Rational Design and Green Fabrication of Antimicrobial Metal Nanoparticle/ Cellulose Nanocrystal Composites

by

Christopher Deutschman

A thesis

presented to the University of Waterloo

in fulfillment of the

thesis requirement for the degree of

Master of Applied Science

in

Chemical Engineering (Nanotechnology)

Waterloo, Ontario, Canada, 2020

Author’s Declaration

This thesis consists of material all of which I authored or co-authored: see Statement of Contributions included in the thesis. This is a true copy of the thesis, including any required final revisions, as accepted by my examiners.

I understand that my thesis may be made electronically available to the public.

Statement of Contributions

Christopher Deutschman was the sole author of Chapters 1, 2, 4, and 5, which were not written for publication. This thesis contains work in Chapter 3 which was written as part of a manuscript pending submission. The contributions for Chapter 3 are as follows:

Christopher Deutschman and Joanna Jardin jointly conceptualized this project under the supervision of Dr. Michael Tam and Dr. Michael Pope. Christopher Deutschman performed all of the data mining, data cleaning, and data analysis. Christopher Deutschman and Joanna Jardin contributed to the writing of the manuscript. Christopher Deutschman generated the figures and tables for the manuscript. Christopher Deutschman contributed to the final editing. All co-authors participated in the intellectual development of the content in the final manuscript. As the lead author of the manuscript, I piloted the majority of the experimental design, set-up, and execution, with valued guidance and input from my co-authors.

Abstract

The primary goals of the work presented in this thesis were to better understand how metal nanoparticles (MNPs) affect antimicrobial activity, and to develop green synthesis protocols for the fabrication of nanocomposites designed specifically for antimicrobial applications. This work utilized a meta-analytical framework to mine data from recent literature and determine which MNP physiochemical properties dictate their antibacterial activity. Linear regression models revealed a size dependence for the antibacterial activity of silver MNPs, where smaller nanoparticles are more effective at combating Gram-negative *E. coli* ($R^2 = 40.3\%$, $p < 0.001$). In contrast, surface charge was determined to be the dominate physiochemical parameter in predicting the efficacy of silver MNPs against Gram-positive *S. aureus*, with potential secondary dependency on MNP size ($R^2 < 44\%$, $p < 0.001$ and < 0.05 for charge and size respectively). Better standardization in antimicrobial testing and reporting protocols will be critical in allowing for more powerful analyses in the future.

Building off of the meta-analytical work, ecofriendly and cost effective synthesis protocols were developed to generate copper nanoparticles using cellulose nanocrystals and tannic acid. Cellulose nanocrystals provided an effective and environmentally benign base for silver and copper MNPs to be deposited using simple one-pot reduction. The developed one-pot synthesis method was also shown to be effective for the generation of silver/cellulose and copper/silver/cellulose nanomaterials. The final morphology of the copper/cellulose MNPs was found to be heavily dependent on the order of reagents during one-pot reduction, where coating of tannic acid on cellulose nanocrystals was a necessary first step to generate small and well-dispersed copper nanoparticles. The copper/cellulose composite was highly effective at suppressing the growth of *S. cerevisiae* microbes at a concentration of 25 μg/mL of copper.

Acknowledgements

I would like to thank my supervisors, Dr. Michael Tam and Dr. Mike Pope, for their guidance and support during the course of my degree at the University of Waterloo. This work would not have been possible without their insight and counsel.

I would also like to thank my committee members, Dr. Bill Anderson and Dr. Boxin Zhao, for their time and effort throughout the thesis defense process.

Thank you to Dr. Juewen Liu for allowing me the use of his lab's time, expertise, and equipment, as zeta potential analysis would not have been possible without it. Thank you also to Mishi Groh for training and assistance with the transmission electron microscope, which enabled a complete characterization for my experimental work.

To my colleagues in the Tam and Pope groups, thank you for an enjoyable and memorable two years!

Table of Contents

List of Figures ..... **viii**
List of Tables ..... **x**
Chapter 1: Introduction 1
1.1 Project Motivation 2
1.2 Project Outcomes 3
1.3 Thesis Outline 4
Chapter 2: Literature Review **5**
2.2 Mechanisms of Antimicrobial Activity of Metal Nanoparticles 7
2.2.1 Physical Adsorption Dependent Pathways 8
2.2.2 Redox Dependent Pathways 11
2.2.3 Metal Ion Dependent Pathways 13
2.2.4 Influence of Surface Coatings on Antimicrobial Activity 14
2.3 Metal Nanoparticle Synthesis 16
2.3.1 Single Metal Nanoparticle Synthesis 16
2.3.2 Bimetallic Nanoparticle Synthesis 19
2.3.3 Green Nanoparticle Synthesis 21
2.3.4 Green Synthesis Using Biopolymers 24
2.4 Conclusions 26
Chapter 3: Determining Critical Physiochemical Properties Affecting Antibacterial Activity of Metal Nanoparticles: A Meta-Analytical Approach **27**
3.2. Experimental Procedure 31
3.2.1 Initial article collection 31
3.2.2 Dataset refinement and inclusion criteria 32
3.2.3 Statistical analysis 34
3.3 Results and Discussion 34
3.3.1 Literature search & data extraction. 34
3.3.2 Trends in antimicrobial nanoparticle evaluation and reporting. 35
3.3.3 Cross-comparative analysis of silver, copper, gold, and zinc antimicrobial MNPs 37
3.3.4 Determining influential physiochemical characteristics of silver MNPs. 38

3.4 Conclusions 42
Chapter 4: Synthesis and Characterization of Copper-, Silver-, and Copper/Silver-Cellulose Nanocrystal Composites with Antimicrobial Activity 44
4.1 Introduction 45
4.2. Experimental Procedure 46
4.2.1 Materials 46
4.2.2 One Pot Preparation of Metal/CNC/Tannic Acid Composites 47
4.2.3 Composite Characterization 47
4.3 Results and Discussion 49
4.3.1 Characterization of Copper/CNC Nanoparticles 49
4.3.2 Effects of Fabrication Parameters on Copper/CNC Morphology 52
4.3.3 Generation and Characterization of Silver/CNC and Copper/Silver/CNC Nanoparticles 55
4.3.4 Preliminary Antimicrobial Testing 60
4.4 Conclusion 62
Chapter 5: Conclusions and Future Recommendations 63
5.1 Conclusions and Recommendations for Work Presented in Chapter 3 64
5.2 Conclusions and Recommendations for Work Presented in Chapter 4 66
References 68

List of Figures

Figure 2.1: Targets of antibacterial metal nanoparticles in various areas of a bacterial cell ……. 7
Figure 2.2: Stretching of the R(C-O) lysozyme sensitive bond by 1, 2, or 5 silver atoms (A). Schematic representation of silver-mediated cell membrane damage (B). Transmission electron micrographs of E. coli cells at 1 and 12 hours of silver nanoparticle exposure, with red arrows indicating silver nanoparticles and black arrows indicating disintegrated bacterial components (C). Adapted from Parashar 2011 ...……...…… 9
Figure 2.3: The conduction and valence band levels of various metal oxide nanoparticles (measured on the absolute vacuum scale). Grey band represents potential range of physiological redox reactions. Adapted from Burello 2011 ...…… 12
Figure 2.4: Difference in toxicity of metal nanoparticles depending on their internalization mechanism. Adapted from Sabella 2014 ……. 14
Figure 2.5: Schematic representation of the critical components for chemical reduction synthesis of metal nanoparticles. Adapted from Jana 2001 ……. 17
Figure 2.6: Growth of highly monodisperse magnetite nanoparticles over time using an 'extended' LaMer mechanism. Adapted from Vreeland 2015 ……..... 18
Figure 2.7: TEM image and formation schematic of gold/palladium bimetallic particles formed with PVP and CTAB as reducing agents (A), TEM images of gold/palladium bimetallic particles formed with increasing concentrations of sodium citrate (B). Adapted from Kuai 2012 and Han 2012 …….. 20
Figure 2.8: Methods of biological synthesis for metal nanoparticles …….. 22
Figure 2.9: Common types of plant derived terpenes, and their role in the reduction and capping of metal nanoparticles. Adapted from Mashwani 2016 ……... 22
Figure 2.10: Reaction schematic for the reduction of metal nanoparticles by eugenol (A) or caffeic acid (B). Adapted from Singh 2010 and Liu 2018 ……... 23
Figure 2.11: TEM images of silver nanoparticles generated with 0.1 wt% (a) 0.25 wt% (b), or 0.5 wt% (c) cellulose nanocrystal solutions as the capping agent. Scale bars represent 100 nm. Range of silver nanoparticles sizes for each solution of CNC (d). Adapted from Lokanathan 2014 … 25

Figure 3.1: Summary of data mined from the literature encompassing information on nanoparticle's physiochemical characteristics, antibacterial assay type, and bacterial models tested …… 35
Figure 3.2: Linear regression models correlating antibacterial efficacy, as measured by minimum inhibitory concentration, with nanoparticle size (A and C) and surface charge (B and D) ……. 39
Figure 4.1: UV-Visible spectra for pristine CNC (red), tannic acid coated CNC (blue), and copper-nanoparticle coated CNC (black) ……..…. 50
Figure 4.2: TEM images of pristine cellulose nanocrystals (A), tannic acid coated cellulose nanocrystals (B), copper nanoparticles generated by tannic acid (C), and copper nanoparticles generated by tannic acid on cellulose nanocrystals (D). Each scale bar represents 100 nm ….. 51
Figure 4.3: TEM and SEM micrographs of bundled copper/CNC colloid (A and B), and TEM micrographs of the copper/CNC composite fabricated without tannic acid (C) and without copper sulfate (D). The proposed mechanism for bundled or networked colloid formation based on reagent addition order (E) ...……. 54
Figure 4.4: UV-Visible spectra for silver/CNC (grey) and copper/silver/CNC (black) composites. Copper/CNC spectrum (blue) is show for comparison ...……. 57
Figure 4.5: TEM micrographs of CuCNC (A) AgCNC (B) and CuAgCNC (C) nanocomposites. All scare bars are 100 nm ……. 58
Figure 4.6: Rate of respiration of yeast (measured as CO_2 produced in mL) when allowed to respirate normally (black) or in the presence of 250 µg of copper/CNC colloid (blue) …….. 61

List of Tables

Table 3.1: Average minimum inhibitory concentration (in µg/mL) for four highly reported types of metal nanoparticles and two broad spectrum antibiotics ……..... 37

Table 4.1: Measured hydrodynamic and nanoparticle core size and zeta potential for copper- and silver-containing CNC nanocomposites …… 59

Chapter 1: Introduction

1.1 Project Motivation

Compound threats of the development of extreme antibiotic resistance in bacterial populations and the slowdown new antibiotic discovery has led to a dearth of new treatments for bacterial infections in humans [1]. With the “golden age of antibiotics” long gone [2], the development of new, non-antibiotic antimicrobial agents will be increasing important for the continuing health and safety of the world’s population. Metal nanoparticles, which have been generated since antiquity for their unique optical properties, have become of interest in the past decades for exactly this application [3]. It has been shown that metal nanoparticles are effective both against common culture strains [4] and against multi-drug resistant strains [5] of human-infecting pathogens, lending promise to the development of metal nanoparticle-based treatment regimes. However, to date, little to no work has been done on the clinical application of antimicrobial nanoparticles [6]. The clinical relevance of metal nanoparticles is in large part hindered because there is not yet a consensus on how they actually function in the suppression or killing of bacteria, nor is there a proven methodology to what makes a nanoparticle maximally effective for this application.

A more rigorous understanding of what makes metal nanoparticles effective is crucial to the translation of these particles from bench to clinic. Determining from the literature what physiochemical parameters are important is challenging due to the high variance in the generated nanoparticles, in the testing procedures, and in the reporting standards. This variance makes it nearly impossible to draw meaningful conclusions about what parameters are or are not important through the comparison of individual articles. A larger and more robust analysis of the literature is needed to determine what overarching trends exist, and this can be achieved through systematic review and meta analytical techniques. Meta-analysis is crucial to increase the

population size and discern trends despite the noise introduced by high inter-study variance, and meta-analytical results are therefore more reliable for clinical translation [7].

Additionally, many antimicrobial metal nanoparticles are generated using highly toxic chemicals, such as sodium borohydride [8] or hydrazine [9], increasing the downstream risk of cyto- and ecotoxicity. Even when the understanding of metal nanoparticles' antimicrobial activity is improved, they will not be translatable until they can be fabricated with sustainable and eco-friendly techniques. The 'green' fabrication of metal nanoparticles is becoming a more prevalent area of research, with a large body of research being published on the use of plant extracts and plant-derived compounds to synthesis metal nanoparticles [10]. However, work remains to be done in the controlled and specific green fabrication of antimicrobial metal nanoparticles. The combination of a thorough understanding of what makes metal nanoparticles optimally antimicrobial and how to fabricate nanoparticles fitting these specifications with green techniques will be an important goal in the generation of clinically relevant solutions.

1.2 Project Outcomes

The overall goal of this project was to understand and create potent new antimicrobials material with minimal negative environmental impact. This was achieved in two simultaneous thrusts: a theoretical component using data mining to clarify what nanoparticle properties are critical for antimicrobial applications, and an applied component on the fabrication and characterization of antimicrobial metal nanoparticles.

The first section of this thesis focused on a theoretical approach to determining what makes metal nanoparticles maximally effective for antimicrobial applications. In this work, data mining and meta-analysis was employed to draw new knowledge from pre-existing literature on antimicrobial nanoparticles. The state of the literature was assessed, and the critical

physiochemical parameters were explored using linear regression models. Both single and multivariate models were used to explore the possibility of interaction terms between important physiochemical parameters.

The second section of this thesis describes the fabrication and characterization of a versatile composite of cellulose nanocrystals and copper, silver, or copper and silver nanoparticles. The impact of fabrication parameters was evaluated to determine optimal fabrication conditions and understand how the fabrication process impacts the final material. The system was then proven to be useable for the fabrication of multiple types of metal nanoparticles, suggesting it's broader applicability for a variety of projects. A preliminary assessment of antimicrobial activity was undertaken. The green system uses a one-pot fabrication method with water as the only solvent, and plant-derived reagents, which minimizes any negative environmental impact the fabrication process may have. The developed CNC/metal composites show promise as an ecofriendly, scalable, and tunable antimicrobial system.

1.3 Thesis Outline

This thesis consists of five chapters. The first chapter provides an introduction to the project, including the motivation and outcomes. The second chapter reviews the recent literature on antimicrobial nanoparticles, highlighting both what is known of their antimicrobial activity and how nanoparticles have previously been synthesized. The ecofriendly synthesis of metal nanoparticles is highlighted. Chapter three presents the results of the undertaken meta-analysis, providing insight into what does and does not influence the antimicrobial activity of metal nanoparticles. Chapter four builds off of the work presented in three and explores the novel green synthesis of metal nanoparticles theoretically optimized for antimicrobial application. Chapter five provides the project conclusions, as well as recommendations for future work.

Chapter 2: Literature Review

2.1 Background on Antibiotic Resistance

Each year, bacterial infections cause severe illness around the world, and the rise of antibiotic resistance in bacteria means that more and more severe illnesses will develop as time goes on [11]. Current reports suggest that at least 26% of reported bacterial infections in Canada alone are resistant to at least one class of first-line antibiotics, and as it stands, reversing antibiotic resistance is immensely challenging at a community level [12]. These drug-resistant infections are associated with one billion dollars in annual healthcare spending in Canada alone [13], and this spending is predicted to increase as drug resistant infections continue to proliferate.

Antibiotics were first used clinically in the 1910s with the synthesis of salvarsan, an organoarsenic compound and the first modern antibiotic [14]. Since then, a large number of antibiotics have been developed and commercialized for widespread use. However, the number of antibiotic compounds being isolated and commercialized has dropped significantly in recent decades, with the most recent new class of antibiotics being discovered in the mid-1980s [2]. Most antibiotics are derived from bacteria or fungi, which produce antibiotic compounds to suppress or kill competing microbes or to mediate interactions with eukaryotic hosts [15]. However, because antibiotic compounds are naturally occurring, there is a chance for bacteria to evolve resistant to these compounds, and the evolution is accelerated by overuse and misuse of antibiotics in human populations [16]. It is therefore crucial to develop novel solutions to address the impending antibiotic resistance crisis.

Nanoparticles, which are materials with at least one dimension of less than 100 nm and physiochemical properties significantly different from their bulk state, have gained attention as a potential solution to the antibiotic resistance crisis [17]. Most nanoparticles, including organic materials such as carbon nanotubes and graphene sheets, and inorganic materials such as quantum dots and metal nanoparticles, display some level of toxicity towards bacteria [18].

Metal nanoparticles in particular are promising antibacterial agents, due to their relatively low cost and ease of fabrication [19]. Metal nanoparticles with antimicrobial properties have been suggested for use in a wide range of applications, including in fabric or surface coating [20], [21], in food packaging [22], and in medical supplies such as hospital surfaces [23], [24] and catheters [25]. This literature review will discuss the current understandings of how metal nanoparticles can act as effective antimicrobial agents, as well as the various methods for synthesizing metal nanoparticles. Special emphasis is placed on the 'green' or sustainable synthesis of metal nanoparticles for antimicrobial applications.

2.2 Mechanisms of Antimicrobial Activity of Metal Nanoparticles

Despite the wide range of research conducted on antimicrobial nanoparticles, the mechanisms by which nanoparticles kill bacteria remain poorly understood. This is in part due to the vast number of interactions that these nanoparticles can have with bacterial cells, including electrostatic, hydrophobic, stereoselective, ligand-receptor, redox-active, or coordination-based interactions

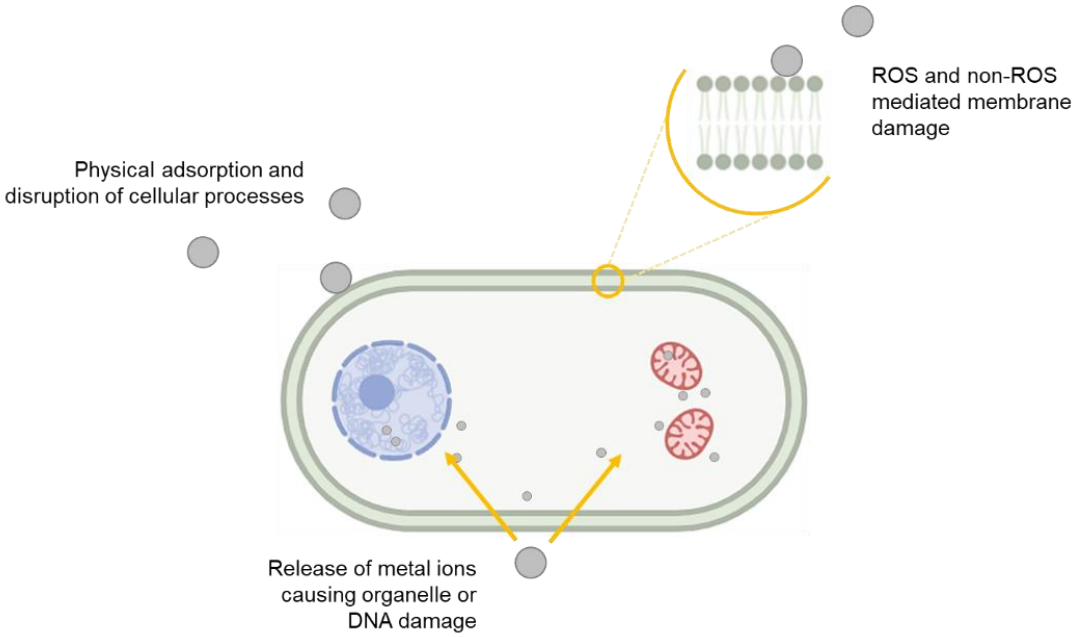

Figure 2.1: Targets of antibacterial metal nanoparticles in various areas of a bacterial cell.

[26]. While the exact interactions that lead to bacterial damage or death remain unclear, there are many pathways that have been explored as potential contributors. These pathways include damage due to physical adsorption of nanoparticles onto the cell (electrostatic or otherwise), oxidative damage via nanoparticle catalyzed redox reactions, and damage caused by heavy metal ions leached from the nanoparticle surface [27]. Each of these pathways can target a variety of biological structures (see Figure 2.1), including the cell membrane [28], DNA [29], and organelles [30]. Understanding the exact pathways will be an important step in designing optimally antimicrobial and clinically relevant nanoparticles.

2.2.1 Physical Adsorption Dependent Pathways

In a study conducted by Choi and coworkers, the antimicrobial activity of silver nanoparticles was compared to silver ions (from $AgNO_3$) and silver colloids (AgCl) against a variety of wastewater-inhabiting bacteria [31]. In a direct comparison, silver nanoparticles were found to be more effective at inhibiting bacterial growth than ionic or colloidal silver. When a suspension of bacteria and silver nanoparticles was studied using high resolution backscattered scanning electron microscopy, the nanoparticles were observed to be physically contacting the bacterial cell membranes. Additionally, the bacterial membranes were seen to be pitting, which could be attributed to the physical adsorption of the nanoparticles onto the cells. Similar results were observed in a study of copper nanoparticle interactions with *E. coli* [32]. The authors evaluated a suspension of bacterial cells and copper nanoparticles using scanning electron microscopy, and found that the bacteria displayed unusual morphology, with shrunken, pitted, or otherwise disfigured membranes. This effect was attributed to the absorption of copper nanoparticles onto the bacteria, and subsequent release of toxic copper ions.

The surface charge of antibacterial nanoparticles may also be important in determining their antimicrobial efficacy, and for both silver and iron, positively charged nanoparticles are more effective than their negatively charged counterparts [33], [34]. While negatively charged nanoparticles may be able to bind electrostatically with the positive residues found in many bacterial membrane proteins [35], both Gram-positive and Gram-negative bacterial membranes bear overall negative charges. Therefore, a positively charged nanoparticle can be expected to be more strongly attracted to bacterial cells, becoming more tightly bound and potentially better disrupting membrane structure or other cellular processes that occur at the interface.

A very interesting study by Parashar and coworkers also explored the impact of silver ions on the peptidoglycan layer that is present in the outer structures of both Gram-negative and Gram-positive bacteria, though in different amounts [36]. The authors modeled the lysozyme sensitive bond that connects N-acetylglucosamine and N-acetylmuramic acid within the peptidoglycan layer, when alone or in the presence, of 1, 2, and 5 silver ions, as shown in Figure 2.2. It was found that the bond length stretches with increasing number of silver ions, effectively

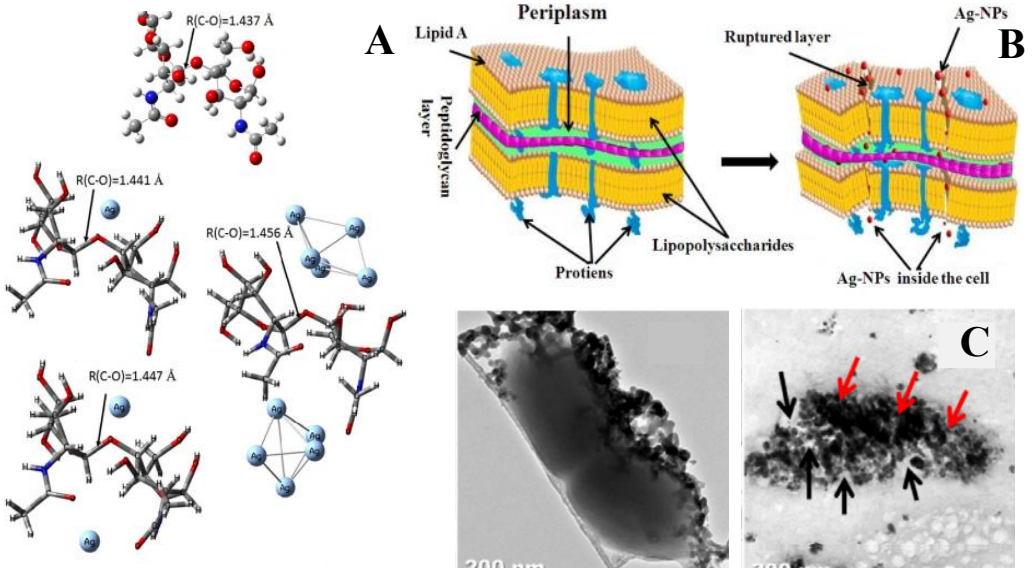

Figure 2.2: Stretching of the R(C-O) lysozyme sensitive bond by 1, 2, or 5 silver atoms (A). Schematic representation of silver-mediated cell membrane damage (B). Transmission electron micrographs of E. coli cells at 1 and 12 hours of silver nanoparticle exposure, with red arrows indicating silver nanoparticles and black arrows indicating disintegrated bacterial components (C). Adapted from Parashar 2011.

weakening the structure and suggesting the possibility of eventual bond breakage. The authors theorized that with enough silver atoms, such as a few hundred in a nanoparticle, the bond could be cleaved, destabilizing the cell wall and eventually lysing the cell. This type of destabilization could only be achieved when the silver nanoparticles are adhered firmly to the bacterial cell membrane, leading the authors to conclude that physical adsorption between the nanoparticle and cell is critical to effective antibacterial action.

Shape dependent nanoparticle behavior has also been observed at the whole-bacteria level. In a study by Hong et al. comparing spherical, cubic, and rod shaped silver nanoparticles, the cubic nanoparticles were found to be most effective against *E. coli* [17]. The authors proposed that both the cubic and spherical nanoparticles, which have much higher specific surface areas than nanorods, were able to pack more tightly to the bacterial cell surfaces, leading to increased membrane damage. Differently shaped nanoparticles have also been shown to have different interactions with the bacterial proteins that adsorb to their surface, which may cause varying states of dysregulation or death of the cell. Soleimani et al. synthesized silver spheres, rods, and cubes, and tested their inhibitory affect against *E. coli*, *P. aeruginosa*, *S. aureus*, and *B. cereus* model bacteria [18]. Cube shaped silver nanoparticles were found to be vastly more effective at inhibiting all strains of bacteria than any other shape. To uncover the potential mechanism, each type of nanoparticle was exposed to human serum albumin, and cubic nanoparticles were found to have the highest binding affinity for the proteins. It was theorized that nanoparticles with sharp edges were able to aggressively bind with and denature proteins, causing increased degradation and cellular damage. However, it is worth noting that unlike the study by Hong et al., which found nanospheres more effective than nanorods for overall bacterial

killing, this study found that nanorods (both sharp and blunt) where more effective than nanospheres.

2.2.2 Redox Dependent Pathways

The catalysis of biologically damaging reactive oxygen species (ROS) by nanoparticles is another pathway by which nanoparticles have been proposed to damage or kill bacteria. Recent work by Angelé-Martínez and colleagues sought to understand the damage caused by copper oxide nanoparticles through the study of DNA damage [37]. In a comparison of copper ions and copper oxide nanoparticles, the damage of nanoparticles was an order of magnitude higher. The authors used EPR spectroscopy to evaluate the reactive oxygen species generated by copper oxide nanoparticles, and found that hydroxyl radicals were the primary species generated when copper oxide particles were incubated with hydrogen peroxide (a common reactive oxygen species found in biological environments), while both hydroxyl and super oxide radicals were generated in the presence of hydrogen peroxide and ascorbate together. The generation of different reactive oxygen species suggests that multiple generation pathways may exist.

Other work has been conducted looking at the impact of reactive oxygen species generated by nanoparticles on bacterial cell membranes. A simple experiment by Ansari et al. [38] used scanning electron microscopy to study changes in bacteria exposed to silver nanoparticles. The authors observed massive pitting in *E. coli*'s cell membranes when exposed to silver nanoparticles, which they attributed to ROS-mediated damage to the cell membrane. Fenton and Fenton-like chemistry, which is the generation of reactive oxygen species by heavy metal ions, has been shown to initiate the peroxidation of lipids, leading to catastrophic membrane failure [39]. Further studies have corroborated these results using reactive oxygen species assays, in which a fluorescent dye is used to label cells which have been damaged by

reactive oxygen species [40]. One such study found that after just two hours of incubation with silver nanoparticles, 40% of exposed *E. coli* cells showed significant reactive oxygen species related damage [41].

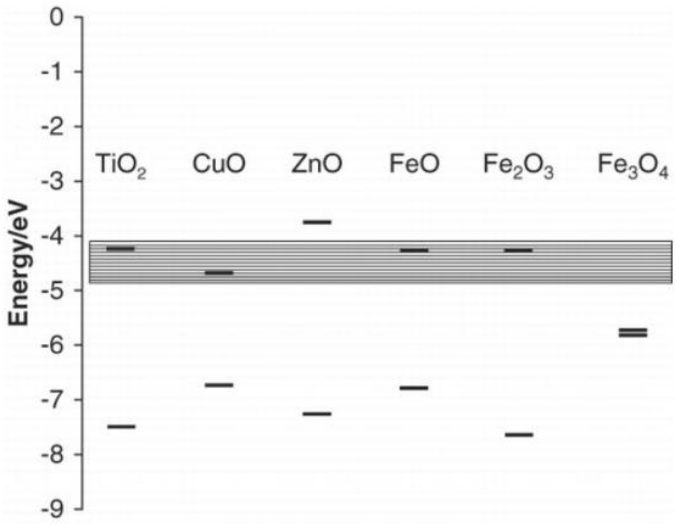

Figure 2.3: The conduction and valence band levels of various metal oxide nanoparticles (measured on the absolute vacuum scale). Grey band represents potential range of physiological redox reactions. Adapted from Burello 2011.

While many studies have focused on the antimicrobial potential of nanoparticles through the catalysis of reactive oxygen species, it is also possible that nanoparticles participate directly in cellular redox processes, inducing oxidative stress more directly. A theoretical study conducted by Burello et al. surveyed a number of metal oxide nanoparticles, evaluating their conduction and valence band levels and comparing them to relevant physiological redox potentials [19]. Many of the evaluated metal oxide nanoparticles had theoretical conduction bands that overlapped with the range of physiological redox potentials, as shown in Figure 2.3. These nanoparticles may therefore be capable of abstracting electrons from biological compounds critical to cell regulation, which could unbalance the cellular redox state and lead to oxidative stress.

2.2.3 Metal Ion Dependent Pathways

Metal nanoparticles have high surface energy, allowing them to solubilize and produce metal ions easily [42]. Heavy metal ions are known to be damaging to bacteria, and thus may represent a major component of nanoparticles toxicity. One study by Hachico et al. [43] examined the impact of silver ions released from silver nanoparticles on the membrane of *P. putida*, and found that relatively low concentrations of silver ions could prevent 100% of bacterial growth in comparison to control. The authors found that the ratio of *cis* to *trans* unsaturated fatty acids in the cell's membrane was greatly increased with the increasing presence of silver ions. This conformational change from *cis* to *trans* isomers rapidly decreases membrane fluidity and permeability and is a common indicator of bacterial cell stress.

Metal ions can also permeate the cells and cause damage to critical internal cellular components. In a study by Chatterjee and coworkers [44], DNA damage in the presence of copper nanoparticles was assessed, and it was found that within 30 minutes of contact time, the copper nanoparticles could completely convert super coiled DNA (the natural form of DNA) to Nick circular or linear confirmations, indicating extensive damage. To determine the source of damage, the authors also incubated the copper nanoparticles and DNA with reactive oxygen species scavengers or with ion chelators and found that only the copper ion chelator protected the DNA from extensive damage. Thus, the authors concluded that the release of ions from nanoparticles, not the generation of reactive oxygen species, was a primary driver in genotoxicity. Another study by Li and coworkers [30] explored the damage of heavy metal ions, and found that within 16 hours of exposure, the vast majority of metal ions localized in the cell's mitochondria. The swelling of the mitochondria and loss of cristae suggested that the mitochondria lost all respiratory function, and the cell would be unable to persist.

2.2.4 Influence of Surface Coatings on Antimicrobial Activity

Some researchers have also proposed alternate pathways for the intracellular toxicity of metal nanoparticles. Sabella et al. conducted a study on the toxicity of a variety of metal nanoparticles, and concluded that the most important factor in predicting nanoparticle toxicity was the uptake of the nanoparticles into the cells through lysosome mediated endocytosis [45]. Two types of gold nanoparticles were studied in detail – one with a surface coating of 11-mercapto undecanesulfonic acid (MUS) and octanethiol (OT), and the other with a surface coating of MUS and 2,7-dimethyl octanethiol (brOT). The gold nanoparticles with the MUS and OT coating were shown to pass through the model cell membranes, whereas the particles with a MUS and brOT coating could only be internalized by the cell through endocytosis. The MUS and brOT particles that could only be internalized through endocytosis showed significantly higher toxicity, both in model cells and in an *in vivo* test with *Drosophila melanogaster*. It was proposed that when internalized in highly acidic lysosomes, the MUS and brOT gold nanoparticles were degraded,

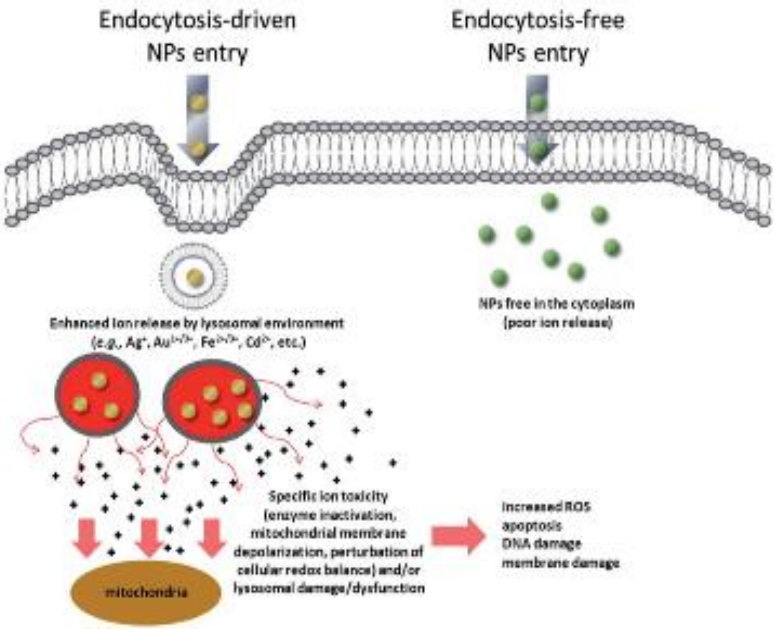

Figure 2.4: Difference in toxicity of metal nanoparticles depending on their internalization mechanism. Adapted from Sabella 2014.

causing a significant release of gold ions which could subsequently cause cell damage and death (shown schematically in Figure 2.4). In comparison, the MUS and OT coated nanoparticles which entered the cell's neutral cytosol did not release cell-damaging ions.

The role that proteins and other biomacromolecules that can adsorb to nanoparticle surfaces has also been investigated as a pathway that can modulate nanoparticle toxicity. Walkey and coauthors created a library of 105 different gold nanoparticles, with 3 different core sizes and 67 potential surface ligands that were subsequently attached [46]. The nanoparticles were each exposed to human serum, and the protein corona that adsorbed to each nanoparticle was quantified. Following serum exposure, the nanoparticles were inoculated into eukaryotic cell type cultures (A549 human lung epithelial carcinoma cells), and cell association of the nanoparticles was quantified. The adsorbed protein fingerprint, which was unique to each type of nanoparticle, was found to be a significantly better predictor of cell association than any other predictor tested, including nanoparticle size or surface charge alone. It is also of note that in general, smaller nanoparticles were found to have a higher protein corona density, which could theoretically amplify the type of interaction it has with a cell.

While the previously proposed endocytosis mediated pathways only apply to eukaryotic cells, it is not a stretch to imagine that nanoparticle surface-adsorbed biomacromolecules would also affect the nanoparticle interactions with bacteria. A study by Jain and coauthors looked at the difference in antibacterial efficacy of silver nanoparticles with either bare surfaces, or with protein capping derived from fungal cells [47]. In general, the authors found that bare nanoparticles were much more effective at damaging the bacteria than the nanoparticles with a cocktail of proteins adsorbed to the surface. Bare surface nanoparticles were found to release nearly twice the amount of silver ions as the protein capped ones, and triggered higher

intracellular ROS generation in all bacterial species tested. Another study by Li et al. observed similar results when testing the antibacterial capacity of iron nanoparticles with either bare surfaces or coatings of polymer or natural organic material (much like the nanoparticles would encounter *in vivo* or in the environment) [48]. The bare surface iron nanoparticles were 20 to 100 times more effective at suppressing bacterial growth than any coated nanomaterial studied. When examined using transmission electron microscopy, the authors found that the bare iron nanoparticles were able to adsorb to the surface of *E. coli* cells, whereas any coating prohibited this interaction. The authors concluded that electrostatic or steric repulsion caused by the nanoparticle surface coatings prevented direct interaction of the nanoparticles with the bacteria, thus significantly lessening their bactericidal ability.

2.3 Metal Nanoparticle Synthesis

2.3.1 Single Metal Nanoparticle Synthesis

Metal nanoparticles, as with most nanomaterials, can be synthesized with a wide variety of processes that can generally be divided into top-down and bottom-up processes. Top-down processes involve the breakdown of a bulk material into nanoparticles, most often through physical or chemical means. Bottom-up processes, in contrast, build nanoparticles up from smaller blocks, most often singular molecules. This includes processes such as chemical [49], [50] or electrochemical reduction [51]–[53] or radiolysis [54], [55]. Bottom-up processes have the advantage of providing more precise control over the composition and morphology of the generated nanoparticles and are often employed for the generation of metal nanoparticles in particular.

Chemical reduction remains a very common method of synthesis for the production of nanoparticles. Colloidal solutions of metal nanoparticles have existed since antiquity [56], but the modern chemical reduction method was pioneered by Turkevich in the early 1950s [57], who

used a boiling solution of sodium citrate to generate monodisperse gold nanoparticles. To generate metal nanoparticles using chemical reduction, three major components are needed: a metal precursor (often a metal salt such as AgNO3 or HAuCl), a reducing agent, and a capping agent [49], though in many cases one molecule can serve as both the reducing and capping agent. This process is represented schematically in Figure 2.5. Using chemical reduction, physiochemical properties such as nanoparticle shape and size, polydispersity, surface charge, surface free energy, and crystallization (ie exposed crystalline face) can be controlled [58]. This flexibility positions chemical reduction as an advantageous choice of fabrication method.

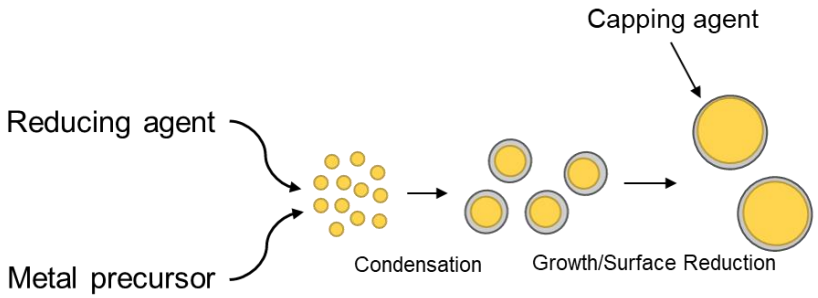

Figure 2.5: Schematic representation of the critical components for chemical reduction synthesis of metal nanoparticles. Adapted from Jana 2001.

Extensive work has been undertaken to identify ways of controlling the final morphology of metal nanoparticles synthesized by chemical reduction. Recent work by Vreeland and coworkers [59] showed that precise shape and size control could be achieved by controlling the amount and addition time of a metal precursor (As shown in Figure 2.6). The authors proposed that in classical nanoparticle synthesis, the concentration of unreacted monomer (metal salt precursor) increases until it reaches supersaturation, after which it is thermodynamically favorable to form nuclei. The formation of nuclei reduces the concentration of the monomer, and from that point onward the largest particles grow larger and the smaller ones dissolve. However, by adding additional unreacted monomer after the 'burst' nucleation phase, the particles can

achieve an extended steady-state growth phase, where the size increases continually and uniformly until no more monomer is added. In this way, the simple supplementation of metal salt precursor over a steady period of time allows for precisely controlled and reproducibly sized nanoparticles to be grown.

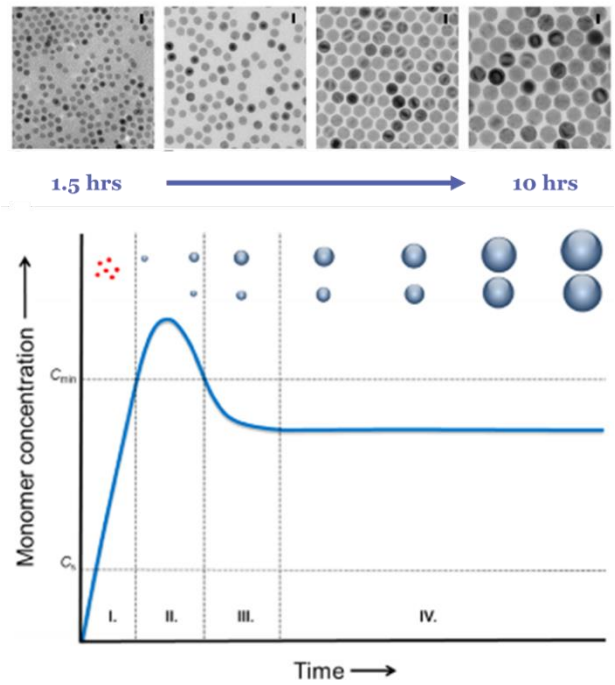

Figure 2.6: Growth of highly monodisperse magnetite nanoparticles over time using an 'extended' LaMer mechanism. Adapted from Vreeland 2015.

Other work has shown that factors such as choice of reducing or capping agent can vastly alter the final shape of a generated metal nanoparticle. A study by Yao et al. [60] showed that platinum nanoparticles could take either an extended wire form or a spherical form, when either a weak reducing agent (such as ethylene glycol) or a strong reducing agent (citric acid) is used. The authors proposed that a strong reducing agent like citric acid would force all the metal precursor to reduce to a zero-valent state, and these atoms will then preferentially aggregate and form spherical nanoparticles. In contrast, the weaker reducing agent complexed with the metal ions without reducing them fully, allowing them to polymerize into wires prior to complete

reduction. In another study [61], hexadecyltrimethylammonium bromide (CTAB), a commonly used surfactant, was used to control the growth of gold nanoparticles into rods or plates rather than spheres. The selective adsorption of CTAB molecules onto {111} planes of gold nanoparticles blocks the further addition of gold ions in those locations, which promotes the observed anisotropic growth.

2.3.2 Bimetallic Nanoparticle Synthesis

The production of bimetallic and multimetallic systems has also been an area of growing interest in the past decades, particularly for application in the area of catalysis [62]. Bimetallic metal nanoparticles may be core/shell particles, where one metal tends entirely to the core and is coated with a 'shell' of the second metal, or they may form 'ordered' or 'true' alloyed structures, in which molecules of each metal are well or homogenously dispersed within the particle [63]. Less commonly, 'Janus' or 'twinned' bimetallic nanoparticles can be formed, where each metal is segregated in one area but still contacting the other on at least one face [64]. There are a variety of synthesis strategies for producing bimetallic nanoparticles, ranging from simple chemical reduction-like methods to more complex ones.

Chemical coreduction is one of the simplest methods that can be employed to generate bimetallic nanoparticles, and generally involves a simple simultaneous chemical reduction with more than one metal precursor. In chemical co-reduction processes, the metal salt precusors for multiple metals can be mixed together, and reduction occurs simultaneously to form multimetal particles. The affinity and strength of the reducing or capping agents used towards each metal plays a large role in dictating the final morphology of the bimetallic structure. Work by Kuai and coworkers [65], for example, showed that gold/palladium particles could be formed with either a core-shell or a true alloy morphology depending on the reducing agent used. When polyvinylpyrrolidone (PVP), a weak reducing agent, was used, gold was reduced first to form a

core and palladium(II) was reduced second to form a core, because the reduction of gold is thermodynamically easier . In contrast, when CTAB (a strong reducing agent under hydrothermal conditions) was used, both gold and palladium could be reduced simultaneously, forming an alloyed particle (represented schematically in Figure 2.7A). Another study by Han et al. [66] showed that the morphology of gold/palladium particles could be changed gradually from quasi-spherical particles to flower-like structures simply by increasing the concentration of sodium citrate used (Figure 2.7B).

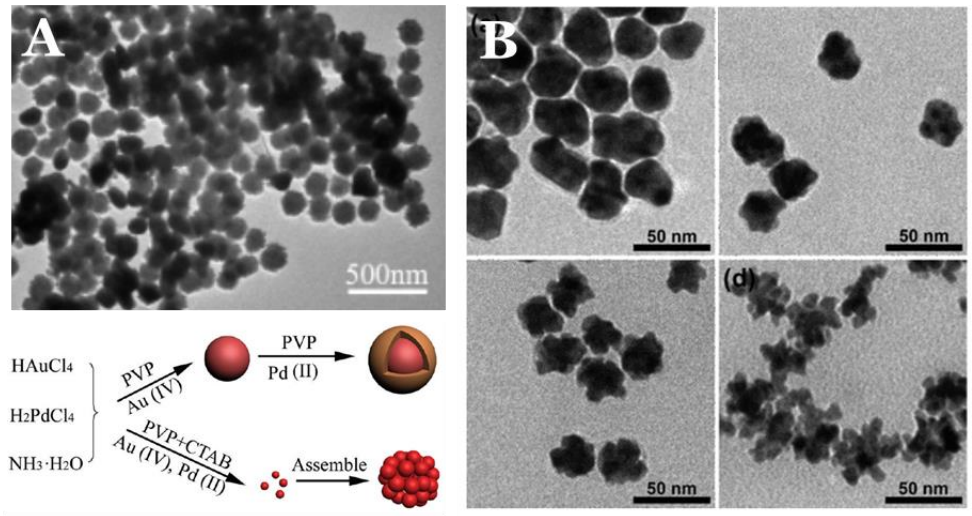

Figure 2.7 TEM image and formation schematic of gold/palladium bimetallic particles formed with PVP and CTAB as reducing agents (A), TEM images of gold/palladium bimetallic particles formed with increasing concentrations of sodium citrate (B). Adapted from Kuai 2012 and Han 2012.

Another relatively facile method for the generation of bimetallic structures employs galvanic displacement. This process relies on a two-step method – first, metal nanoparticles 'seeds' are generated with one metal salt precursor, and then these seeds are exposed to a second metal salt precursor, often in the presence of additional reducing agents [67]. This process relies on ions of the second metal, which must be a metal of higher reduction potential than the seed material, to solubilize and replace the core metal, effectively etching parts of the core away and

depositing the secondary metal. Galvanic displacement has been used to fabricate a wide range of particles, including silver/copper [68], silver/gold [67], and gold/palladium particles [69].

2.3.3 Green Nanoparticle Synthesis

The synthesis of metal nanoparticles using green, or environmentally sustainable, methods has grown greatly in the past years. A multitude of green fabrication strategies have been developed for metal nanoparticle synthesis, primarily based either on synthesis using single-cell cultures or synthesis using plant components (illustrated in Figure 2.8). Cellular synthesis most commonly leverages either whole cell culture, or cell-free supernatant (containing biomacromolecules produced by the cells) for synthesis. In whole cell synthesis, a metal precursor is introduced into a culture of living cells (either bacteria, algae, or some yeasts), and metal nanoparticles are generated within the cells themselves [70]. It has been proposed that the intracellular synthesis of nanoparticles is a byproduct of the cells' inherent heavy-metal defense systems. The metal ions which enter the cells are sequestered, often either in the cell wall or within vacuoles in the cell, and then reduced as a strategy to mitigate their toxicity. As a result, the zero-valent ions in close proximity to one another are able to nucleate and form nanoparticles, similar to a chemical reduction strategy. Extracellular synthesis, on the other hand, utilizes biomacromolecules commonly produced by cells as reducing and capping agents, removing the cells from the solution prior to the start of the reaction [71]. In this case, nanoparticles are thought to be generated through simple chemical reduction pathways, where secondary metabolites produced by the cells act as reducing and capping agents [72].

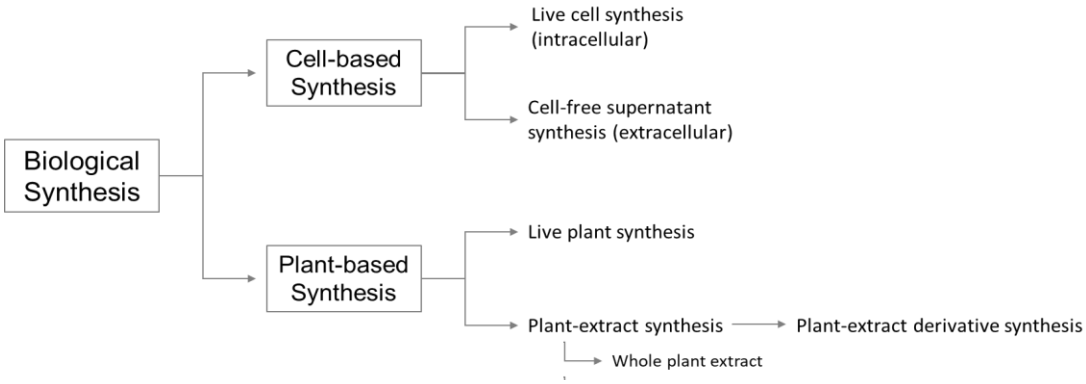

Figure 2.8: Methods of biological synthesis for metal nanoparticles.

Plant-based synthesis is the other common route of biological synthesis, and may involve the use of whole plant extract [73], or extract from specific components of a plant, such as the roots [74], leaves [75], or bark [76]. Most commonly, the plant matter is boiled in distilled or deionized water to extract phytochemicals, which can then be used directly in the synthesis of metal nanoparticles. Terpenoids and plant polyphenols are most commonly cited as playing a major role in the reduction and capping of metal nanoparticles, though organic acids and proteins may also contribute.

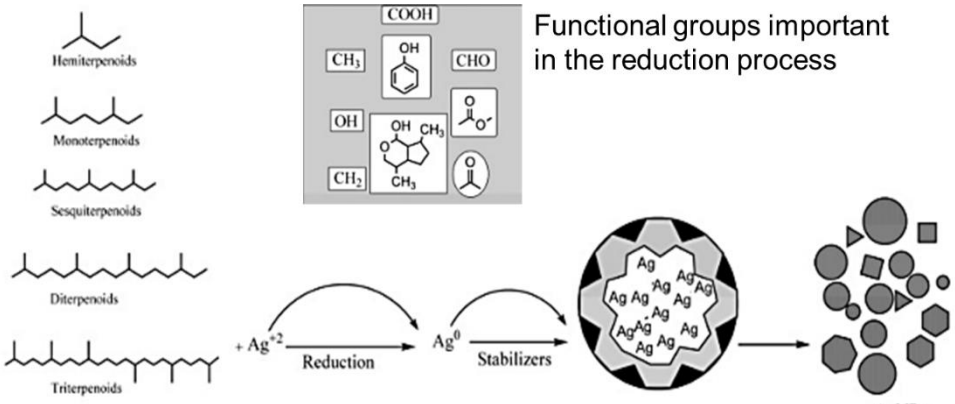

Figure 2.9: Common types of plant derived terpenes, and their role in the reduction and capping of metal nanoparticles. Adapted from Mashwani 2016.

Terpenes are cyclic or chained hydrocarbons built from isoprene units, and are considered the largest class of secondary metabolites found in nature [77]. Many plant-derived terpenoids contain functional moieties such as carboxylic acid or hydroxyl groups, which play a key role in

the reduction of metal ions to zero-valent atoms (as shown in Figure 2.9) [78]. For example, work by Dubey et al. [79] showed that extract of Tansy fruit could easily form silver or gold nanoparticles, which was attributed to reduction of the metal salt precursors by terpenoids found in the essential oil extract. The authors proposed specifically that the terpenoids containing a carbonyl group could undergo conversion from =C=O to –C(O)=O, providing the necessary electron for reduction.

Plant polyphenols are another major class of biomolecules that participate in the synthesis of metal nanoparticles. These molecules all contain a hydroxy-substituted benzene ring in their structure, and can range from very simple to very complex. As of 2015, over eight thousand types of polyphenols had been identified [80]. Singh and workers showed that clove extract could be used to successfully synthesize both gold and silver nanoparticles [81], which contains a high concentration of the polyphenol eugenol. The reaction scheme, shown in Figure 2.10A,

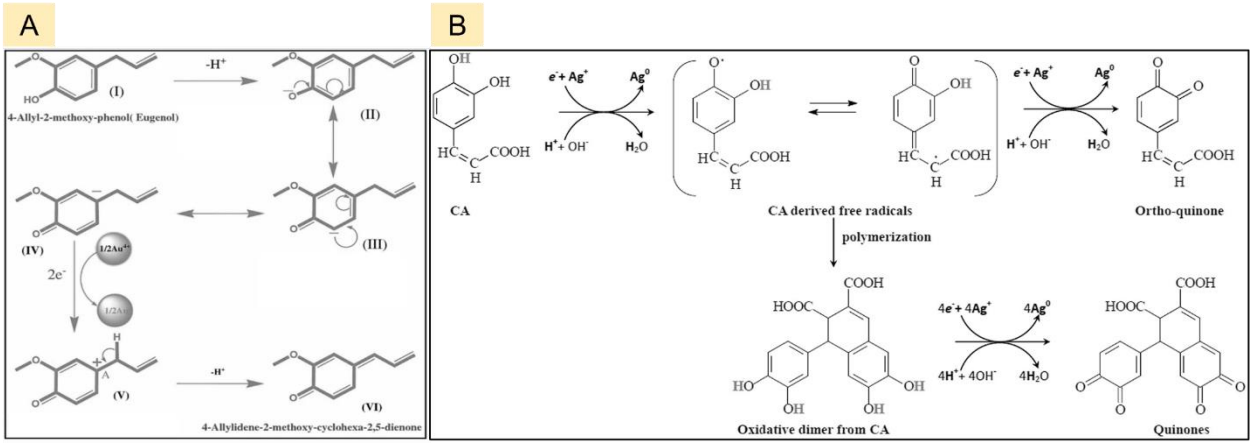

Figure 2.10: Reaction schematic for the reduction of metal nanoparticles by eugenol (A) or caffeic acid (B). Adapted from Singh 2010 and Liu 2018.

shows that when eugenol is deprotonated, it can either exist in a resonance stabilized form, or oxidize and expel 2 electrons. These two electrons can then participate in the reduction of either two Ag^{+} ions or half an Au^{4+} ion. A study by Liu et al. showed that polyphenolic compounds from rice husk extract could be used to synthesize silver nanoparticles [82]. Caffeic acid (CA), a

polyphenolic acid, was proposed to play a major role in the reduction, as one molecule of CA is able to donate up to 5 electrons to a metal precursor (Figure 2.10B).

2.3.4 Green Synthesis Using Biopolymers

Synthesis of metal nanoparticles using naturally derived biopolymers is a specific area of interest, as many biopolymers provide a combination of reducing or capping capabilities, and improved colloidal stability. Work has been done to generate nanoparticles using polymers such as chitosan, alginate, and cellulose [83]–[86]. Nanoparticles generated using cellulose nanocrystals (CNC) are of particular interest, as CNC has useful properties including high thermal stability, high mechanical strength, and low cytotoxicity [87]. Additionally, cellulose is considered the most abundant biopolymer on earth, and pristine nanocellulose can be biodegraded in a span of just weeks [88]. CNC has been used extensively as a capping agent in the synthesis of metal nanoparticles, and has been shown to promote the generation of monodisperse and stable colloids [89]. Lokanathan and colleagues explored the impact of increasing concentrations of CNC on the formation of silver nanoparticles [90], and found that a higher concentration of CNC generated significantly smaller nanoparticles (shown in Figure 2.11). The authors proposed that the hydroxyl groups on the surface of the CNC play a role in coordinating the metal ions, causing the deposition of the nanoparticles directly on the surface. An increase in CNC concentration increases the number of potential nucleation sites, therefore generating more, smaller nanoparticles. Additionally, the sulfate half ester groups, present on the surface of cellulose nanocrystals generated via sulfuric acid hydrolysis, play a role in the capping of the nanoparticles.

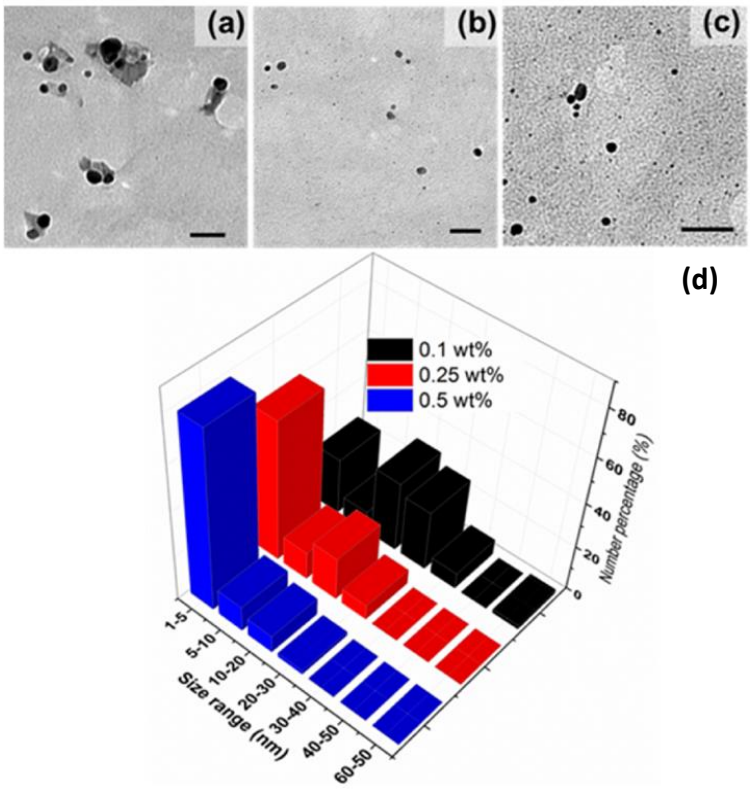

Figure 2.11: TEM images of silver nanoparticles generated with 0.1 wt% (a), 0.25 wt% (b), or 0.5 wt% (c) cellulose nanocrystal solutions as the capping agent. Scale bars represent 100 nm. Range of silver nanoparticles sizes for each solution of CNC (d). Adapted from Lokanathan 2014.

Recent work has also shown that cellulose nanocrystals can be used for 'reductant-free' synthesis of metal nanoparticles, in which the cellulose acts as both the reducing and capping agent. Reductant free synthesis has been achieved either under hydrothermal synthesis conditions [91] or using chemical reduction in a highly basic environment [92]. In both cases, the reduction of the metal salt precursor to a nanoparticle was attributed to the hydroxyl groups present on CNC's surface. At high enough temperature or in highly basic conditions, the hydroxyl groups become deprotonated, exposing an electron-rich oxygen anion that can participate in redox reactions. Additionally, the exposed oxygen may be capable of anchoring the metal nanoparticles to the CNC surface through electrostatic interactions [93]. Given the ability of CNC to act as both a reducing and capping agent, and its superior physical properties and sustainability, it is a promising choice for use in the synthesis of metal nanoparticles for a wide range of applications.

2.4 Conclusions

A narrow summary of the literature on the fabrication and antimicrobial activity of nanoparticles has been presented in this section. While much work has attempted to determine how metal nanoparticles suppress or kill bacteria, there exists no field-wide consensus on the most important or true mechanisms. A lack of mechanistic understanding makes it challenging to understand which physiochemical parameters make metal nanoparticles maximally effective. More work therefore remains to be done in the generation of nanoparticles with specifically targeted physiochemical characteristics ideal for use in antimicrobial applications. The synthesis of metal nanoparticles using cost effective and eco-friendly methods has also been highlighted. Biopolymers, and particularly cellulose nanocrystals, show promise for use in the generation of controlled metal nanoparticles. CNC-capped silver nanoparticles have been successfully generated through a variety of methods, and more work remains to be done on the synthesis of other metal nanoparticles using CNC. This thesis work aims to contribute to the fabrication of maximally antimicrobial and sustainable metal nanoparticles both by furthering the mechanistic understanding of antimicrobial nanoparticles using data mining and meta-analysis, and by developing novel preparation methods for CNC-capped metal nanoparticles that have antimicrobial activity.

Chapter 3: Determining Critical Physiochemical Properties Affecting Antibacterial Activity of Metal Nanoparticles: A Meta-Analytical Approach

3.1 Introduction

Within the last century, antibiotics have become the primary treatment for harmful bacterial infections. Most antibiotics are developed by exploiting the natural ability of specific bacteria to produce secondary metabolites that play a role in defending against competing microbes [94]. These compounds are identified and isolated from the bacteria based on their toxicity towards select human-infecting microorganisms, and then reproduced on the mass-scale as antibiotics to combat infection. Because antibiotic chemicals are synthesized by bacteria themselves, small portions of bacterial populations may naturally evolve to contain mutations that result in antibiotic resistance. In recent years, high rates of antibiotic use have allowed the propagation of resistant strains, some of which are virtually untreatable with currently developed antibiotics [95]. In response to this crisis, ways to manage and mitigate bacterial infection are being developed.

Metal nanoparticles (MNPs) are well known to be antimicrobial, and could play a major role in addressing drug resistant infections. MNPs have already been extensively investigated for their antibacterial properties, with nearly 14,000 publications on the subject in 2019 alone. Additionally, numerous reviews have been compiled to distill the vast body of literature on the efficacy of MNPs [96]–[98]. There is a myriad of pathways through which MNPs are proposed to exert cellular toxicity, though there remains no consensus on which pathways are most true or most important. Until the activity of MNPs is better understood, it will be very challenging to design optimally bactericidal MNPs, limiting the scope of their clinical application.

While there is yet to be agreement on a singular bactericidal mode of action, there are a number of widely referenced hypotheses. One commonly cited mechanism suggests that there are electrostatic interactions between positively charged metal ions and the negatively charged cell membranes of microorganisms [99], [100]. The adsorption of metal ions on the surface of

bacterial cells may damage the phospholipid bilayer of Gram negative bacteria [101] or the peptidoglycan layer of Gram positive bacteria [36]. Negatively charged metal nanoparticles may also be attracted to positive residues found in many bacterial membrane proteins [35], and MNPs adsorbed to bacteria have been shown to induce pits in the membrane, indicating severe damage [31], [32].

Another hypothesis is that metal ions leached from nanoparticles can infiltrate bacterial cells and cause damage to integral proteins or organelles within the cell. Silver ions have been shown to chelate sulfur-containing or phosphorous-containing compounds such as DNA, preventing cell replication [35]. Likewise, copper ions have been found to significantly damage or destroy bacterial DNA [44]. In addition to direct damage caused by chelation, released metal ions (as well as MNPs themselves) can generate reactive oxygen species (ROS), which induce oxidative stress and eventual apoptosis [102].

All proposed routes of MNP toxicity depend heavily on the nanoparticle's specific physiochemical properties, such as metal type, size, surface charge, and attached surface ligands. MNP size and exposed crystalline face are known to affect catalytic activity, dictating which ROS byproducts are produced [103], [104]. The surface charge of MNPs also dictates their colloidal stability, preventing agglomeration and helping nanoparticles retain high specific surface area [105]. This in turn may affect the catalytic behavior of the nanoparticles and the magnitude of ion dissolution from their surface [106].

Some studies have sought to correlate fundamental physiochemical characteristics of MNPs, such as size or surface charge, with their antimicrobial performance [35], [107], [108]. However, there are so many permutations of metal type, size, charge, capping agent, and post fabrication functionalization that it is impossible to ascertain, at the bench level, whether a single

physiochemical characteristic dominates the response. Only a few studies have attempted to create a library of nanoparticles and understand their biological activity, and those have focused solely on the effects of MNPs on eukaryotic cell lines, not bacteria [46].

In addition to the challenge posed by the vast variance in physiochemical properties that may influence MNP's antimicrobial activity, the cross comparability of individual MNP studies is low due to a lack of standardization in the testing of the MNPs. There are several common in vitro testing methods for evaluating antimicrobial efficacy, including broth dilution tests, such as minimum inhibitory concentration (MIC) or minimum bactericidal concentration (MBC), and zone of inhibition (ZOI) tests, such as disk diffusion or well diffusion [109]. While these tests are often assumed to be comparable in evaluating the overall performance of MNPs, broth MIC and MBC tests measure the dilution (or dose) of the MNPs, whereas ZOI tests measure the diffusion of the MNPs, rendering them incomparable.

The actual interaction of the MNPs with the testing method chosen also must be considered before comparability can be assumed. In ZOI tests, if a compound being tested has poor solubility in the chosen agar, the test may incorrectly show low or no efficacy [110], [111]. ZOI tests were developed for antibiotic molecules, which can be an order of magnitude smaller than MNPs. Most nanoparticles have comparatively low diffusivity in the ZOI tests, and only soluble ions that are released from the nanoparticles will be able to participate in antibacterial activity. Dilution techniques such as MIC and MBC are therefore generally considered more robust, but the specific assay set-up can still influence the measured efficacy of MNPs. The chosen incubation broth, initial inoculum size, and specific strain of the bacterial model have all been shown to affect the measured efficacy of MNPs [112]–[114].

The massive heterogeneity in the literature on metal nanoparticles makes it incredibly challenging to identify real trends in what makes a nanoparticle an effective antimicrobial agent. To determine what MNP properties are likely influential, we employ a meta-analytical technique, which is a process that systematically combines the results of hundreds of studies and allows for significantly increased statistical explanatory power. Meta-analysis has very recently been used to predict the interactions of select nanomaterials with eukaryotic models [115], [116], but to the best of our knowledge, no one has undertaken this work with antibacterial MNPs. The goal of this meta-analysis is therefore two-fold: to determine how well standardized the field currently is (in essence, to understand the cross comparability of the knowledge that has been generated), and to identify statistically robust trends around the influential physiochemical properties of antimicrobial MNPs. This in-depth analysis may also provide a starting point to make the case for the necessity of standardization in antimicrobial MNP testing.

3.2. Experimental Procedure

3.2.1 Initial article collection

Peer reviewed original articles on antimicrobial metal nanoparticles published between January 2015 and January 2019 were collected from Web of Science using advanced topic search. For each of the four metals of interest (silver, copper, gold, and zinc), a search was performed to find articles whose topics included reference to both a metal nanoparticle and antimicrobial activity. Variance in reporting language was accounted for in the search by including multiple potential search terms for each topic (searching antibacterial OR antimicrobial, silver OR Ag). In total, the initial search yielded 9252 articles across the four metals, which were further assessed for inclusion in the qualitative and/or quantitative meta-analysis.

3.2.2 Dataset refinement and inclusion criteria

All identified articles were screened for relevance and reliability before being included in the meta-analysis, as detailed in Scheme 1. The systematic screening process followed methods previous laid out for use in meta-analysis [117]. Following initial article identification, the author defined keywords of all articles were compiled and assessed for mention of both metal nanoparticle(s) and antimicrobial activity. Of the original 9252 potential articles identified, 2907 contained keywords relating both to metal nanoparticle(s) and antimicrobial activity. These 2907 articles were then manually screened for relevance to the meta-analysis. Publications were considered relevant if they (1) reported on a single, unmodified metal nanoparticle (i.e. not multimetallic, not loaded with additional antimicrobial agents, not incorporated into a composite), and (2) included a quantitative assessment of the antimicrobial performance of said nanoparticle. Only articles that utilized a minimum inhibitory concentration (MIC) assay were considered eligible for use in the quantitative analysis, to minimize heterogeneity and allow for reasonable cross-comparison between articles. The 113 articles [33], [106], [110], [111], [117 – 221] To prepare the data for analysis, each article was divided into individual records containing one nanoparticle evaluated against one strain of bacteria. Articles yielded between 1 and 18 records each, with modal value of 4 records per article, for a total of 398 records.

Scheme 3.1. Selection process for article identification through inclusion.

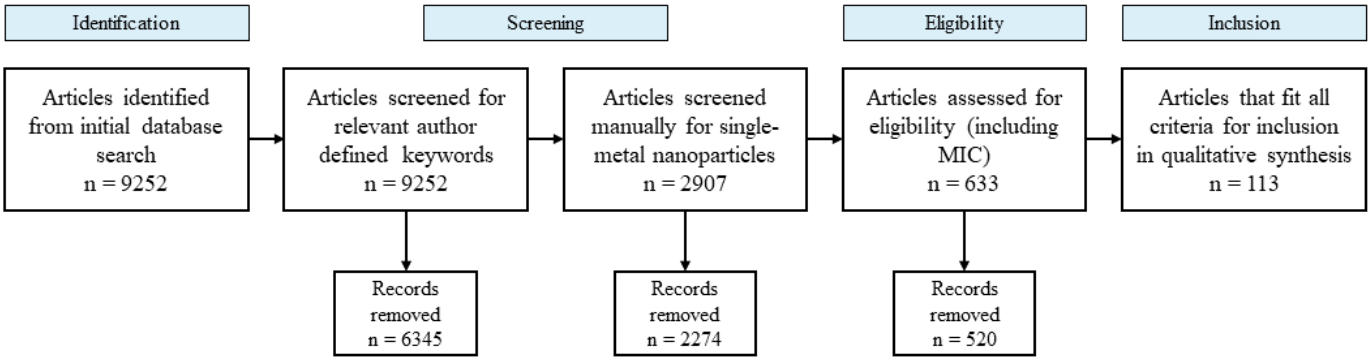

All articles that were included in the qualitative analysis were manually assessed, and data was extracted on both physiochemical characteristics of the nanoparticle and testing parameters for antimicrobial performance. A total of 15 variables – 6 continuous and 9 categorical – were documented for each article mined. The physiochemical properties noted were nanoparticle type (silver, copper, gold, or zinc), capping agent used during synthesis (grouped into either plant extract, cell culture extract, or others), nanoparticle size (in nm) as well as the size evaluation method (TEM, DLS, or others), nanoparticle shape, and nanoparticle surface charge as measured by zeta potential (in mV). For the MIC assay parameters, broth formulation (Mueller Hinton, Nutrient Broth, Luria Bertani, Tryptic Soy, or others), incubation time and temperature (in h and ˚C respectively), inoculum size (in colony forming units per mL), and nanoparticle minimum inhibitory concentration (in number of particles per mL) were catalogued. Lastly, information on the bacterial species, Gram type, and specific strain was collected.

In addition to raw data, grouping variables were added to improve comprehension and allow for the identification of overall trends. These grouping variables included capping agent type (divided simply into plant-based synthesis, cell culture-based synthesis, and others) and the gram type of the bacteria. An ‘unknown’ designation was given for any single category not reported within a paper. The units for numeric categories of size, zeta potential, MIC, time, temperature, and inoculum size were standardized to nm, mV, µq/mL, h, ˚C, and number of colony forming units (# CFU) respectively. CFU values were additionally normalized using the natural log transform (ln(X+1)) prior to analysis.

3.2.3 Statistical analysis

All statistical analysis was performed using Systat 13. Simple descriptive statistics were used to understand the trends in information reported, including the range of continuous variables and the frequency with which each variable was reported. ANOVA testing was used to determine differences in mean values for cross-comparative analysis and was performed for any population with greater than 5 records. ANOVA results were considered significant when $p < 0.05$. Linear regression was used to correlate physiochemical parameters with antibacterial efficacy. For data quality control during the building of regression models, any records with standardized residuals of > 5 were considered outliers and discarded, after which regressions were recalculated. This process continued iteratively until no outliers remained. All regression fits were linear, with 95% confidence bounds. Regression results (slope fit) were considered statistically significant when $p < 0.05$.

3.3 Results and Discussion

3.3.1 Literature search & data extraction.

Original research articles published over a four-year span on silver, copper, gold, or zinc antimicrobial metal nanoparticles (MNPs) were identified using the Thomson Reuters Web of Science database. 9252 articles were initially identified as potentially relevant (see Methods), the majority of which (73%) reported on silver nanoparticles, followed by those that reported on zinc (14%), gold (7%), and copper (6%) MNPs. The texts were assessed to determine the antibacterial assay used. A majority of the papers initially identified from the literature (60%) used some form of ZOI test, such as disk or well diffusion, while only 20% of the articles reported an MIC test. A small minority of studies used more qualitative methods such as growth kinetics (4%) or plate streaking (3%) as their primary method of evaluation, and singular papers assessed antimicrobial activity through other techniques such as live/dead staining, flow cytometry, and cellular

respiration quantification. Zone of inhibition tests are likely the most common evaluation method due to their relative ease of use and comparatively low cost. However, ZOI tests are qualitative, not quantitative, so they cannot be directly used when trying to compare the relative efficacy of two separate studies [223]. Additionally, the solubility of the metal [111] in the chosen agar can drastically decrease or eliminate the measured inhibition zone of an otherwise antimicrobial MNP. Thus, only studies that employed an MIC test were included in the quantitative dataset. These articles were further assessed to determine reported information on the physiochemical characteristics of the MNPs fabricated, the MIC assay parameters used, and the bacterial models (reported in Figure 3.1).

3.3.2 Trends in antimicrobial nanoparticle evaluation and reporting.

While MIC broth dilution tests are considered to be more robust than ZOI tests, large variance in the specific methodological parameters used in individual studies was noted, which poses a significant barrier to rigorous cross-comparison of antimicrobial MNP studies. Standards for broth dilution methodologies have already been developed [224], but the adherence to these protocols is currently low in the field. Less than 8 percent of the articles considered in this study both provided a complete report on the utilized testing set-up and followed a standard protocol. Determining which studies are maximally cross-comparable is hindered by the vast number of reports that do not provide full and complete details on the nanoparticle synthesized, the experimental set-up used, or the model organism(s) tested. Only 27.75% of the articles considered in this study reported all 15 variables of interest, while 35.85% were missing one value, 23.58% were missing two values, and 19.81% were missing three or more values. The most commonly underreported variables were the surface charge of the synthesized nanoparticle (measured with zeta potential or otherwise), the number of colony forming units in the initial bacterial inoculum, and the specific strain of the model bacteria tested. All three of these

commonly unreported factors have been shown to affect the observed antimicrobial efficacy [112], [113], [225], suggesting that without report of these factors, it is impossible to understand the true behavior of a nanoparticle studied.

Going forward, a standardized characterization and reporting protocol is suggested to ensure studies are similar enough for meaningful cross comparison. At minimum, nanoparticle material characteristics including the metal type, nanoparticle size, nanoparticle shape, capping agent used, and surface charge should be reported. The testing environment parameters, including the broth type used, the initial bacterial inoculum size, the time and temperature of incubation, and the concentration(s) of nanoparticles tested should also be reported. Lastly, the

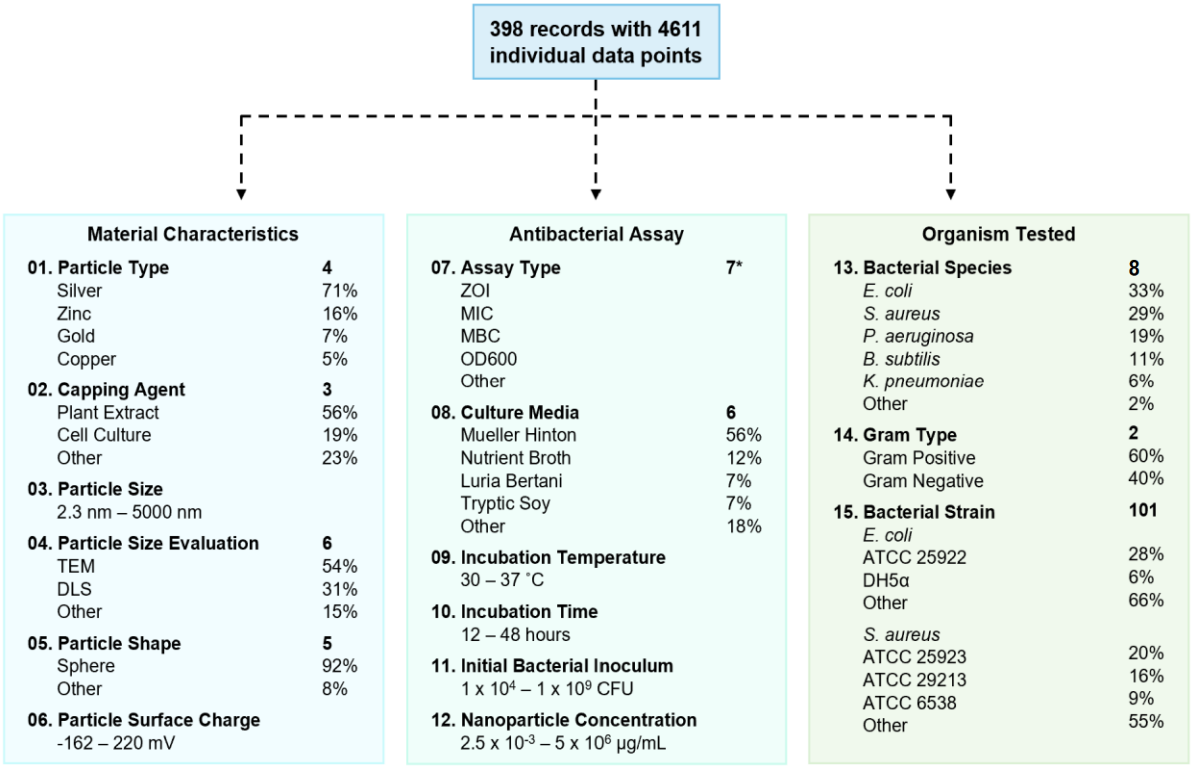

*Figure 3.1: Summary of information on nanoparticle's physiochemical characteristics, antibacterial assay used, and bacterial models tested for publications included in the quantitative dataset. For categorical variables (1-2, 4-5, 7-8, & 13-15), the total number of categories for that variable is bolded, and the percent of the population belonging to the most frequent categories are provided (*n/a for assay type, which encompasses all publications mined). For all continuous variables (3, 6, 9-12), the complete range as pulled from the quantitative dataset is presented.*

species and specific strain of the bacteria tested for susceptibility should be considered and reported.

3.3.3 Cross-comparative analysis of silver, copper, gold, and zinc antimicrobial MNPs.

For all metal types, the three most commonly used model bacteria were *E. coli*, *S. aureus*, and *P. aeruginosa*, representing 33.1%, 28.6%, and 19.1% of the overall records respectively. *E. coli* is frequently used as a model Gram-negative bacterium, and *S. aureus* holds the same status for Gram-positive bacteria. *P. aeruginosa*, another Gram-negative bacteria, is a clinically relevant target for nanoparticle therapy, as this bacteria is naturally highly drug resistant [226], [227].

*Table 3.1: Average minimum inhibitory concentration (in µg/mL) for four highly reported types of metal nanoparticles and two broad spectrum antibiotics. * signifies the value is significantly different from silver for the same bacterium, $p < 0.01$.*
*** signifies the values is significantly different from silver for the same bacterium, $p < 0.001$. n/a indicates too few data points for analysis.*

	Antimicrobial Nanoparticle MIC (µg/mL)				Antibiotic MIC (µg/mL)	
Bacteria	**Silver**	**Copper**	**Gold**	**Zinc**	**Imipenem**	**Ciprofloxacin**
E. coli	32.9 ± 65.9	83.2 ± 55.6	91.6 ± 90.1	124.4 ± 110.4 *	0.628 ± 0.795 **	0.024 ± 0.020 **
S. aureus	15.4 ± 15.4	71.6 ± 71.1	116.7 ± 104.7	116.6 ± 96.3 *	0.067 ± 0.041 **	0.375 ± 0.177 **
P. aeruginosa	13.7 ± 9.8	n/a	188.5 ± 212.6	98.4 ± 66.7 *	3.47 ± 1.58 **	0.508 ± 0.351 **

The variance in MIC values derived from the literature was high for all four metal types, irrespective of the bacterial species used as a model. The average MIC value for silver MNPs in this study did not differ significantly from the average MICs of copper or gold MNPs ($p >> 0.05$), but it is not possible to determine from simple aggregate analysis whether the lack of significant difference in MIC between silver, copper, and gold is because metal type is not a driving factor in antimicrobial activity, or because of confounding factors adding noise to the system. Zinc MNPs, in contrast to copper and gold, were found to have a statistically significantly higher average MIC value than silver for all bacterial species tested ($p < 0.01$),

despite the high levels of variance in the datasets. Zinc can therefore be concluded to be a less effective antimicrobial material than silver.

While silver nanoparticles do display the lowest average MIC value, a significant difference in performance of silver MNPs when compared to traditionally used antibiotics was found, as seen in Table 1 ($p < .001$). Ciprofloxacin and imipenem, two broad-spectrum medications belonging to two different classes of antibiotics (quinolone antibiotics and carbapenem antibiotics respectively), have reported MIC values that often fall well below 1 µg/mL, depending on bacterial species and strain tested [228]–[241]. Further improvement to the antimicrobial efficacy of MNPs on a per mass basis will be an important milestone in achieving medically translatable antimicrobial treatments using MNPs.

3.3.4 Determining influential physiochemical characteristics of silver MNPs.

Physiochemical parameters such as MNP size and surface charge have previously been proposed to influence the antimicrobial efficacy of a nanoparticle. However, the very disparate nature of individual MNPs that have been fabricated and tested makes it challenging to draw reliable proof from the literature. To increase the explanatory power of the work that has been done, this study sought to evaluate the effect of physical parameters on antimicrobial activity (as measured with minimum inhibitory concentrations) from a meta-analytical standpoint. Studies were considered as singular records of a physiochemical parameter and an MIC value, and the aggregate data from multiple articles was analyzed using linear regression techniques.

As regression techniques are more reliable and more effective with larger bodies of data, regression analysis was only performed using data on silver MNPs that were tested against E. coli or S. aureus models of any strain, as these combinations of metal type and bacterial model constituted the vast majority (71%) of the publications available in our dataset. Not all data is

equally valuable, so to control for assumed rigor, only the papers that reported all 14 experimental variables (those described in Fig. 1) were included. With all these considerations, 57 records were included in the initial dataset. Prior to final analysis, data quality control was performed, and any record with a reported MIC value that lay 3 standard deviations or more away from the mean, or with a residual value greater than 5 in a simple one variable regression model, were considered outliers and removed. This process was repeated iteratively until there were no outliers, leaving a final set of 48 records on antimicrobial silver nanoparticles to be analyzed. It is worth noting that the data set for regression analysis naturally contained a much more normal and homogenous group of studies than the total set originally mined from the literature. The range of MIC values in the final set was 10 to 58 μg/mL, the range of surface charge (zeta potential) values was -58 to -10.5 mV, and the range of MNP size values was 0.78 to 32 nm in diameter.

Nanoparticle size had a significant effect ($p < .0001$) on the measured MIC for *E. coli*. As seen in Fig. 2A, there is a positive relationship between size and minimum inhibitory concentration, demonstrating that smaller nanoparticles are more effective against E. coli, and potentially against Gram-negative bacteria at large. The measured R^2 value of 40.3% shows that despite the heterogeneity of the specific MNPs included in the analysis, over 40% of the variance in results is driven exclusively by nanoparticle size. 96.2% of the observed data points fell within the prediction limits of the size-only model, showing very good agreement between the model and the literature-derived values. In stark contrast to this result, nanoparticle size was not a statistically significant predictor of MIC for *S. aureus* when using the same model.

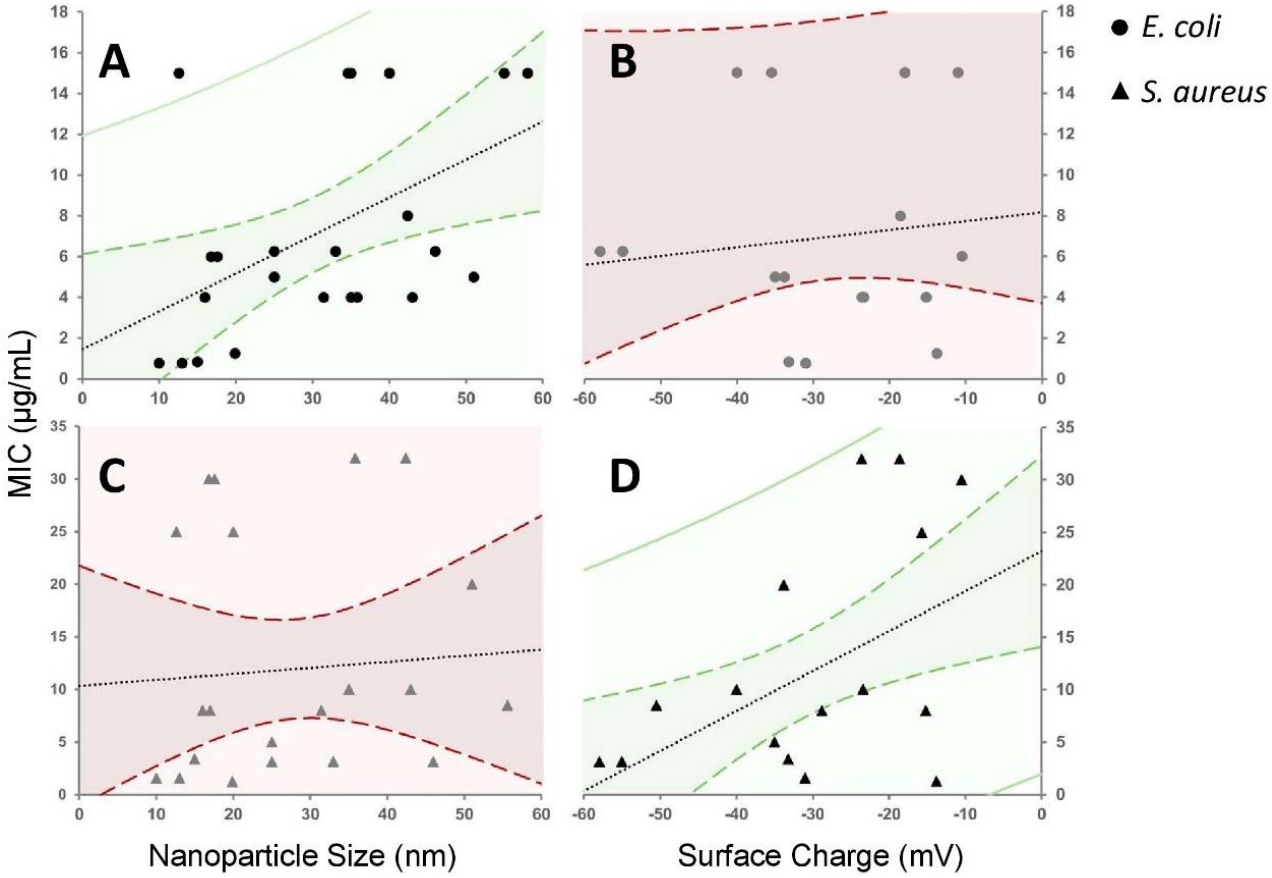

Figure 3.2: Linear regression models correlating antibacterial efficacy, as measured by minimum inhibitory concentration, with nanoparticle size (A and C) and surface charge (B and D). Black dotted lines represent regression lines of best fit, dashed colored lines represent upper and lower confidence intervals (95% confidence), and solid colored lines represent upper and lower prediction intervals. Models highlighted in green where a statistically significant correlation exists.

Nanoparticle size has previously been proposed as a driving factor in determining MNP antimicrobial activity, with the assumption that smaller nanoparticles are broadly more effective against all types of bacteria. A number of studies [242], [243] have suggested that the MNPs must be below a critical size (for example, 10 nm in diameter) to cross a bacterial cell membrane and damage the cell directly. MNP size has also been shown to modulate the interaction of the nanoparticle with biological molecules. It has also been shown that for very small MNPs, complex protein adsorption occurs almost instantly in *in vivo* like conditions [244], and the proteins adsorbed change the extent of the nanoparticle/bacterial interaction [245]. However, very little previous work exploring the relationship between nanoparticle size and antimicrobial

efficacy has considered the effect of Gram type as a driving factor. The aggregate data from this study clarifies the linear correlation of MNP size with MIC when tested against *E. coli*, but not *S. aureus*, indicating that a physiochemical characterization alone is not sufficient to describe how size influences the antibacterial efficacy. Rather, the specific characteristics of the bacteria, most notably the Gram type, play a simultaneous role.

The effect of MNP surface charge was also explored with a single variable regression. For *E. coli*, no statistically significant trend was observed, suggesting that surface charge does not dictate the effect of MNPs when used against Gram-negative bacteria. However, a very strong linear dependence was shown for *S. aureus* ($p < .005$), where more negatively charged particles are much more effective than less negatively charged particles. The model fit (R^2) was found to be 30.1%, indicating that a third of the variability in MNP efficacy can be explained singularly by surface charge. It is of note that the dataset did not include any MNPs with a positive surface charge, so it is not possible to determine from this model whether the greater effect of more negatively charged particles is due to the increasing negativity or the increasing magnitude of charge.

As with size, surface charge has previously been proposed to affect the activity of nanoparticles against bacteria. When comparing nanoparticles with zeta potentials that are highly positive or highly negative, the more positively charged nanoparticles are found to be most effective. It is commonly proposed that the increased efficacy of positively charged particles is due to the stronger electrostatic interactions between the particles and the negatively charged bacterial cells. However, very little research has been done on the effect of magnitude of charge, particularly in negatively charged particles, despite the fact that most metal nanoparticles are negatively charged unless specific positive charge is otherwise induced. The effect of surface

charge on the Gram selectivity of nanoparticles has only recently been explored, and only for mixed or positively charged nanoparticles [108].

In addition to singularly looking at size and surface charge regression, multivariate models were built to explore the interaction between these parameters. An additive model of size and surface charge was built, effectively allowing each parameter to be understood while the other was controlled for. The additive model of size and surface charge did not differ in significance or fit from the size model for *E. coli*, increasing the evidence that size is the most important physiochemical parameter for Gram-negative bacteria. However, the additive model for *S. aureus* had an improved R^2 of 44.6%, up almost 15% from the single variable surface charge model. Additionally, in the additive model, both size and surface charge were statistically significant ($p < 0.05$ and $p < 0.001$ respectively). This suggests that while surface charge does dominate the response, size may also play a smaller but significant role for MNPs used against Gram-positive bacteria.

3.4 Conclusions

Meta-analysis was performed on data mined from the literature over a five-year span to determine the trends in testing and reporting on antimicrobial metal nanoparticles. Simple aggregate analysis shows that silver nanoparticles are statistically more effective than zinc oxide nanoparticles at killing or suppressing both Gram-negative and Gram-positive bacteria, but that there is not a significant difference in the antimicrobial activity of copper or gold particles when compared to silver. It is not possible to determine whether metal type would emerge as a driving factor in antimicrobial activity when the heterogeneity in testing and reporting protocols is minimized.

Nanoparticle size is a defining factor in predicting the antimicrobial activity of silver NPs against Gram-negative bacterium ($p < 0.0001$). The compiled papers indicate a positive correlation between size and MIC (R^2 of 40.3%), where smaller MNPs are more effective and thus require lower concentrations to inhibit bacterial growth. In contrast, size alone is not shown to affect the MIC of silver NPs against Gram-positive bacteria. Differences in the cell wall and membrane structures of these bacteria may modulate the bactericidal mechanism(s) of MNPs. Surface charge does not show any significant correlation with MIC for Gram-negative bacteria. However, the efficacy of silver MNPs against Gram-positive bacteria is considerably affected by zeta potential ($p < .005$) where highly negative MNPs require lower concentrations to inhibit bacterial growth than less negative MNPs. Interestingly, multivariate regression using both size and surface charge as independent variables creates a more rigorous model (R^2 of 44.6%), indicating that the antibacterial efficacy of MNPs against Gram positive bacteria is dominated by charge, but is also somewhat affected by the size of silver NP used.

Due to the sheer number of papers that did not report significant material and testing parameters (such as surface charge, number of bacterial colony forming units used in the inoculum, and the specific bacterial strain tested), more intricate analysis is not possible. It is critical that common antimicrobial testing and reporting methods are adopted, to allow further insight on the exact mechanisms of MNP antimicrobial activity to be obtained. This study demonstrates that while improvement in standardization is needed, meta-analytical techniques can still be employed to successfully generate new knowledge by data-mining and analyzing the current literature.

Chapter 4: Synthesis and Characterization of Copper-, Silver-, and Copper/Silver-Cellulose Nanocrystal Composites with Antimicrobial Activity

4.1 Introduction

The green synthesis of metal nanoparticles is very desirable to reduce cyto- and ecotoxicity and increase their range of applications. A large body of work on the synthesis of metal nanoparticles using living cells [246]–[248], cell culture extract [249]–[251], and plant extracts [252]–[254] has been generated in the past decades. Of particular interest is the fabrication of metal nanoparticles using cellulose nanocrystals as an ecofriendly substrate. Cellulose nanocrystals (CNC) can be derived from plant matter, bacteria, and tunicates, and have been shown to have no toxicity to human cells [255]. Additionally, they have desirable physical properties such as good dispersibility [256] and high mechanical strength [257]. CNC derived from acid-hydrolyzed wood pulp has been shown to be highly effective at coordinating nanoparticles [86], where the hydrolysis-generated sulfate half ester groups act participate in nanoparticle capping and the abundant hydroxyl groups participate in the capture of metal ions [90].

Much work has been done on the preparation of cellulose nanocrystal-bound metal nanoparticles, for applications such as food packaging [258], [259], sensing [260], [261], water purification [262], and catalysis [89], [91]. Antimicrobial metal and CNC composites have also been developed through a variety of routes, including hydrothermal synthesis [263] and chemical reduction [264]. However, much of this work involves the use of toxic or environmentally harmful reducing agents, such as sodium borohydride [8], or non-biodegradable polymers, such as polyethylenimine [265]. This precludes these composites from being considered completely green and increases the risk of downstream cyto- or ecotoxicity.

The development of more sustainable metal/CNC composites has been recently explored, using natural compounds for both the reducing and capping of metal nanoparticles. Shi and coworkers [266] developed a silver and CNC composite by coating polydopamine, a mussel-associated polymer, onto the CNC surface [99]. The abundance of catechol groups in

polydopamine were able to successfully coordinate with and reduce the silver ion precursor to silver nanoparticles, resulting in a multitude of well dispersed nanoparticles on the CNC surface.

While this is a relatively effective strategy, the polymerization of polydopamine from dopamine requires a significant time period, which limits the scalability of the product. In this work, a similar one-pot reduction method was employed, with tannic acid used as the CNC coating instead of dopamine. Tannic acid is a plant derived polyphenol, and has previously been used as a coating in biomedical applications due to its biodegradability and self-coating behavior [267]. Tannic acid has also been extensively used in the synthesis of metal nanoparticles, and can act as both a reducing and capping agent [268].

In this chapter, metal nanoparticles were deposited on tannic acid-coated cellulose nanocrystals using a simple one-pot chemical reduction method. The impact of fabrication parameters was explored, and the order of reagent addition was found to have a strong influence on the final morphology of the composite. The generated copper/CNC and silver/CNC composites had high colloidal stability, and the metal nanoparticles were found to be very small (<10 nm average in diameter), which indicates that they may be promising for antimicrobial application. Additionally, the same one-pot system can be used to reduce copper and silver onto CNC simultaneously, demonstrating a desirable versatility.

4.2. Experimental Procedure

4.2.1 Materials

Cellulose nanocrystals, with length of 100 to 200 nm and width of 5 to 20 nm, were donated by CelluForce Inc. Tannic acid ($C_{76}H_{52}O_{46}$) , silver nitrate ($AgNO_3$), copper sulfate ($CuSO_4$), and sodium hydroxide (NaOH) pellets were purchased from Sigma-Aldrich and used as received. Milli-Q water (resistance of greater than or equal to 18 MΩ cm) was used as the sole solvent for all procedures, and was generated by a Millipore Mill-A purification system.

4.2.2 One Pot Preparation of Metal/CNC/Tannic Acid Composites

Cellulose nanocrystals (CNC) were mixed into 15 mL of Milli-Q (MQ) water at a concentration of 0.01 wt% with a vortex mixer and thoroughly dispersed via bath sonication for 25 minutes at 10˚C. Powdered tannic acid (0.255 g) was dispersed in 15 mL of MQ water (a concentration of 1 mM) with vigorous shaking and vortex mixing. Stock solutions of metal salt precursors (either $CuSO_4$, $AgNO_3$, or an equal combination of the two) were dispersed in MQ water with vigorous shaking and vortex mixing. The CNC and tannic acid solutions were combined with vortex mixing, and then the pH of the CNC/tannic acid solution was adjusted to 9.0 used aliquots of freshly prepared 1.0 M NaOH solution. The CNC/tannic acid was then transferred to a round bottom flask and heated to 50˚C under stirring at 400 RPM. Metal salt precursor solution was added dropwise to the CNC/tannic acid solution to achieve a molar ratio of 0.06 (for copper) or 0.03 (for silver or copper/silver), following the procedure for rapid generate of metal nanoparticles with tannic acid previously laid out [269]. The reaction began immediately, and was allowed to proceed for 4 hours at elevated temperature. The metal/CNC/tannic acid solution was then centrifuged at 4250 RPM for 30 minutes, and the supernatant was decanted. The pellet (containing the CNC-bound metal nanoparticles) was re-dispersed in fresh MQ water and stored for further use.

4.2.3 Composite Characterization

4.2.3.1 UV-Visible Spectra

A UV-Visible Spectrometer was used to generate spectra from 200 to 800 nm. All samples were prepared in MQ water at a 0.1 wt% concentration, and bath sonicated for 2 minutes directly prior to measurement. Scans were performed at room temperature and latent pH. Each spectrum was normalized based on the broadband scattering peak of cellulose nanocrystals from that sample.

4.2.3.2 Hydrodynamic Size and Zeta Potential

Hydrodynamic size and zeta potential (ZP) were both determined using a Malvern Nano-ZS90 Zetasizer. Samples were diluted to a 0.1 wt% (w/w) concentration in MQ water and bath sonicated for 2 minutes directly prior to measurement. Hydrodynamic size was determined using single angle (90˚) dynamic light scattering at room temperature. Zeta potential was determined based on electrophoretic mobility at room temperature. All measurements were taken 5 times and the average is presented.

4.2.3.3 Transmission Electron Microscopy

Samples were diluted to a concentration of 0.1 wt% (w/w) in MQ water and bath sonicated for 30 minutes at 10˚C to assure dispersion. 25 µL of sample was drop-cast on a carbon-coated copper grid (200 mesh) and allowed to dry for 24 hours in ambient conditions. A Philips CM 10 transmission electron microscope with a 60 kV accelerating voltage was used to take all images. All image analysis was performed using ImageJ software. Nanoparticle sizes derived from ImageJ software represent the average value no less than 100 particles.

4.2.3.4 Scanning Electron Microscopy

Samples were diluted to a concentration of 0.1 wt% (w/w) in MQ water and bath sonicated for 30 minutes at 10˚C to assure dispersion. 25 µL of sample was drop-cast on a new silicon wafer chip and allowed to dry for 24 hours in ambient conditions. The wafer was coated in a thin layer of gold (thickness < 5 nm) using a simple sputter-coating process to improve conductivity of the samples. An FEI Quanta Feg 250 Environmental scanning electron microscope with EDX was used to take all images.

4.2.3.5 Antifungal Testing

Active dry yeast (*Saccharomyces cerevisiae*) was used as the model organism for antifungal testing. Yeast was added to deionized water at 37˚C under stirring to disperse, and glucose was added to the solution to prompt activation and respiration. The extent of fungal respiration was

measured as carbon dioxide produced (in mL) using simple water displacement. A small aliquot of metal/CNC/tannic acid sample (1 mL, 0.025 wt% w/w) was added to the flask, and the rate of respiration (CO_2 produced over time) was tracked for a 25 minute period. Control experiments were performed using the same protocol, but with 1 mL of deionized water added instead of sample.

4.3 Results and Discussion

4.3.1 Characterization of Copper/CNC Nanoparticles

Copper nanoparticles bound to nanocellulose substrates were successfully fabricated using a simple one-pot chemical reduction method. Copper sulfate ($CuSO_4$) was used as the metal salt precursor, tannic acid (TA) was used as the reducing agent, and cellulose nanocrystals (CNC) were used as the capping agent. Tannic acid, a plant polyphenol, has been shown to be an effective reducing agent in the synthesis of a variety of metal nanoparticles, as each molecule can donate up to 20 electrons to reduce a metal cation [270]. When dispersed in water, tannic acid undergoes partial hydrolysis, exposing gallic acid moieties that act as reductants, and glucose moieties that act as weak capping agents under basic conditions [268]. For complexation with a metal cation, the gallic acid units must be deprotonated, which occurs around pH 8 and above [271], [272].

Previous studies have been undertaken to coat cellulose nanocrystals with tannic acid and with other catechol-containing monomers such as dopamine [273], [274]. While the exact interaction is not well understood, it has been shown that the oxidized phenolic moieties of tannic acid can react with the cellulose nanocrystals to form strong bonds, which may be based on covalent, hydrogen, or π–π stacking interactions. To induce a strong coating, the pH of the tannic acid and CNC solution in this study was adjusted to 9 using freshly prepared 0.1 M NaOH. Copper sulfate was then added to the basic tannic acid/CNC solution and allowed to react

to form copper oxide particles on the surface of the CNC. The presence of tannic acid on CNC and the formation of copper nanoparticles were monitored using UV-visible spectroscopy (Figure 4.1). The UV-visible spectrum of tannic acid is highly pH dependent, and at pH 9, it shows two characteristic peaks around 235 and 323 nm [275]. The tannic acid/CNC solution at pH 9 generated in this study showed peaks at 254 and 358 nm, indicating relatively good agreement with the literature. The composite with copper nanoparticles shows one primary peak at 285 nm, which is characteristic of the surface plasmon resonance peak displayed by copper oxide nanoparticles [276], [277]. Additionally, a small shoulder at 358 nm can be seen, which is indicative of a small amount of unreacted tannic acid remaining in the system. According to Mie's theory, the presence of only one metal-associated peak indicates that the copper oxide particles are spherical in shape. [278]

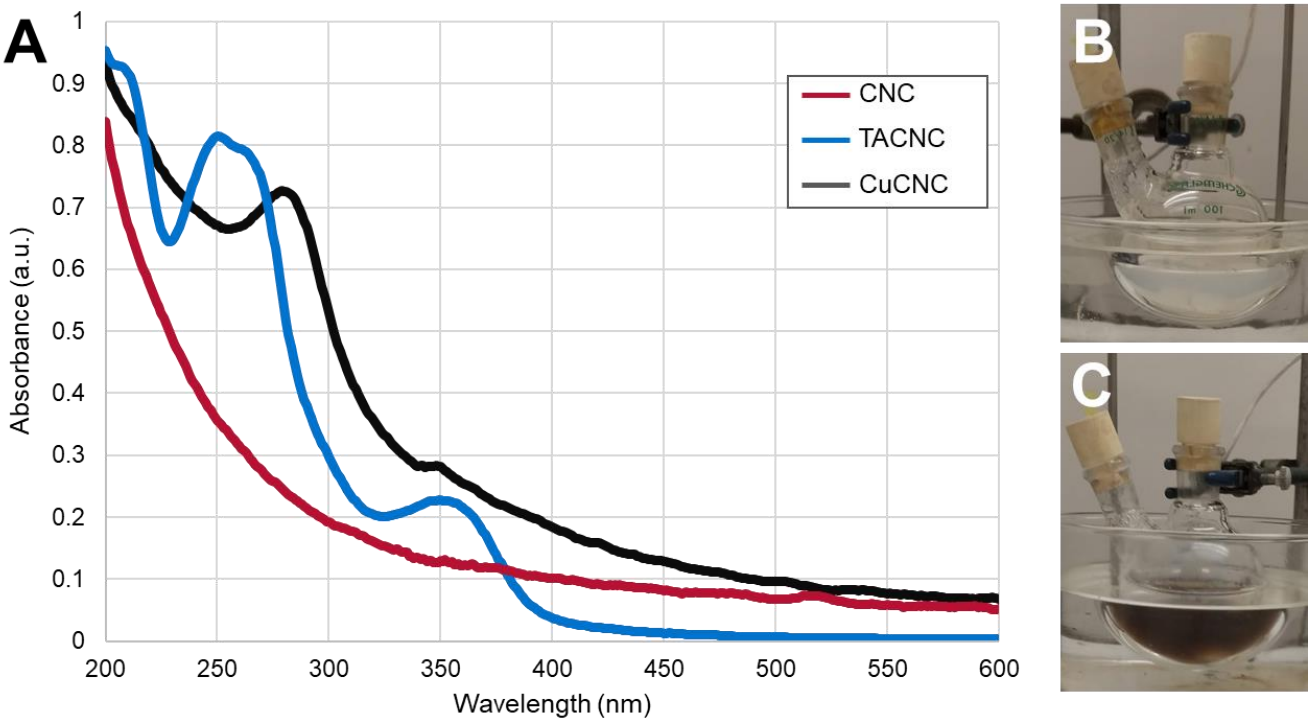

Figure 4.1: UV-Visible spectra taken at room temperature and native pH for pristine CNC (red), tannic acid coated CNC (blue), and copper-nanoparticle coated CNC (black) (A). Photographs of CNC (B) and CuCNC (C) dispersions.

The copper/tannic acid/CNC composites (CuCNC) were stable after 5 months storage in ambient conditions, with no obvious precipitation and no shift in UV-vis spectrum (indicating metal nanoparticle aggregation or agglomeration). The high stability is attributed in large part to the colloidal stability of cellulose nanocrystals, which bear highly negative surface charges, and thus experience high electrostatic repulsion. The stability of the system was probed using zeta potential measurements. A pristine CNC suspension had a zeta potential of -43.6 mV, which shows good agreement with previous literature [266]. The zeta potential of the CuCNC composite was -25.6 mV, which is still high enough to have good colloidal stability. In contrast, copper nanoparticles generated using tannic acid but without CNC as a control had a zeta potential of -20.2 mV, which verges on colloidal instability.

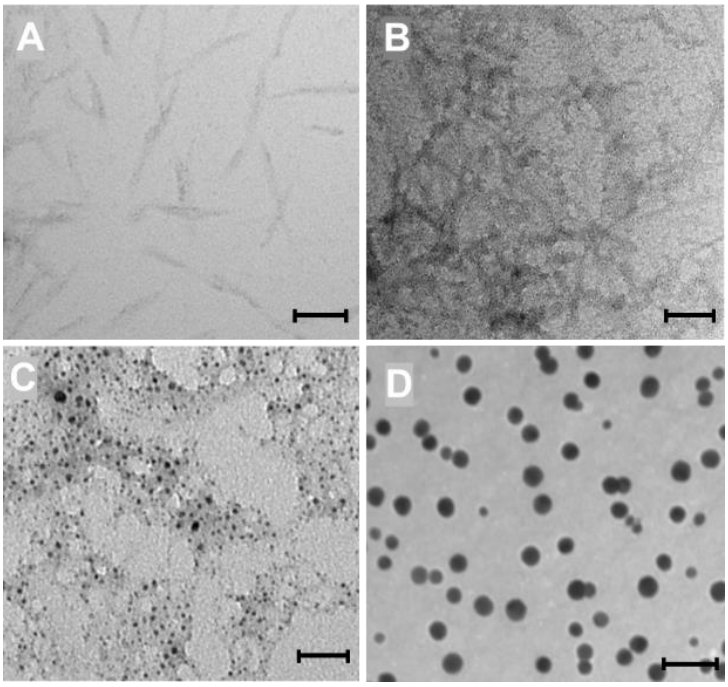

Figure 4.2: TEM images of pristine cellulose nanocrystals (A), tannic acid coated cellulose nanocrystals (B), copper nanoparticles generated by tannic acid (C), and copper nanoparticles generated by tannic acid on cellulose nanocrystals (D). Each scale bar represents 100 nm.

The morphology of the copper composites was examined using a transmission electron microscope. Pristine cellulose nanocrystals have very low electron density, and are thus hard to visualize with TEM (Fig 4.2A). The addition of the tannic acid coating improves the contract somewhat, and a network-like structure can be observed with the tannic acid wrapping the CNC closely (Fig 4.2B). The copper-coated CNC show a similar network-like structure, with many very small and very well dispersed spherical copper nanoparticles dispersed along the tannic acid coated CNC rods. Copper nanoparticles generated tannic acid but without CNC are also spherical, but are much larger and have a higher polydispersity, indicating that they are less stable and more prone to agglomeration than the CNC-bound copper nanoparticles.

4.3.2 Effects of Fabrication Parameters on Copper/CNC Morphology

Factors such as reaction pH and concentration have been shown to affect the synthesis of metal nanoparticles when using tannic acid [279]–[281] , but even in the case where co-reductants such as sodium citrate have been used, little previous work has explored the effect of reagent addition order on the final material morphology. This study therefore sought to understand how reagent addition order might affect the generated CuCNC composite. In order to investigate this, copper/CNC composites and controls were fabricated using a variety of reagent addition orders, as shown in Scheme 4.1.

Scheme 4.1: Tested reagent addition orders and controls for CuCNC composites.

Dispersed CNC → Tannic Acid → NaOH → $CuSO_4$ (Original)

Dispersed CNC → $CuSO_4$ → NaOH → Tannic Acid (Reversed)

Dispersed CNC → $CuSO_4$ → NaOH (Control)

Dispersed CNC → Tannic Acid → NaOH (Control)

Transmission electron microscopy was used to characterize the generated CuCNC composites. When tannic acid was added to the CNC dispersion first, followed by the addition of NaOH to adjust the pH to 9 and then copper sulfate, the metallization of CNC proceeds as expected, yielding many well dispersed copper oxide nanoparticles. However, when copper sulfate was added first, a unique 'bundled' morphology arose, as shown in Fig. 4.3A. These bundles were an average of 54 nm wide and 320 nm long, which is 2 to 5 times the average dimensions of pristine cellulose nanocrystals [256], and were coated in small nanoparticles. Scanning electron micrographs were also generated of these bundles to assure that the morphology was not an artifact of the TEM sample preparation, and very good agreement between the two types of micrographs was found (Fig 4.3B). The SEM images also suggest that the primary composite is in a 'bundled' form, some individual CNC still exist, forming a network between the bundles. Elemental analysis was performed directly during SEM measurement using EDX, which confirmed the presence of copper.

To determine the source of the bundling, control experiments were undertaken using either just tannic acid and cellulose, or just copper sulfate and cellulose, and following an otherwise identical reaction procedure (as laid out in section 4.2.2). These control composites were also investigated with TEM imaging. The tannic acid/CNC composite without any copper sulfate (Fig 4.3D) showed a simple network structure, similar to those previously observed for other catechol-coated CNC composites [273], suggesting that the tannic acid is not the source of the bundling. The $CuSO_4$/CNC control (Fig. 4.3C), in contrast, showed nearly identical 'bundled' morphology to the original reversed-fabrication CuCNC composite. Unexpectedly, not only did the bundling occur with the addition of $CuSO_4$, but a large number of very small copper oxide nanoparticles also appeared (average diameter of 4.02 nm), as seen by the high density of

dark circles in the TEM image. This can be explained by the reductive nature of cellulose nanocrystals in basic environments. While tannic acid was used as the primary reducing agent in this composite, CNC has previously been shown to generate nanoparticles in a 'reducant-free' synthesis [92]. The authors of this work proposed that the hydroxyl groups of CNC become deprotonated at higher pH, exposing an oxygen anion that can participate in reduction of metal nanoparticles. The authors further elaborate that this deprotonation lowers the ability of CNC to participate in hydrogen bonding, which means it has higher surface energy and is therefore more reactive than at a neutral or acidic pH.

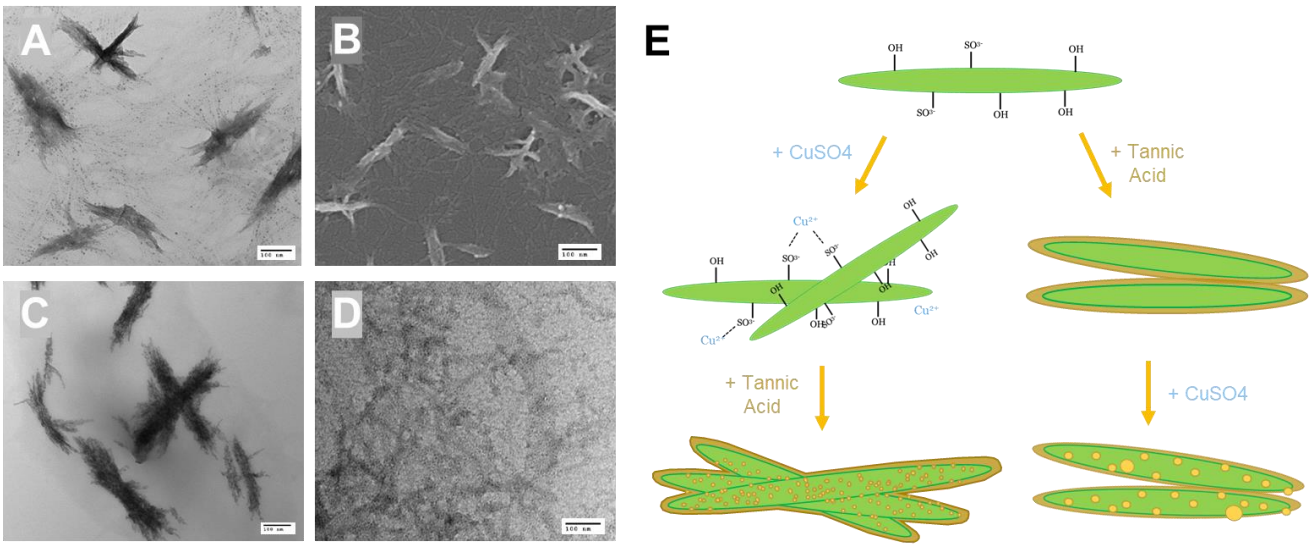

Figure 4.3: TEM and SEM micrographs of bundled copper/CNC colloid (A and B), and TEM micrographs of the copper/CNC composite fabricated without tannic acid (C) and without copper sulfate (D). The proposed mechanism for bundled or networked colloid formation based on reagent addition order (E).

The presence of the bundling only when copper sulfate was added first (with or without tannic acid) clarifies that copper cations play a major role in causing the bundled morphology. Cellulose nanocrystals generated through sulfuric acid hydrolysis of plant matter bear numerous sulfate half ester groups on their surface [282], which impart their characteristic high negative charge. At basic pH, the hydroxyl groups on the surface of CNC are deprotonated, exposing an

oxygen anion. Either of these negatively charged function groups may interact strongly with the positive copper cations. The divalency of copper cations also means that they can interact with two non-adjacent positively charged sites [283], which could lead to the 'bridging' of two CNC rods, eventually causing bundling of many CNC rods at once (as shown schematically in Fig. 4.3E). It can be assumed, in contrast, when CNC is first coated with a tannic acid layer, the exposed o-dihydroxyphenyl groups directly chelate and reduce the copper cations to copper nanoparticles before any strong electrostatic interactions occur. Thus, changing the order of addition of reagents in this system generates vastly different nanostructures from an otherwise identical fabrication protocol.

4.3.3 Generation and Characterization of Silver/CNC and Copper/Silver/CNC Nanoparticles

Following the successful fabrication of the copper oxide/CNC composite, a silver/CNC composite (AgCNC) was fabricated using the same one-pot method, with tannic acid as the reducing agent and cellulose nanocrystals as the capping agent. As with the CuCNC composite, tannic acid and colloidal CNC were first combined, and then silver salt precursor (silver nitrate) was added dropwise. The solution changed immediately from light orange to dark brown with the addition of the silver nitrate. Colloidal suspensions of silver nanoparticles have been shown to display a large range of colors, mostly commonly light yellow through dark red or brown depending on the shape and concentration [284], [285]. Thus, the visual results of this one-pot process are in good agreement with the previous reports. The generated AgCNC nanomaterial was stable after 5 months of storage at ambient conditions, with no change in color and no visual precipitation.

Bimetallic composites with both copper and silver bound to CNC (CuAgCNC) were also generated. There are a variety of ways to generate bimetallic materials, such as using galvanic

replacement or digestive ripening processes [286]–[288]. Here, the simplest method, chemical coreduction, was used. Chemical coreduction has been used successfully to generate bimetallic nanoparticles [65], [66], and is advantageous in that it requires no additional preparation steps and is very scalable. For the chemical coreduction process, the metal salt precusors are mixed prior to the start of the reaction, and then the reduction can proceed unchanged. In this work, $CuSO_4$ and $AgNO_3$ were mixed in a 1:1 molar ratio, and added dropwise to a solution of tannic-acid coated CNC. As with the single metal synthesis, the color of the solution changed immediately to a dark brown/black color, indicating the successful synthesis of metal nanoparticles.

The AgCNC and CuAgCNC suspensions were analyzed using UV-visible spectroscopy (Fig. 4.4). The characteristic SPR peak of spherical silver nanoparticles ranges between 410 and 430 nm [289], though the peak wavelength varies based on nanoparticle size and concentration [290]. The AgCNC composite displayed a peak at 420 nm, falling well within the expected limits for silver nanoparticles. An additional shoulder around 251 nm may be indicative of a small amount of residual tannic acid. The CuAgCNC composite showed two distinct peaks at 275 nm and 420 nm, aligning nearly perfectly with the copper oxide and silver peaks found for the single metal/CNC composites in this study. The relative peak intensity of both the copper and silver peak is lower than for the single metal composites, indicating the formation of fewer particles. This aligns well with the expected results, as half the amount of each precursor was used for the bimetallic composite as for either single metal composite.

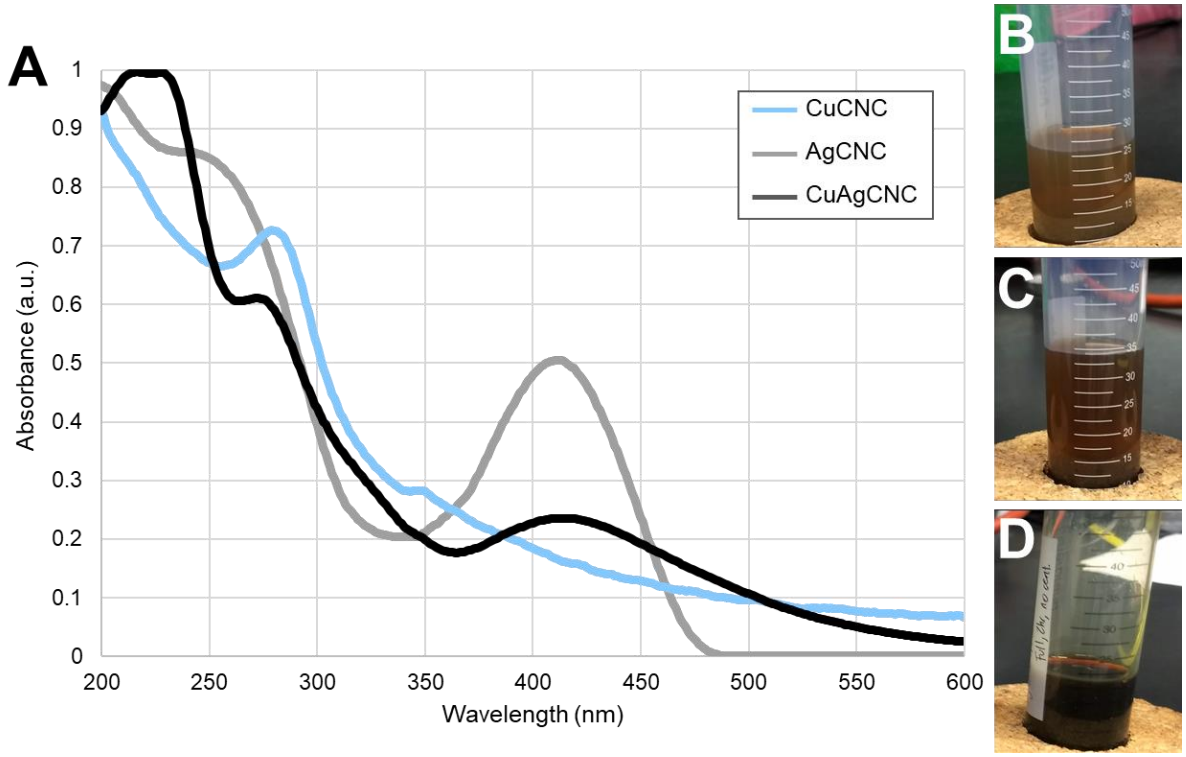

Figure 4.4: UV-Visible spectra for silver/CNC (grey) and copper/silver/CNC (black) composites. Copper/CNC spectrum (blue) is show for comparison (A). Photographs of CuCNC (B), AgCNC (C), and CuAgCNC (D) dispersions.

Truly alloyed metal nanoparticles generally display only one SPR peak, at a wavelength in between those of the two individual metals [291]. Core-shell nanoparticles with a complete shell with display only one SPR peak at the same location as the shell's SPR peak, and core-shell nanoparticles with an incomplete shell will display two SPR peaks or 'humps' that appear closer to each other than the individual peaks for each metal would otherwise be [292], [293]. Colloidal solutions of two metal nanoparticles that are not alloyed in any way, but simply mixed, will display two peaks at the characteristic locations for each individual metal [294]. The presence of two distinct peaks in the location of silver and copper oxide SPR peaks suggest either that the chemical coreduction process simply yielded separate copper and silver particles on CNC, rather than any type of bimetallic particle. This is likely because there is a large difference in lattice size between copper and silver, rendering them relatively immiscible. Previous work has shown

that copper/silver core/shell nanoparticles that are not treated with an annealing process post-fabrication will undergo dewetting, in which the silver nanoparticles form very small free-floating particles around a bare copper core [68].

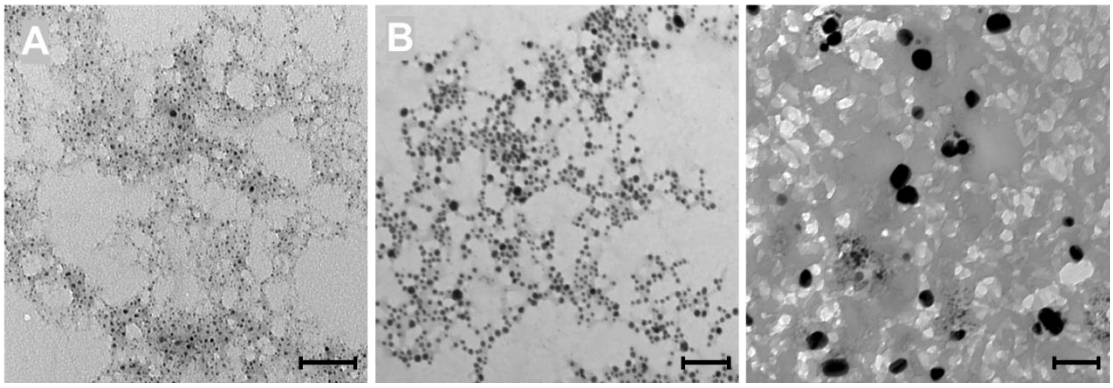

Figure 4.5: TEM micrographs of CuCNC (A) AgCNC (B) and CuAgCNC (C) nanocomposites. All scare bars are 100 nm.

To better understand the morphology of the AgCNC and CuAgCNC composites, TEM imaging was employed, the results of which are shown in Fig. 4.5. The Ag/CNC composite showed similar morphology to the CuCNC composite, with many well dispersed spherical nanoparticles generated along a network of tannic acid-coated CNC. Both the CuCNC and AgCNC composites show no metal nanoparticles separate from the CNC network, suggesting most or all of the nanoparticles are well attached to the substrate. The CuAgCNC composite had a markedly different morphology than the single metal and CNC composites, containing a bimodal distribution of large (40 nm) darker particles and smaller (<10 nm) lighter particles. Based on mass diffraction principles [295], silver nanoparticles should diffract more electrons and thus appear darker in brightfield TEM images. However, increased electron diffusion due to Bragg's diffraction off of crystalline materials can also play a large role, confounding the interpretation of the TEM results without also using selected area diffraction to determine the

presence of crystalline metal. More work to determine the specific composition of the CuAgCNC composites is therefore recommended.

Table 4.1: Measured hydrodynamic and nanoparticle core size and zeta potential for copper- and silver-containing CNC nanocomposites.

Material	Hydrodynamic Diameter (nm)	Nanoparticle Diameter (nm)	Zeta Potential (mV)
CNC	104.2	n/a	-43.6
CuCNC	147.9	5.32 ± 1.88	-25.5
AgCNC	261.0	7.11 ± 4.08	-47.0
CuAgCNC	186.9	24.9 ± 21.0	-33.9

The average sizes and stabilities of the AgCNC and CuAgCNC composites were measured and compared with pristine CNC and with CuCNC, as shown in Table 4.1. The hydrodynamic diameters, as determined by single angle dynamic light scattering, reflect the total size of the composite, including the CNC, the tannic acid coating, and the bound metal nanoparticles, and any hydration shell. As expected, the hydrodynamic diameter of each metal/CNC colloid is larger than the hydrodynamic diameter of pristine CNC, with the largest composite being the AgCNC composite. This larger size may be due to the relatively homogenous coating of larger silver nanoparticles, or because of a strong networking between some of the individual AgCNC particles, leading to slightly larger agglomerates. The actual metal nanoparticle core size was measured using TEM micrographs, and the copper oxide and silver nanoparticles from the monometallic composites were found to be quite small (under 10 nanometers). The average metal core diameter for the CuAgCNC composite was much larger, at nearly 25 nm, with a high standard deviation of 21 nm. The high deviation is in part due to the bimodality of the system, where some nanoparticles were very small (averaging 11 nm), and others very large (upwards of 44 nm). The colloidal stability of the AgCNC and CuAgCNC composites was assessed with zeta potential, and was found to be -47 and -33.9 mV respectively,

indicating very good stability. This is consistent with the visual aging results, which showed no precipitation or sedimentation over a 5 month period in ambient conditions.

4.3.4 Preliminary Antimicrobial Testing

To assess the antimicrobial activity of these particles, CuCNC were tested against yeast (*Saccharomyces cerevisiae*), a single-celled eukaryotic model organism. Antifungal testing is a facile method for the preliminary evaluation of antimicrobial nanoparticles, and previous work has shown extensively that nanoparticles that are antifungal are also antimicrobial [296], [297]. Yeast produces carbon dioxide gas (CO_2) as a byproduct of normal respiration, and a change in the rate of CO_2 production can be used to evaluate the health of the yeast. While measurement of CO_2 produced cannot directly delineate between reduced yeast growth rate and reduced cell viability, decrease in fermentation has previously been shown to correlate with both of these outcomes [298]. *S. cerevisiae* treated with 250 µg of CuCNC, which corresponds to a dose of 26 µg of copper oxide nanoparticles, showed a 40% decrease in respiration with just 25 minutes of exposure time (Fig. 4.6). This high rate of respiratory decrease suggests that CuCNC is a highly effective antimicrobial agent.

As previously discussed, metal nanoparticles are well-known to be antimicrobial, and a variety of inhibition pathways have been proposed, including the release of toxic heavy metal ions and the disruption of the cell membrane due to physical adsorption. Previous work has shown that metal nanoparticles bound to cellulose substrates are more antimicrobial than comparable free-floating nanoparticles [266]. The authors suggested that the high surface area of the cellulose substrate allowed for improved adsorption of the metal/CNC composite on the surface of bacteria, inducing more localized release of antimicrobial metal ions. Another recent work looking at the toxicity of cellulose-associated copper nanoparticles towards *S. cerevisiae* found that treatment of yeast with the CuCNC composite generated significantly higher levels of

reactive oxygen species that a copper ion precursor (CuSO4) alone [299], suggesting that the CNC plays a large role in increasing the composite's toxicity. The authors found that the primary target of the generated reactive oxygen species was the lipid membrane of the yeast, which would an equally attainable target in bacterial model systems.

As discussed in Chapter 3, smaller nanoparticles are generally expected to be more effective at combating Gram negative bacteria, and more negatively charged particles are expected to be more effective at combating Gram positive bacteria. Thus, it would be expected that the nanocomposites generated in this study, with metal core sizes under 10 nm and zeta potentials of -25 mV (somewhat negative) to -47 mV (highly negative) would be highly effective as a broad-spectrum antimicrobial agent. The model organism used in this study, yeast, also showed susceptibility to CuCNC composites. As the method of antimicrobial activity for metal/CNC composites has been shown to target primarily microbial cell membranes, the CuCNC, AgCNC, and CuAgCNC composites would all be expected to be highly translatable to specific antibacterial applications.

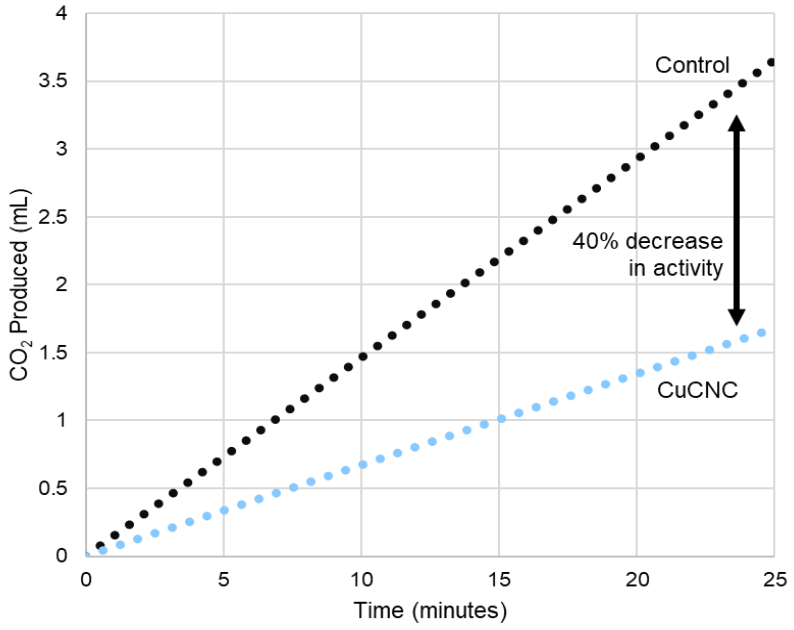

Figure 4.6: Rate of respiration of yeast (measured as CO_2 produced in mL) when allowed to respirate normally (black line) or in the presence of 250 µg of copper/CNC colloid (blue line).

4.4 Conclusion

This chapter discusses the fabrication and characterization of nanocellulose-bound metal nanoparticles generated with a simple and green one-pot method. Tannic acid was successfully deposited onto cellulose nanocrystals, and copper, silver, or a combination of copper and silver nanoparticles were nucleated onto the substrate with dropwise addition of a metal salt precursor. Zeta potential analysis revealed that all of the metal/cellulose nanocrystal composites were colloidally stable, with average zeta potentials of -25.5, -47.0, and -33.9 mV for the CuCNC, AgCNC, and CuAgCNC nanocomposites, respectively. No agglomeration or precipitation was observed for any of the composites over a period of 5 months storage under ambient conditions. The copper and CNC composite showed good antimicrobial activity against *S. cerevisiae,* and previous literature indicates this damage may take place through reactive oxygen species generation and through physical adsorption and metal ion release. This system provides an ecofriendly and facile base for various metal nanoparticles to be fabricated, and the generated nanocomposites well suited to antimicrobial applications. Further studies will clarify the magnitude of antimicrobial activity of these metal and cellulose composites.

Chapter 5: Conclusions and Future Recommendations

5.1 Conclusions and Recommendations for Work Presented in Chapter 3

Data mining and meta-analytical techniques were employed for the first time to understand larger trends in the efficacy of antimicrobial metal nanoparticles. For this work, over 9,000 original research articles published between 2015 and 2019 were distilled down into a workable body of 600+ articles on single metal antimicrobial nanoparticles. The testing methodologies each article used to assess antimicrobial activity were documented, and zone of inhibition tests were found to be most common tests used, despite evidence in the literature that this class of tests cannot accurately measure the efficacy of nanoparticles. Of the articles published that did employ the more robust broth dilution techniques, there was little standardization found in the testing or reporting process. A large majority of tests used varying incubation broths, times, and temperatures, started with different bacterial inoculums, and tested different species and strains of bacteria. Additionally, over two-thirds of the publications included in the data set did not report critical information about the testing conditions, such as the bacterial strain or inoculum size, or about the material tested, such as its surface charge or shape.

Simple analysis of variance testing was undertaken to determine the difference in efficacy of different metal types, including silver, copper, gold, and zinc nanoparticles. There was a very significant ($p < 0.01$) difference between the efficacy of zinc oxide nanoparticles when compared to silver nanoparticles, but no significant different could be found when comparing copper or gold nanoparticles to silver. It cannot be concluded at this time whether the lack of significant difference is due to the massive variance in the publications, or due to similarity in silver, copper, and gold nanoparticles for this application.

Silver nanoparticles, which represented the focus of over 70% of the publications included in this study, were further used as a model to understand other influential characteristics

of antimicrobial nanoparticles. When using linear regression models, it was found that the Gram-type of the bacteria being used as a model is a critical parameter. There was a strong linear correlation between size and efficacy for Gram negative bacteria, indicating that Gram-negative bacteria are increasingly susceptible to smaller nanoparticles. No such correlation existed for Gram-positive bacteria. In contrast, a strong linear correlation existed between surface charge and efficacy against Gram-positive bacteria, indicating that more negatively charged particles are more effective at damaging Gram-positive bacteria. No such correlation existed for Gram negative bacteria.

The conclusion of this work is therefore twofold. The first conclusion is that the literature around antimicrobial metal nanoparticles is yet to be sufficiently standardized, which severely limits the ability to draw new and reliable knowledge from the literature. Improvement in the testing and reporting standards will be critical in allowing the advancement of the field. The second conclusion is that physiochemical parameters such as metal type, nanoparticle size, and nanoparticle surface charge do predict the efficacy of the nanoparticles against bacteria. However, the Gram type of the bacteria vastly modulates which parameters are important and must be considered when designing nanoparticles for specific applications.

In the future, further statistical modeling could be undertaken to explore the effects of size and surface charge on the activity of non-silver nanoparticles, such as gold or copper. This could help elucidate whether or not the mechanism(s) of antimicrobial activity are consistent across these metals, or whether each one functions differently. Additionally, modeling should be performed on the activity of nanoparticles against bacteria aside from *S. aureus* and *E. coli*, to confirm that the difference in activity is indeed modulated by Gram type, and is not simply species specific.

5.2 Conclusions and Recommendations for Work Presented in Chapter 4

This chapter detailed the fabrication and characterization of cellulose nanocrystal-bound metal nanoparticles. Tannic acid and CNC were used for the fabrication of copper, silver, and copper/silver metal nanoparticles in mild synthesis conditions, where water was the sole solvent and the reaction could proceed at near-room temperature. The system was shown to produce relatively monodisperse and highly stable nanoparticles of any metal type tested. The nanoparticles had an average size of 5, 7, and 25 nm diameters for the Cu, Ag, and CuAgCNC composites, respectively. All composites had a zeta potential of at least -25 mV, indicating good colloidal stability, which is attributed in large part to the high stability of cellulose nanocrystals themselves.

Optimization of the fabrication parameters was undertaken, and the order of reagent addition was found to have a large effect on the final product for CuCNC. When copper salt precursor and cellulose nanocrystals are mixed prior to the addition of tannic acid, highly 'bundled' CNC structures occur, with copper acting as a crosslinker between adjacent CNC molecules. However, the coating of tannic acid on CNC prior to the addition of copper salt produces well-dispersed and individual copper coated CNC nanoparticles, due to the direct chelation and reduction of copper ions by tannic acid. The pre-coating of CNC with tannic acid also works to fabricate silver CNC-bound particles. A mixture of silver and copper nanoparticles can be bound simultaneously to tannic acid-coated CNC using simple chemical coreduction.

The CuCNC composite was found to have good antimicrobial activity, and is able to reduce the activity of yeast after just 25 minutes of contact time with a copper dosing of 25 µg/mL (total composite dose of 250 µg/mL). It is expected that this antimicrobial activity is owing primarily to the presence of copper nanoparticles, as cellulose nanocrystals have no

measurable toxicity at such a low dose. Additionally, copper nanoparticles are likely able to generate damaging reactive oxygen species, which can easily cause peroxidation of the lipid membranes and therefore cause catastrophic membrane failure in yeast.

In conclusion, a simple one-pot and ecofriendly method was shown to produce antimicrobial metal/CNC nanocomposites. In the future, more work should be undertaken exploring the exact mechanisms of antimicrobial activity for each composite. It would also be advantageous to generate bimetallic alloys of silver and copper and compare their activity to each individual metal and a mixture of metals. Such work would help to elucidate the antibacterial mechanisms and help guide work towards the fabrication of maximally antimicrobial metal nanomaterials.

References

[1] S. B. Zaman, M. A. Hussain, R. Nye, V. Mehta, K. T. Mamun, and N. Hossain, "A Review on Antibiotic Resistance: Alarm Bells are Ringing," *Cureus*, vol. 9, no. 6, doi: 10.7759/cureus.1403.

[2] M. I. Hutchings, A. W. Truman, and B. Wilkinson, "Antibiotics: past, present and future," *Curr. Opin. Microbiol.*, vol. 51, pp. 72–80, Oct. 2019, doi: 10.1016/j.mib.2019.10.008.

[3] K. Gold, B. Slay, M. Knackstedt, and A. K. Gaharwar, "Antimicrobial Activity of Metal and Metal-Oxide Based Nanoparticles," *Adv. Ther.*, vol. 1, no. 3, p. 1700033, 2018, doi: 10.1002/adtp.201700033.

[4] W.-R. Li, X.-B. Xie, Q.-S. Shi, H.-Y. Zeng, Y.-S. OU-Yang, and Y.-B. Chen, "Antibacterial activity and mechanism of silver nanoparticles on Escherichia coli," *Appl. Microbiol. Biotechnol.*, vol. 85, no. 4, pp. 1115–1122, Jan. 2010, doi: 10.1007/s00253-009-2159-5.

[5] A. Nanda and M. Saravanan, "Biosynthesis of silver nanoparticles from Staphylococcus aureus and its antimicrobial activity against MRSA and MRSE," *Nanomedicine Nanotechnol. Biol. Med.*, vol. 5, no. 4, pp. 452–456, Dec. 2009, doi: 10.1016/j.nano.2009.01.012.

[6] H. Palza, M. Nuñez, R. Bastías, and K. Delgado, "In situ antimicrobial behavior of materials with copper-based additives in a hospital environment," *Int. J. Antimicrob. Agents*, vol. 51, no. 6, pp. 912–917, Jun. 2018, doi: 10.1016/j.ijantimicag.2018.02.007.

[7] N. Mikolajewicz and S. V. Komarova, "Meta-Analytic Methodology for Basic Research: A Practical Guide," *Front. Physiol.*, vol. 10, 2019, doi: 10.3389/fphys.2019.00203.

[8] Kandarp Mavani and Mihir Shah, "Synthesis of Silver Nanoparticles by using Sodium Borohydride as a Reducing Agent," 2013, doi: 10.13140/2.1.3116.8648.

[9] V. V. Tatarchuk, A. P. Sergievskaya, T. M. Korda, I. A. Druzhinina, and V. I. Zaikovsky, "Kinetic Factors in the Synthesis of Silver Nanoparticles by Reduction of Ag+ with Hydrazine in Reverse Micelles of Triton N-42," *Chem. Mater.*, vol. 25, no. 18, pp. 3570–3579, Sep. 2013, doi: 10.1021/cm304115j.

[10] S. Ahmed, M. Ahmad, B. L. Swami, and S. Ikram, "A review on plants extract mediated synthesis of silver nanoparticles for antimicrobial applications: A green expertise," *J. Adv. Res.*, vol. 7, no. 1, pp. 17–28, Jan. 2016, doi: 10.1016/j.jare.2015.02.007.

[11] A. Prüss, D. Kay, L. Fewtrell, and J. Bartram, "Estimating the burden of disease from water, sanitation, and hygiene at a global level.," *Environ. Health Perspect.*, vol. 110, no. 5, pp. 537–542, May 2002.

[12] D. I. Andersson and D. Hughes, "Antibiotic resistance and its cost: is it possible to reverse resistance?," *Nat. Rev. Microbiol.*, vol. 8, no. 4, Art. no. 4, Apr. 2010, doi: 10.1038/nrmicro2319.

[13] Agence de santé publique du Canada, *Tackling antimicrobial resistance and antimicrobial use: a pan-Canadian framework for action.* 2017.

[14] L. Zaffiri, J. Gardner, and L. H. Toledo-Pereyra, "History of Antibiotics. From Salvarsan to Cephalosporins," *J. Invest. Surg.*, vol. 25, no. 2, pp. 67–77, Mar. 2012, doi: 10.3109/08941939.2012.664099.

[15] R. F. Seipke, M. Kaltenpoth, and M. I. Hutchings, "Streptomyces as symbionts: an emerging and widespread theme?," *FEMS Microbiol. Rev.*, vol. 36, no. 4, pp. 862–876, Jul. 2012, doi: 10.1111/j.1574-6976.2011.00313.x.

[16] H. Wj and D. L, “Antibiotic resistance and the need for the rational use of antibiotics.,” *J. Med. Liban.*, vol. 49, no. 5, pp. 246–256, Sep. 2001.
[17] A. Gupta, S. Mumtaz, C.-H. Li, I. Hussain, and V. M. Rotello, “Combatting antibiotic-resistant bacteria using nanomaterials,” *Chem. Soc. Rev.*, vol. 48, no. 2, pp. 415–427, Jan. 2019, doi: 10.1039/c7cs00748e.
[18] P. V. Baptista *et al.*, “Nano-Strategies to Fight Multidrug Resistant Bacteria-"A Battle of the Titans",” *Front. Microbiol.*, vol. 9, p. 1441, 2018, doi: 10.3389/fmicb.2018.01441.
[19] M. Gholipourmalekabadi*, M. Mobaraki, M. Ghaffari, A. Zarebkohan, V. F. Omrani, and A. M. U. and A. Seifalian*, “Targeted Drug Delivery Based on Gold Nanoparticle Derivatives,” *Current Pharmaceutical Design*, May 31, 2017. https://www.eurekaselect.com/151692/article (accessed Aug. 08, 2020).
[20] E. Tabesh, H. Salimijazi, M. Kharaziha, and M. Hejazi, “Antibacterial chitosan-copper nanocomposite coatings for biomedical applications,” *Mater. Today Proc.*, vol. 5, no. 7, Part 3, pp. 15806–15812, Jan. 2018, doi: 10.1016/j.matpr.2018.05.078.
[21] Z. A. Raza, F. Anwar, S. Ahmad, and M. Aslam, “Fabrication of ZnO incorporated chitosan nanocomposites for enhanced functional properties of cellulosic fabric,” *Mater. Res. Express*, vol. 3, no. 11, p. 115001, Nov. 2016, doi: 10.1088/2053-1591/3/11/115001.
[22] L. Al-Naamani, S. Dobretsov, and J. Dutta, “Chitosan-zinc oxide nanoparticle composite coating for active food packaging applications,” *Innov. Food Sci. Emerg. Technol.*, vol. 38, pp. 231–237, Dec. 2016, doi: 10.1016/j.ifset.2016.10.010.
[23] P. Choudhary, T. Parandhaman, B. Ramalingam, N. Duraipandy, M. S. Kiran, and S. K. Das, “Fabrication of Nontoxic Reduced Graphene Oxide Protein Nanoframework as Sustained Antimicrobial Coating for Biomedical Application,” *ACS Appl. Mater. Interfaces*, vol. 9, no. 44, pp. 38255–38269, Nov. 2017, doi: 10.1021/acsami.7b11203.
[24] M. Ahonen *et al.*, “Proactive Approach for Safe Use of Antimicrobial Coatings in Healthcare Settings: Opinion of the COST Action Network AMiCI,” *Int. J. Environ. Res. Public. Health*, vol. 14, no. 4, Art. no. 4, Apr. 2017, doi: 10.3390/ijerph14040366.
[25] R. Thomas, S. Mathew, A. R. Nayana, J. Mathews, and E. K. Radhakrishnan, “Microbially and phytofabricated AgNPs with different mode of bactericidal action were identified to have comparable potential for surface fabrication of central venous catheters to combat Staphylococcus aureus biofilm,” *J. Photochem. Photobiol. B*, vol. 171, pp. 96–103, Jun. 2017, doi: 10.1016/j.jphotobiol.2017.04.036.
[26] Y. Wang, R. Cai, and C. Chen, “The Nano–Bio Interactions of Nanomedicines: Understanding the Biochemical Driving Forces and Redox Reactions,” *Acc. Chem. Res.*, vol. 52, no. 6, pp. 1507–1518, Jun. 2019, doi: 10.1021/acs.accounts.9b00126.
[27] N. Durán, M. Durán, M. B. de Jesus, A. B. Seabra, W. J. Fávaro, and G. Nakazato, “Silver nanoparticles: A new view on mechanistic aspects on antimicrobial activity,” *Nanomedicine Nanotechnol. Biol. Med.*, vol. 12, no. 3, pp. 789–799, Apr. 2016, doi: 10.1016/j.nano.2015.11.016.
[28] M. Premanathan, K. Karthikeyan, K. Jeyasubramanian, and G. Manivannan, “Selective toxicity of ZnO nanoparticles toward Gram-positive bacteria and cancer cells by apoptosis through lipid peroxidation,” *Nanomedicine Nanotechnol. Biol. Med.*, vol. 7, no. 2, pp. 184–192, Apr. 2011, doi: 10.1016/j.nano.2010.10.001.
[29] K. Giannousi, K. Lafazanis, J. Arvanitidis, A. Pantazaki, and C. Dendrinou-Samara, “Hydrothermal synthesis of copper based nanoparticles: Antimicrobial screening and

interaction with DNA," *J. Inorg. Biochem.*, vol. 133, pp. 24–32, Apr. 2014, doi: 10.1016/j.jinorgbio.2013.12.009.
[30] N. Li *et al.*, "Ultrafine particulate pollutants induce oxidative stress and mitochondrial damage," *Environ. Health Perspect.*, vol. 111, no. 4, pp. 455–460, Apr. 2003, doi: 10.1289/ehp.6000.
[31] O. Choi, K. K. Deng, N.-J. Kim, L. Ross, R. Y. Surampalli, and Z. Hu, "The inhibitory effects of silver nanoparticles, silver ions, and silver chloride colloids on microbial growth," *Water Res.*, vol. 42, no. 12, pp. 3066–3074, Jun. 2008, doi: 10.1016/j.watres.2008.02.021.
[32] M. Raffi *et al.*, "Investigations into the antibacterial behavior of copper nanoparticles against Escherichia coli," *Ann. Microbiol.*, vol. 60, no. 1, pp. 75–80, Mar. 2010, doi: 10.1007/s13213-010-0015-6.
[33] A. Ahmad *et al.*, "The effects of bacteria-nanoparticles interface on the antibacterial activity of green synthesized silver nanoparticles," *Microb. Pathog.*, vol. 102, pp. 133–142, Jan. 2017, doi: 10.1016/j.micpath.2016.11.030.
[34] M. Arakha *et al.*, "Antimicrobial activity of iron oxide nanoparticle upon modulation of nanoparticle-bacteria interface," *Sci. Rep.*, vol. 5, Oct. 2015, doi: 10.1038/srep14813.
[35] S. Agnihotri, S. Mukherji, and S. Mukherji, "Size-controlled silver nanoparticles synthesized over the range 5–100 nm using the same protocol and their antibacterial efficacy," *RSC Adv.*, vol. 4, no. 8, pp. 3974–3983, 2014, doi: 10.1039/C3RA44507K.
[36] U. K. Parashar *et al.*, "Study of mechanism of enhanced antibacterial activity by green synthesis of silver nanoparticles," *Nanotechnology*, vol. 22, no. 41, p. 415104, Oct. 2011, doi: 10.1088/0957-4484/22/41/415104.
[37] C. Angelé-Martínez, K. V. T. Nguyen, F. S. Ameer, J. N. Anker, and J. L. Brumaghim, "Reactive Oxygen Species Generation by Copper(II) Oxide Nanoparticles Determined by DNA Damage Assays and EPR Spectroscopy," *Nanotoxicology*, vol. 11, no. 2, pp. 278–288, Mar. 2017, doi: 10.1080/17435390.2017.1293750.
[38] M. A. Ansari *et al.*, "Interaction of silver nanoparticles with Escherichia coli and their cell envelope biomolecules," *J. Basic Microbiol.*, vol. 54, no. 9, pp. 905–915, 2014, doi: 10.1002/jobm.201300457.
[39] M. M. Gaschler and B. R. Stockwell, "Lipid peroxidation in cell death," *Biochem. Biophys. Res. Commun.*, vol. 482, no. 3, pp. 419–425, Jan. 2017, doi: 10.1016/j.bbrc.2016.10.086.
[40] B. Das *et al.*, "Green synthesized silver nanoparticles destroy multidrug resistant bacteria via reactive oxygen species mediated membrane damage," *Arab. J. Chem.*, vol. 10, no. 6, pp. 862–876, 2017, doi: 10.1016/j.arabjc.2015.08.008.
[41] H.-L. Su *et al.*, "The disruption of bacterial membrane integrity through ROS generation induced by nanohybrids of silver and clay," *Biomaterials*, vol. 30, no. 30, pp. 5979–5987, Oct. 2009, doi: 10.1016/j.biomaterials.2009.07.030.
[42] Y. J. Tang, S. G. Wu, L. Huang, J. Head, D. Chen, and I. C. Kong, "Phytotoxicity of Metal Oxide Nanoparticles is Related to Both Dissolved Metals Ions and Adsorption of Particles on Seed Surfaces," *J. Pet. Environ. Biotechnol.*, vol. 03, no. 04, 2012, doi: 10.4172/2157-7463.1000126.
[43] N. Hachicho, P. Hoffmann, K. Ahlert, and H. J. Heipieper, "Effect of silver nanoparticles and silver ions on growth and adaptive response mechanisms of Pseudomonas putida mt-

2," *FEMS Microbiol. Lett.*, vol. 355, no. 1, pp. 71–77, 2014, doi: 10.1111/1574-6968.12460.
[44] A. K. Chatterjee, R. Chakraborty, and T. Basu, "Mechanism of antibacterial activity of copper nanoparticles," *Nanotechnology*, vol. 25, no. 13, p. 135101, 2014, doi: 10.1088/0957-4484/25/13/135101.
[45] S. Sabella *et al.*, "A general mechanism for intracellular toxicity of metal-containing nanoparticles," *Nanoscale*, vol. 6, no. 12, p. 7052, 2014, doi: 10.1039/c4nr01234h.
[46] C. D. Walkey *et al.*, "Protein Corona Fingerprinting Predicts the Cellular Interaction of Gold and Silver Nanoparticles," *ACS Nano*, vol. 8, no. 3, pp. 2439–2455, Mar. 2014, doi: 10.1021/nn406018q.
[47] N. Jain, A. Bhargava, M. Rathi, R. V. Dilip, and J. Panwar, "Removal of Protein Capping Enhances the Antibacterial Efficiency of Biosynthesized Silver Nanoparticles," *PLoS ONE*, vol. 10, no. 7, Jul. 2015, doi: 10.1371/journal.pone.0134337.
[48] Z. Li, K. Greden, P. J. J. Alvarez, K. B. Gregory, and G. V. Lowry, "Adsorbed Polymer and NOM Limits Adhesion and Toxicity of Nano Scale Zerovalent Iron to E. coli," *Environ. Sci. Technol.*, vol. 44, no. 9, pp. 3462–3467, May 2010, doi: 10.1021/es9031198.
[49] N. R. Jana, L. Gearheart, and C. J. Murphy, "Evidence for Seed-Mediated Nucleation in the Chemical Reduction of Gold Salts to Gold Nanoparticles," *Chem. Mater.*, vol. 13, no. 7, pp. 2313–2322, Jul. 2001, doi: 10.1021/cm000662n.
[50] M. Brust, M. Walker, D. Bethell, D. J. Schiffrin, and R. Whyman, "Synthesis of thiol-derivatised gold nanoparticles in a two-phase Liquid–Liquid system," *J Chem Soc Chem Commun*, vol. 0, no. 7, pp. 801–802, 1994, doi: 10.1039/C39940000801.
[51] M. T. Reetz and W. Helbig, "Size-Selective Synthesis of Nanostructured Transition Metal Clusters," *J. Am. Chem. Soc.*, vol. 116, no. 16, pp. 7401–7402, Aug. 1994, doi: 10.1021/ja00095a051.
[52] L. Rodríguez-Sánchez, M. C. Blanco, and M. A. López-Quintela, "Electrochemical Synthesis of Silver Nanoparticles," *J. Phys. Chem. B*, vol. 104, no. 41, pp. 9683–9688, Oct. 2000, doi: 10.1021/jp001761r.
[53] Y. Ma, C. Liu, D. Qu, Y. Chen, M. Huang, and Y. Liu, "Antibacterial evaluation of sliver nanoparticles synthesized by polysaccharides from Astragalus membranaceus roots," *Biomed. Pharmacother.*, vol. 89, pp. 351–357, May 2017, doi: 10.1016/j.biopha.2017.02.009.
[54] A. Abedini, A. R. Daud, M. A. Abdul Hamid, N. Kamil Othman, and E. Saion, "A review on radiation-induced nucleation and growth of colloidal metallic nanoparticles," *Nanoscale Res. Lett.*, vol. 8, no. 1, p. 474, Nov. 2013, doi: 10.1186/1556-276X-8-474.
[55] J. Belloni, "Nucleation, growth and properties of nanoclusters studied by radiation chemistry: Application to catalysis," *Catal. Today*, vol. 113, no. 3, pp. 141–156, Apr. 2006, doi: 10.1016/j.cattod.2005.11.082.
[56] M.-C. Daniel and D. Astruc, "Gold Nanoparticles: Assembly, Supramolecular Chemistry, Quantum-Size-Related Properties, and Applications toward Biology, Catalysis, and Nanotechnology," p. 54.
[57] J. Turkevich, P. C. Stevenson, and J. Hillier, "A study of the nucleation and growth processes in the synthesis of colloidal gold," *Discuss. Faraday Soc.*, vol. 11, no. 0, pp. 55–75, Jan. 1951, doi: 10.1039/DF9511100055.

[58] Y. Xia, Y. Xiong, B. Lim, and S. E. Skrabalak, “Shape-Controlled Synthesis of Metal Nanocrystals: Simple Chemistry Meets Complex Physics?,” *Angew. Chem. Int. Ed Engl.*, vol. 48, no. 1, pp. 60–103, 2009, doi: 10.1002/anie.200802248.
[59] E. C. Vreeland *et al.*, “Enhanced Nanoparticle Size Control by Extending LaMer’s Mechanism,” *Chem. Mater.*, vol. 27, no. 17, pp. 6059–6066, Sep. 2015, doi: 10.1021/acs.chemmater.5b02510.
[60] T. Yao *et al.*, “Probing Nucleation Pathways for Morphological Manipulation of Platinum Nanocrystals,” *J. Am. Chem. Soc.*, vol. 134, no. 22, pp. 9410–9416, Jun. 2012, doi: 10.1021/ja302642x.
[61] Y. Huang, W. Wang, H. Liang, and H. Xu, “Surfactant-Promoted Reductive Synthesis of Shape-Controlled Gold Nanostructures,” *Cryst. Growth Des.*, vol. 9, no. 2, pp. 858–862, Feb. 2009, doi: 10.1021/cg800500c.
[62] N. Toshima and T. Yonezawa, “Bimetallic nanoparticles—novel materials for chemical and physical applications,” *New J. Chem.*, vol. 22, no. 11, pp. 1179–1201, Jan. 1998, doi: 10.1039/A805753B.
[63] R. Ghosh Chaudhuri and S. Paria, “Core/Shell Nanoparticles: Classes, Properties, Synthesis Mechanisms, Characterization, and Applications,” *Chem. Rev.*, vol. 112, no. 4, pp. 2373–2433, Apr. 2012, doi: 10.1021/cr100449n.
[64] R. Ferrando, J. Jellinek, and R. L. Johnston, “Nanoalloys: From Theory to Applications of Alloy Clusters and Nanoparticles,” *Chem. Rev.*, vol. 108, no. 3, pp. 845–910, Mar. 2008, doi: 10.1021/cr040090g.
[65] L. Kuai, X. Yu, S. Wang, Y. Sang, and B. Geng, “Au–Pd Alloy and Core–Shell Nanostructures: One-Pot Coreduction Preparation, Formation Mechanism, and Electrochemical Properties,” *Langmuir*, vol. 28, no. 18, pp. 7168–7173, May 2012, doi: 10.1021/la300813z.
[66] J. Han *et al.*, “One-pot, seedless synthesis of flowerlike Au–Pd bimetallic nanoparticles with core-shell-like structure via sodium citrate coreduction of metal ions,” *CrystEngComm*, vol. 14, no. 20, pp. 7036–7042, Sep. 2012, doi: 10.1039/C2CE25824B.
[67] T. Ghosh, B. Satpati, and D. Senapati, “Characterization of bimetallic core–shell nanorings synthesized via ascorbic acid-controlled galvanic displacement followed by epitaxial growth,” *J. Mater. Chem. C*, vol. 2, no. 13, pp. 2439–2447, Mar. 2014, doi: 10.1039/C3TC32340D.
[68] S.-S. Chee and J.-H. Lee, “Preparation and oxidation behavior of Ag-coated Cu nanoparticles less than 20 nm in size,” *J. Mater. Chem. C*, vol. 2, no. 27, pp. 5372–5381, Jun. 2014, doi: 10.1039/C4TC00509K.
[69] Y. Yang *et al.*, “Combination of Digestive Ripening and Seeding Growth As a Generalized Route for Precisely Controlling Size of Monodispersed Noble Monometallic, Shell Thickness of Core−Shell and Composition of Alloy Nanoparticles,” *J. Phys. Chem. C*, vol. 114, no. 1, pp. 256–264, Jan. 2010, doi: 10.1021/jp909065y.
[70] N. I. Hulkoti and T. C. Taranath, “Biosynthesis of nanoparticles using microbes—A review,” *Colloids Surf. B Biointerfaces*, vol. 121, pp. 474–483, Sep. 2014, doi: 10.1016/j.colsurfb.2014.05.027.
[71] R. Singh *et al.*, “Synthesis, optimization, and characterization of silver nanoparticles from Acinetobacter calcoaceticus and their enhanced antibacterial activity when combined with antibiotics,” *Int. J. Nanomedicine*, vol. 8, pp. 4277–4290, 2013, doi: 10.2147/IJN.S48913.

[72] R. K. Gupta, V. Kumar, R. K. Gundampati, M. Malviya, S. H. Hasan, and M. V. Jagannadham, “Biosynthesis of silver nanoparticles from the novel strain of Streptomyces Sp. BHUMBU-80 with highly efficient electroanalytical detection of hydrogen peroxide and antibacterial activity,” *J. Environ. Chem. Eng.*, vol. 5, no. 6, pp. 5624–5635, Dec. 2017, doi: 10.1016/j.jece.2017.09.029.
[73] C. Mahendra *et al.*, “Antibacterial and antimitotic potential of bio-fabricated zinc oxide nanoparticles of Cochlospermum religiosum (L.),” *Microb. Pathog.*, vol. 110, pp. 620–629, Sep. 2017, doi: 10.1016/j.micpath.2017.07.051.
[74] J. Judith Vijaya *et al.*, “Bioreduction potentials of dried root of Zingiber officinale for a simple green synthesis of silver nanoparticles: Antibacterial studies,” *J. Photochem. Photobiol. B*, vol. 177, pp. 62–68, Dec. 2017, doi: 10.1016/j.jphotobiol.2017.10.007.
[75] D. K. Verma, S. H. Hasan, and R. M. Banik, “Photo-catalyzed and phyto-mediated rapid green synthesis of silver nanoparticles using herbal extract of Salvinia molesta and its antimicrobial efficacy,” *J. Photochem. Photobiol. B*, vol. 155, pp. 51–59, Feb. 2016, doi: 10.1016/j.jphotobiol.2015.12.008.
[76] S. Iravani and B. Zolfaghari, “Green Synthesis of Silver Nanoparticles Using Pinus eldarica Bark Extract,” *BioMed Research International*, Sep. 08, 2013. https://www.hindawi.com/journals/bmri/2013/639725/ (accessed Aug. 01, 2020).
[77] B. Singh and R. A. Sharma, “Plant terpenes: defense responses, phylogenetic analysis, regulation and clinical applications,” *3 Biotech*, vol. 5, no. 2, pp. 129–151, Apr. 2015, doi: 10.1007/s13205-014-0220-2.
[78] Z.-R. Mashwani, M. A. Khan, T. Khan, and A. Nadhman, “Applications of plant terpenoids in the synthesis of colloidal silver nanoparticles,” *Adv. Colloid Interface Sci.*, vol. 234, pp. 132–141, Aug. 2016, doi: 10.1016/j.cis.2016.04.008.
[79] S. P. Dubey, M. Lahtinen, and M. Sillanpää, “Tansy fruit mediated greener synthesis of silver and gold nanoparticles,” *Process Biochem.*, vol. 45, no. 7, pp. 1065–1071, Jul. 2010, doi: 10.1016/j.procbio.2010.03.024.
[80] S. Piccolella and S. Pacifico, “Chapter Five - Plant-Derived Polyphenols: A Chemopreventive and Chemoprotectant Worth-Exploring Resource in Toxicology,” in *Advances in Molecular Toxicology*, vol. 9, J. C. Fishbein and J. M. Heilman, Eds. Elsevier, 2015, pp. 161–214.
[81] A. K. Singh, M. Talat, D. P. Singh, and O. N. Srivastava, “Biosynthesis of gold and silver nanoparticles by natural precursor clove and their functionalization with amine group,” *J. Nanoparticle Res.*, vol. 12, no. 5, pp. 1667–1675, Jun. 2010, doi: 10.1007/s11051-009-9835-3.
[82] Y.-S. Liu, Y.-C. Chang, and H.-H. Chen, “Silver nanoparticle biosynthesis by using phenolic acids in rice husk extract as reducing agents and dispersants,” *J. Food Drug Anal.*, vol. 26, no. 2, pp. 649–656, Apr. 2018, doi: 10.1016/j.jfda.2017.07.005.
[83] H. Huang and X. Yang, “Synthesis of Chitosan-Stabilized Gold Nanoparticles in the Absence/Presence of Tripolyphosphate,” *Biomacromolecules*, vol. 5, no. 6, pp. 2340–2346, Nov. 2004, doi: 10.1021/bm0497116.
[84] M. Adlim, M. Abu Bakar, K. Y. Liew, and J. Ismail, “Synthesis of chitosan-stabilized platinum and palladium nanoparticles and their hydrogenation activity,” *J. Mol. Catal. Chem.*, vol. 212, no. 1, pp. 141–149, Apr. 2004, doi: 10.1016/j.molcata.2003.08.012.
[85] J. Díaz-Visurraga, C. Daza, C. Pozo, A. Becerra, C. von Plessing, and A. García, “Study on antibacterial alginate-stabilized copper nanoparticles by FT-IR and 2D-IR correlation

spectroscopy," *Int. J. Nanomedicine*, vol. 7, pp. 3597–3612, 2012, doi: 10.2147/IJN.S32648.
[86] G. Biliuta and S. Coseri, "Cellulose: A ubiquitous platform for ecofriendly metal nanoparticles preparation," *Coord. Chem. Rev.*, vol. 383, pp. 155–173, Mar. 2019, doi: 10.1016/j.ccr.2019.01.007.
[87] X. Wu, Z. Shi, S. Fu, J. Chen, R. M. Berry, and K. C. Tam, "Strategy for Synthesizing Porous Cellulose Nanocrystal Supported Metal Nanocatalysts," *ACS Sustain. Chem. Eng.*, vol. 4, no. 11, pp. 5929–5935, Nov. 2016, doi: 10.1021/acssuschemeng.6b00551.
[88] G. Singh, C. Chandoha-Lee, W. Zhang, S. Renneckar, P. J. Vikesland, and A. Pruden, "Biodegradation of nanocrystalline cellulose by two environmentally-relevant consortia.," *Water Res.*, vol. 104, pp. 137–146, Nov. 2016, doi: 10.1016/j.watres.2016.07.073.
[89] W. Yan *et al.*, "Facile and green synthesis of cellulose nanocrystal-supported gold nanoparticles with superior catalytic activity," *Carbohydr. Polym.*, vol. 140, pp. 66–73, Apr. 2016, doi: 10.1016/j.carbpol.2015.12.049.
[90] A. R. Lokanathan, K. M. A. Uddin, O. J. Rojas, and J. Laine, "Cellulose Nanocrystal-Mediated Synthesis of Silver Nanoparticles: Role of Sulfate Groups in Nucleation Phenomena," *Biomacromolecules*, vol. 15, no. 1, pp. 373–379, Jan. 2014, doi: 10.1021/bm401613h.
[91] X. Wu, C. Lu, Z. Zhou, G. Yuan, R. Xiong, and X. Zhang, "Green synthesis and formation mechanism of cellulose nanocrystal-supported gold nanoparticles with enhanced catalytic performance," *Environ. Sci. Nano*, vol. 1, no. 1, pp. 71–79, 2014, doi: 10.1039/C3EN00066D.
[92] Y. Han, X. Wu, X. Zhang, Z. Zhou, and C. Lu, "Reductant-Free Synthesis of Silver Nanoparticles-Doped Cellulose Microgels for Catalyzing and Product Separation," *ACS Sustain. Chem. Eng.*, vol. 4, no. 12, pp. 6322–6331, Dec. 2016, doi: 10.1021/acssuschemeng.6b00889.
[93] J. Morère, M. J. Tenorio, M. J. Torralvo, C. Pando, J. A. R. Renuncio, and A. Cabañas, "Deposition of Pd into mesoporous silica SBA-15 using supercritical carbon dioxide," *J. Supercrit. Fluids*, vol. 56, no. 2, pp. 213–222, Mar. 2011, doi: 10.1016/j.supflu.2010.12.012.
[94] J. Clardy, M. Fischbach, and C. Currie, "The natural history of antibiotics," *Curr. Biol. CB*, vol. 19, no. 11, pp. R437–R441, Jun. 2009, doi: 10.1016/j.cub.2009.04.001.
[95] D. I. Andersson, "Persistence of antibiotic resistant bacteria," *Current Opinion in Microbiology*, vol. 6, no. 5. Elsevier Ltd, pp. 452–456, 2003, doi: 10.1016/j.mib.2003.09.001.
[96] L.-E. Shi, Z.-H. Li, W. Zheng, Y.-F. Zhao, Y.-F. Jin, and Z.-X. Tang, "Synthesis, antibacterial activity, antibacterial mechanism and food applications of ZnO nanoparticles: a review," *Food Addit. Contam. Part A*, vol. 31, no. 2, pp. 173–186, Feb. 2014, doi: 10.1080/19440049.2013.865147.
[97] Y. N. Slavin, J. Asnis, U. O. Häfeli, and H. Bach, "Metal nanoparticles: understanding the mechanisms behind antibacterial activity," *J. Nanobiotechnology*, vol. 15, no. 1, p. 65, Oct. 2017, doi: 10.1186/s12951-017-0308-z.
[98] T. M. Tolaymat, A. M. El Badawy, A. Genaidy, K. G. Scheckel, T. P. Luxton, and M. Suidan, "An evidence-based environmental perspective of manufactured silver nanoparticle in syntheses and applications: A systematic review and critical appraisal of

peer-reviewed scientific papers," *Sci. Total Environ.*, vol. 408, no. 5, pp. 999–1006, Feb. 2010, doi: 10.1016/j.scitotenv.2009.11.003.
[99] H. Li, Q. Chen, J. Zhao, and K. Urmila, "Enhancing the antimicrobial activity of natural extraction using the synthetic ultrasmall metal nanoparticles," *Sci. Rep.*, vol. 5, p. 11033, Jun. 2015, doi: 10.1038/srep11033.
[100] P. K. Stoimenov, R. L. Klinger, G. L. Marchin, and K. J. Klabunde, "Metal Oxide Nanoparticles as Bactericidal Agents," *Langmuir*, vol. 18, no. 17, pp. 6679–6686, Aug. 2002, doi: 10.1021/la0202374.
[101] I. Sondi and B. Salopek-Sondi, "Silver nanoparticles as antimicrobial agent: a case study on E. coli as a model for Gram-negative bacteria," *J. Colloid Interface Sci.*, vol. 275, no. 1, pp. 177–182, Jul. 2004, doi: 10.1016/j.jcis.2004.02.012.
[102] K. K. Y. Wong and X. Liu, "Silver nanoparticles—the real 'silver bullet' in clinical medicine?," *MedChemComm*, vol. 1, no. 2, pp. 125–131, Aug. 2010, doi: 10.1039/C0MD00069H.
[103] N. Tian, Y.-H. Wen, Z.-Y. Zhou, S.-G. Sun, J. H. Soh, and Z. Gao, "Shape-Controlled Synthesis of Metal Nanoparticles of High Surface Energy and Their Applications in Electrocatalysis Metal Nanoparticles in Biomedical Applications Index," *Complex-Shaped Met. Nanoparticles*, pp. 117–165, Jun. 2012, doi: doi:10.1002/9783527652570.ch3 10.1002/9783527652570.ch3 doi:10.1002/9783527652570.ch15 10.1002/9783527652570.ch15 doi:10.1002/9783527652570.index 10.1002/9783527652570.index.
[104] J. R. Morones *et al.*, "The bactericidal effect of silver nanoparticles," *Nanotechnology*, vol. 16, no. 10, pp. 2346–2353, Aug. 2005, doi: 10.1088/0957-4484/16/10/059.
[105] J. D. Aiken and R. G. Finke, "A review of modern transition-metal nanoclusters: their synthesis, characterization, and applications in catalysis," *J. Mol. Catal. Chem.*, vol. 145, no. 1, pp. 1–44, Sep. 1999, doi: 10.1016/S1381-1169(99)00098-9.
[106] S. Prabhu and E. K. Poulose, "Silver nanoparticles: mechanism of antimicrobial action, synthesis, medical applications, and toxicity effects," *Int. Nano Lett.*, vol. 2, no. 1, p. 32, Oct. 2012, doi: 10.1186/2228-5326-2-32.
[107] P. Orlowski *et al.*, "Tannic acid-modified silver nanoparticles for wound healing: the importance of size," *Int. J. Nanomedicine*, vol. 13, pp. 991–1007, Feb. 2018, doi: 10.2147/IJN.S154797.
[108] P. P. Pillai, B. Kowalczyk, K. Kandere-Grzybowska, M. Borkowska, and B. A. Grzybowski, "Engineering Gram Selectivity of Mixed-Charge Gold Nanoparticles by Tuning the Balance of Surface Charges," *Angew. Chem. Int. Ed.*, vol. 55, no. 30, pp. 8610–8614, 2016, doi: 10.1002/anie.201602965.
[109] M. Balouiri, M. Sadiki, and S. K. Ibnsouda, "Methods for in vitro evaluating antimicrobial activity: A review," *J. Pharm. Anal.*, vol. 6, no. 2, pp. 71–79, Apr. 2016, doi: 10.1016/j.jpha.2015.11.005.
[110] A. Klančnik, S. Piskernik, B. Jeršek, and S. S. Možina, "Evaluation of diffusion and dilution methods to determine the antibacterial activity of plant extracts," *J. Microbiol. Methods*, vol. 81, no. 2, pp. 121–126, May 2010, doi: 10.1016/j.mimet.2010.02.004.
[111] A. Kourmouli *et al.*, "Can disc diffusion susceptibility tests assess the antimicrobial activity of engineered nanoparticles?," *J. Nanoparticle Res.*, vol. 20, no. 3, p. 62, Mar. 2018, doi: 10.1007/s11051-018-4152-3.

[112] D. T. Thuc, T. Q. Huy, L. H. Hoang, T. H. Hoang, A.-T. Le, and D. D. Anh, "Antibacterial Activity of Electrochemically Synthesized Colloidal Silver Nanoparticles Against Hospital-Acquired Infections," *J. Electron. Mater.*, vol. 46, no. 6, pp. 3433–3439, Jun. 2017, doi: 10.1007/s11664-017-5315-1.
[113] J. P. Ruparelia, A. K. Chatterjee, S. P. Duttagupta, and S. Mukherji, "Strain specificity in antimicrobial activity of silver and copper nanoparticles," *Acta Biomater.*, vol. 4, no. 3, pp. 707–716, May 2008, doi: 10.1016/j.actbio.2007.11.006.
[114] G. Maiorano *et al.*, "Effects of Cell Culture Media on the Dynamic Formation of Protein−Nanoparticle Complexes and Influence on the Cellular Response," *ACS Nano*, vol. 4, no. 12, pp. 7481–7491, Dec. 2010, doi: 10.1021/nn101557e.
[115] H. I. Labouta, N. Asgarian, K. Rinker, and D. T. Cramb, "Meta-Analysis of Nanoparticle Cytotoxicity via Data-Mining the Literature," *ACS Nano*, vol. 13, no. 2, pp. 1583–1594, Feb. 2019, doi: 10.1021/acsnano.8b07562.
[116] E. Oh *et al.*, "Meta-analysis of cellular toxicity for cadmium-containing quantum dots," *Nat. Nanotechnol.*, vol. 11, no. 5, pp. 479–486, May 2016, doi: 10.1038/nnano.2015.338.
[117] D. Moher, A. Liberati, J. Tetzlaff, D. G. Altman, and T. P. Group, "Preferred Reporting Items for Systematic Reviews and Meta-Analyses: The PRISMA Statement," *PLOS Med.*, vol. 6, no. 7, p. e1000097, Jul. 2009, doi: 10.1371/journal.pmed.1000097.
[118] Z. Abbasi, S. Feizi, E. Taghipour, and P. Ghadam, "Green synthesis of silver nanoparticles using aqueous extract of dried Juglans regia green husk and examination of its biological properties," *Green Process. Synth.*, vol. 6, no. 5, Jan. 2017, doi: 10.1515/gps-2016-0108.
[119] F. Abul Qais, Samreen, and I. Ahmad, "Broad-spectrum inhibitory effect of green synthesised silver nanoparticles from Withania somnifera (L.) on microbial growth, biofilm and respiration: a putative mechanistic approach," *IET Nanobiotechnol.*, vol. 12, no. 3, pp. 325–335, 2018, doi: 10.1049/iet-nbt.2017.0193.
[120] M. R. Ajdari, G. H. Tondro, N. Sattarahmady, A. Parsa, and H. Heli, "Phytosynthesis of Silver Nanoparticles Using Myrtus communis L. Leaf Extract and Investigation of Bactericidal Activity," *J. Electron. Mater.*, vol. 46, no. 12, pp. 6930–6935, 2017, doi: 10.1007/s11664-017-5784-2.
[121] S. Arokiyaraj, S. Vincent, M. Saravanan, Y. Lee, Y. K. Oh, and K. H. Kim, "Green synthesis of silver nanoparticles using Rheum palmatum root extract and their antibacterial activity against Staphylococcus aureus and Pseudomonas aeruginosa," *Artif. Cells Nanomedicine Biotechnol.*, vol. 45, no. 2, pp. 372–379, Feb. 2017, doi: 10.3109/21691401.2016.1160403.
[122] A. A. Ashour, D. Raafat, H. M. El-Gowelli, and A. H. El-Kamel, "Green synthesis of silver nanoparticles using cranberry powder aqueous extract: characterization and antimicrobial properties," *Int. J. Nanomedicine*, vol. 10, pp. 7207–7221, Dec. 2015, doi: 10.2147/ijn.s87268.
[123] M. Azizi, H. K. Farshchi, F. Oroojalian, and H. Orafaee, "Green Synthesis of Silver Nanoparticles Using Kelussia odoratissima Mozaff. Extract and Evaluation of its Antibacterial Activity," p. 11.
[124] O. Azizian-Shermeh, A. Einali, and A. Ghasemi, "Rapid biologically one-step synthesis of stable bioactive silver nanoparticles using Osage orange (Maclura pomifera) leaf extract and their antimicrobial activities," *Adv. Powder Technol.*, vol. 28, no. 12, pp. 3164–3171, Dec. 2017, doi: 10.1016/j.apt.2017.10.001.

[125] A. Barbasz, M. Oćwieja, and J. Barbasz, “Cytotoxic Activity of Highly Purified Silver Nanoparticles Sol Against Cells of Human Immune System,” *Appl. Biochem. Biotechnol.*, vol. 176, no. 3, pp. 817–834, 2015, doi: 10.1007/s12010-015-1613-3.
[126] T. Baygar and A. Ugur, “In vitro evaluation of antimicrobial and antibiofilm potentials of silver nanoparticles biosynthesised by Streptomyces griseorubens,” *IET Nanobiotechnol.*, vol. 11, no. 6, pp. 677–681, 2017, doi: 10.1049/iet-nbt.2016.0199.
[127] B. Buszewski *et al.*, “Antimicrobial activity of biosilver nanoparticles produced by a novel Streptacidiphilus durhamensis strain,” *J. Microbiol. Immunol. Infect.*, vol. 51, no. 1, pp. 45–54, Feb. 2018, doi: 10.1016/j.jmii.2016.03.002.
[128] N. Chauhan, A. K. Tyagi, P. Kumar, and A. Malik, “Antibacterial Potential of Jatropha curcas Synthesized Silver Nanoparticles against Food Borne Pathogens,” *Front. Microbiol.*, vol. 7, Nov. 2016, doi: 10.3389/fmicb.2016.01748.
[129] N. R. Chowdhury, M. MacGregor-Ramiasa, P. Zilm, P. Majewski, and K. Vasilev, “‘Chocolate’ silver nanoparticles: Synthesis, antibacterial activity and cytotoxicity,” *J. Colloid Interface Sci.*, vol. 482, pp. 151–158, Nov. 2016, doi: 10.1016/j.jcis.2016.08.003.
[130] J. Chumpol and S. Siri, “Simple green production of silver nanoparticles facilitated by bacterial genomic DNA and their antibacterial activity,” *Artif. Cells Nanomedicine Biotechnol.*, vol. 46, no. 3, pp. 619–625, Apr. 2018, doi: 10.1080/21691401.2017.1332638.
[131] B. Das *et al.*, “Green synthesized silver nanoparticles destroy multidrug resistant bacteria via reactive oxygen species mediated membrane damage,” *Arab. J. Chem.*, vol. 10, no. 6, pp. 862–876, 2017, doi: 10.1016/j.arabjc.2015.08.008.
[132] A. Devadiga, K. V. Shetty, and M. B. Saidutta, “Timber industry waste-teak (Tectona grandis Linn.) leaf extract mediated synthesis of antibacterial silver nanoparticles,” *Int. Nano Lett.*, vol. 5, no. 4, pp. 205–214, 2015, doi: 10.1007/s40089-015-0157-4.
[133] A. Devadiga, K. Vidya Shetty, and M. B. Saidutta, “Highly stable silver nanoparticles synthesized using Terminalia catappa leaves as antibacterial agent and colorimetric mercury sensor,” *Mater. Lett.*, vol. 207, pp. 66–71, Nov. 2017, doi: 10.1016/j.matlet.2017.07.024.
[134] R. Dobrucka and J. Długaszewska, “Antimicrobial Activities of Silver Nanoparticles Synthesized by Using Water Extract of Arnicae anthodium,” *Indian J. Microbiol.*, vol. 55, no. 2, pp. 168–174, Jun. 2015, doi: 10.1007/s12088-015-0516-x.
[135] L. Du, S. Zeng, Q. Xu, and J.-X. Feng, “Biosynthesis of Ag Nanoparticles Using Liquefied Cassava Mash and Its Antibacterial Activity Against *Staphylococcus aureus* and *Escherichia coli*,” *J. Nanosci. Nanotechnol.*, vol. 16, no. 8, pp. 8741–8747, Aug. 2016, doi: 10.1166/jnn.2016.12571.
[136] E. E. Elemike, D. C. Onwudiwe, A. C. Ekennia, R. C. Ehiri, and N. J. Nnaji, “Phytosynthesis of silver nanoparticles using aqueous leaf extracts of Lippia citriodora: Antimicrobial, larvicidal and photocatalytic evaluations,” *Mater. Sci. Eng. C*, vol. 75, pp. 980–989, Jun. 2017, doi: 10.1016/j.msec.2017.02.161.
[137] E. E. Elemike, D. C. Onwudiwe, O. E. Fayemi, A. C. Ekennia, E. E. Ebenso, and L. R. Tiedt, “Biosynthesis, Electrochemical, Antimicrobial and Antioxidant Studies of Silver Nanoparticles Mediated by Talinum triangulare Aqueous Leaf Extract,” *J. Clust. Sci.*, vol. 28, no. 1, pp. 309–330, Jan. 2017, doi: 10.1007/s10876-016-1087-7.
[138] K. Elumalai, S. Velmurugan, S. Ravi, V. Kathiravan, and G. Adaikala Raj, “Bio-approach: Plant mediated synthesis of ZnO nanoparticles and their catalytic reduction of methylene

blue and antimicrobial activity," *Adv. Powder Technol.*, vol. 26, no. 6, pp. 1639–1651, Nov. 2015, doi: 10.1016/j.apt.2015.09.008.
[139] C. E. Escárcega-González *et al.*, "In vivo antimicrobial activity of silver nanoparticles produced via a green chemistry synthesis using Acacia rigidula as a reducing and capping agent," *Int. J. Nanomedicine*, vol. 13, pp. 2349–2363, Apr. 2018, doi: 10.2147/ijn.s160605.
[140] M. Ghaedi, M. Yousefinejad, M. Safarpoor, H. Z. Khafri, and M. K. Purkait, "Rosmarinus officinalis leaf extract mediated green synthesis of silver nanoparticles and investigation of its antimicrobial properties," *J. Ind. Eng. Chem.*, vol. 31, pp. 167–172, 2015, doi: 10.1016/j.jiec.2015.06.020.
[141] V. Gopinath *et al.*, "Biogenic synthesis, characterization of antibacterial silver nanoparticles and its cell cytotoxicity," *Arab. J. Chem.*, vol. 10, no. 8, pp. 1107–1117, Dec. 2017, doi: 10.1016/j.arabjc.2015.11.011.
[142] R. K. Gupta, V. Kumar, R. K. Gundampati, M. Malviya, S. H. Hasan, and M. V. Jagannadham, "Biosynthesis of silver nanoparticles from the novel strain of Streptomyces Sp. BHUMBU-80 with highly efficient electroanalytical detection of hydrogen peroxide and antibacterial activity," *J. Environ. Chem. Eng.*, vol. 5, no. 6, pp. 5624–5635, Dec. 2017, doi: 10.1016/j.jece.2017.09.029.
[143] S. M. Hoseini-Alfatemi, A. Karimi, S. Armin, S. Fakharzadeh, F. Fallah, and S. Kalanaky, "Antibacterial and antibiofilm activity of nanochelating based silver nanoparticles against several nosocomial pathogens," *Appl. Organomet. Chem.*, vol. 32, no. 5, p. e4327, 2018, doi: 10.1002/aoc.4327.
[144] H. M. M. Ibrahim, "Green synthesis and characterization of silver nanoparticles using banana peel extract and their antimicrobial activity against representative microorganisms," *J. Radiat. Res. Appl. Sci.*, vol. 8, no. 3, pp. 265–275, Jul. 2015, doi: 10.1016/j.jrras.2015.01.007.
[145] S. Jaiswal and P. Mishra, "Antimicrobial and antibiofilm activity of curcumin-silver nanoparticles with improved stability and selective toxicity to bacteria over mammalian cells," *Med. Microbiol. Immunol. (Berl.)*, vol. 207, no. 1, pp. 39–53, Feb. 2018, doi: 10.1007/s00430-017-0525-y.
[146] A. Jamali, S. Razavizadeh, A. Aliahmadi, and H. Ghomi, "Antibacterial activity of silver and zinc oxide nanoparticles produced by spark discharge in deionized water," *Contrib. Plasma Phys.*, vol. 57, no. 8, pp. 316–321, 2017, doi: 10.1002/ctpp.201600021.
[147] R. Janthima, A. Khamhaengpol, and S. Siri, "Egg extract of apple snail for eco-friendly synthesis of silver nanoparticles and their antibacterial activity," *Artif. Cells Nanomedicine Biotechnol.*, vol. 46, no. 2, pp. 361–367, Feb. 2018, doi: 10.1080/21691401.2017.1313264.
[148] M. A. Karimi, M. A. Mozaheb, H. Tavallali, A. M. Attaran, and G. Deilamy-Rad, "Green synthesis of silver nanoparticles using pollen extract of rose ower and their antibacterial activity," *Sci. Iran.*, p. 9, 2015.
[149] A. H. A. Kelkawi, A. Abbasi Kajani, and A.-K. Bordbar, "Green synthesis of silver nanoparticles using Mentha pulegium and investigation of their antibacterial, antifungal and anticancer activity," *IET Nanobiotechnol.*, vol. 11, no. 4, pp. 370–376, Jun. 2017, doi: 10.1049/iet-nbt.2016.0103.
[150] S. Khorrami, A. Zarrabi, M. Khaleghi, M. Danaei, and M. R. Mozafari, "Selective cytotoxicity of green synthesized silver nanoparticles against the MCF-7 tumor cell line

and their enhanced antioxidant and antimicrobial properties," *Int. J. Nanomedicine*, vol. 13, pp. 8013–8024, Nov. 2018, doi: 10.2147/ijn.s189295.
[151] D.-Y. Kim, J. Suk Sung, M. Kim, and G. Ghodake, "Rapid production of silver nanoparticles at large-scale using gallic acid and their antibacterial assessment," *Mater. Lett.*, vol. 155, pp. 62–64, 2015, doi: 10.1016/j.matlet.2015.04.138.
[152] A. J. Kora and R. B. Sashidhar, "Biogenic silver nanoparticles synthesized with rhamnogalacturonan gum: Antibacterial activity, cytotoxicity and its mode of action," *Arab. J. Chem.*, vol. 11, no. 3, pp. 313–323, Mar. 2018, doi: 10.1016/j.arabjc.2014.10.036.
[153] M. Kumar *et al.*, "Synthesis, characterization, mechanistic studies and antimicrobial efficacy of biomolecule capped and pH modulated silver nanoparticles," *J. Mol. Liq.*, vol. 249, pp. 1145–1150, Jan. 2018, doi: 10.1016/j.molliq.2017.11.143.
[154] V. Kumar, R. K. Gundampati, D. K. Singh, D. Bano, M. V. Jagannadham, and S. H. Hasan, "Photoinduced green synthesis of silver nanoparticles with highly effective antibacterial and hydrogen peroxide sensing properties," *J. Photochem. Photobiol. B*, vol. 162, pp. 374–385, 2016, doi: 10.1016/j.jphotobiol.2016.06.037.
[155] K. D. Lee, P. Kuppusamy, D. H. Kim, N. Govindan, G. P. Maniam, and K. C. Choi, "Forage Crop Lolium multiflorum Assisted Synthesis of AgNPs and Their Bioactivities Against Poultry Pathogenic Bacteria in In Vitro," *Indian J. Microbiol.*, vol. 58, no. 4, pp. 507–514, Dec. 2018, doi: 10.1007/s12088-018-0755-8.
[156] A. B. Leila and A. Parinaz, "Biofabrication of silver nanoparticles using Lactobacillus casei subsp. Casei and its efficacy against human pathogens bacteria and cancer cell lines," p. 12, 2018.
[157] D. Li, Z. Liu, Y. Yuan, Y. Liu, and F. Niu, "Green synthesis of gallic acid-coated silver nanoparticles with high antimicrobial activity and low cytotoxicity to normal cells," *Process Biochem.*, vol. 50, no. 3, pp. 357–366, Mar. 2015, doi: 10.1016/j.procbio.2015.01.002.
[158] K. Li *et al.*, "Making good use of the byproducts of cultivation: green synthesis and antibacterial effects of silver nanoparticles using the leaf extract of blueberry," *J. Food Sci. Technol.*, vol. 54, no. 11, pp. 3569–3576, Oct. 2017, doi: 10.1007/s13197-017-2815-1.
[159] Y. Y. Loo *et al.*, "In Vitro Antimicrobial Activity of Green Synthesized Silver Nanoparticles Against Selected Gram-negative Foodborne Pathogens," *Front. Microbiol.*, vol. 9, Jul. 2018, doi: 10.3389/fmicb.2018.01555.
[160] Y. Ma, C. Liu, D. Qu, Y. Chen, M. Huang, and Y. Liu, "Antibacterial evaluation of sliver nanoparticles synthesized by polysaccharides from Astragalus membranaceus roots," *Biomed. Pharmacother.*, vol. 89, pp. 351–357, 2017, doi: 10.1016/j.biopha.2017.02.009.
[161] W. M. Mahmoud, T. S. Abdelmoneim, and A. M. Elazzazy, "The Impact of Silver Nanoparticles Produced by Bacillus pumilus As Antimicrobial and Nematicide," *Front. Microbiol.*, vol. 7, Nov. 2016, doi: 10.3389/fmicb.2016.01746.
[162] D. A. Marrez *et al.*, "Phenolic profile and antimicrobial activity of green synthesized Acalypha wilkesiana seed's silver nanoparticles against some food borne pathogens," vol. 14, p. 14, 2017.
[163] S. Mathew, A. Prakash, and E. K. Radhakrishnan, "Sunlight mediated rapid synthesis of small size range silver nanoparticles using Zingiber officinale rhizome extract and its antibacterial activity analysis," *Inorg. Nano-Met. Chem.*, vol. 48, no. 2, pp. 139–145, Feb. 2018, doi: 10.1080/24701556.2017.1373295.

[164] S. Mohan *et al.*, “Synthesis, antibacterial, cytotoxicity and sensing properties of starch-capped silver nanoparticles,” *J. Mol. Liq.*, vol. 213, pp. 75–81, 2016, doi: 10.1016/j.molliq.2015.11.010.
[165] J. S. Moodley, S. B. N. Krishna, K. Pillay, and P. Govender, “PRODUCTION, CHARACTERIZATION AND ANTIMICROBIAL ACTIVITY OF SILVER NANOPARTICLES PRODUCED BY PEDIOCOCCUS ACIDILACTICI,” p. 11.
[166] S. Paosen, J. Saising, A. Wira Septama, and S. Piyawan Voravuthikunchai, “Green synthesis of silver nanoparticles using plants from Myrtaceae family and characterization of their antibacterial activity,” *Mater. Lett.*, vol. 209, pp. 201–206, Dec. 2017, doi: 10.1016/j.matlet.2017.07.102.
[167] M. Parlinska-Wojtan, M. Kus-Liskiewicz, J. Depciuch, and O. Sadik, “Green synthesis and antibacterial effects of aqueous colloidal solutions of silver nanoparticles using camomile terpenoids as a combined reducing and capping agent,” *Bioprocess Biosyst. Eng.*, vol. 39, no. 8, pp. 1213–1223, Aug. 2016, doi: 10.1007/s00449-016-1599-4.
[168] M. P. Patil, A. A. Rokade, D. Ngabire, and G.-D. Kim, “Green Synthesis of Silver Nanoparticles Using Water Extract from Galls of Rhus Chinensis and Its Antibacterial Activity,” *J. Clust. Sci.*, vol. 27, no. 5, pp. 1737–1750, Sep. 2016, doi: 10.1007/s10876-016-1037-4.
[169] M. P. Patil *et al.*, “Antibacterial potential of silver nanoparticles synthesized using Madhuca longifolia flower extract as a green resource,” *Microb. Pathog.*, vol. 121, pp. 184–189, Aug. 2018, doi: 10.1016/j.micpath.2018.05.040.
[170] A. Pompilio *et al.*, “Electrochemically Synthesized Silver Nanoparticles Are Active Against Planktonic and Biofilm Cells of Pseudomonas aeruginosa and Other Cystic Fibrosis-Associated Bacterial Pathogens,” *Front. Microbiol.*, vol. 9, Jul. 2018, doi: 10.3389/fmicb.2018.01349.
[171] W. R. Rolim *et al.*, “Green tea extract mediated biogenic synthesis of silver nanoparticles: Characterization, cytotoxicity evaluation and antibacterial activity,” *Appl. Surf. Sci.*, vol. 463, pp. 66–74, Jan. 2019, doi: 10.1016/j.apsusc.2018.08.203.
[172] H. I. Salaheldin, M. H. K. Almalki, A. E. M. Hezma, and G. E. H. Osman, “Facile synthesis of silver nanoparticles mediated by polyacrylamide-reduction approach to antibacterial application,” *IET Nanobiotechnol.*, vol. 11, no. 4, pp. 448–453, 2017, doi: 10.1049/iet-nbt.2016.0135.
[173] G. M. Sangaonkar and K. D. Pawar, “Garcinia indica mediated biogenic synthesis of silver nanoparticles with antibacterial and antioxidant activities,” *Colloids Surf. B Biointerfaces*, vol. 164, pp. 210–217, Apr. 2018, doi: 10.1016/j.colsurfb.2018.01.044.
[174] R. G. Saratale, G. Benelli, G. Kumar, D. S. Kim, and G. D. Saratale, “Bio-fabrication of silver nanoparticles using the leaf extract of an ancient herbal medicine, dandelion (Taraxacum officinale), evaluation of their antioxidant, anticancer potential, and antimicrobial activity against phytopathogens,” *Environ. Sci. Pollut. Res.*, vol. 25, no. 11, pp. 10392–10406, Apr. 2018, doi: 10.1007/s11356-017-9581-5.
[175] K. Saravanakumar *et al.*, “Green synthesis and characterization of biologically active nanosilver from seed extract of Gardenia jasminoides Ellis,” *J. Photochem. Photobiol. B*, vol. 185, pp. 126–135, Aug. 2018, doi: 10.1016/j.jphotobiol.2018.05.032.
[176] M. Shaaban and A. M. El-Mahdy, “Biosynthesis of Ag, Se, and ZnO nanoparticles with antimicrobial activities against resistant pathogens using waste isolateStreptomyces

enissocaesilis," *IET Nanobiotechnol.*, vol. 12, no. 6, pp. 741–747, 2018, doi: 10.1049/iet-nbt.2017.0213.
[177] M. A. Shaker and M. I. Shaaban, "Synthesis of silver nanoparticles with antimicrobial and anti-adherence activities against multidrug-resistant isolates from Acinetobacter baumannii," *J. Taibah Univ. Med. Sci.*, vol. 12, no. 4, pp. 291–297, Aug. 2017, doi: 10.1016/j.jtumed.2017.02.008.
[178] C. S. Shivananda *et al.*, "Biosynthesis of colloidal silver nanoparticles: Their characterization and potential antibacterial activity," *Macromol. Res.*, vol. 24, no. 8, pp. 684–690, 2016, doi: 10.1007/s13233-016-4086-5.
[179] S. N. Sinha and D. Paul, "Phytosynthesis of Silver Nanoparticles Using Andrographis paniculata Leaf Extract and Evaluation of Their Antibacterial Activities," *Spectrosc. Lett.*, vol. 48, no. 8, pp. 600–604, Sep. 2015, doi: 10.1080/00387010.2014.938756.
[180] N. Skandalis *et al.*, "The Effect of Silver Nanoparticles Size, Produced Using Plant Extract from Arbutus unedo, on Their Antibacterial Efficacy," *Nanomaterials*, vol. 7, no. 7, p. 178, 2017, doi: 10.3390/nano7070178.
[181] M. Składanowski, P. Golinska, K. Rudnicka, H. Dahm, and M. Rai, "Evaluation of cytotoxicity, immune compatibility and antibacterial activity of biogenic silver nanoparticles," *Med. Microbiol. Immunol. (Berl.)*, vol. 205, no. 6, pp. 603–613, Dec. 2016, doi: 10.1007/s00430-016-0477-7.
[182] F. F. Soleimani, T. Saleh, S. A. Shojaosadati, and R. Poursalehi, "Green Synthesis of Different Shapes of Silver Nanostructures and Evaluation of Their Antibacterial and Cytotoxic Activity," *BioNanoScience*, vol. 8, no. 1, pp. 72–80, Mar. 2018, doi: 10.1007/s12668-017-0423-1.
[183] T. Suwan, S. Khongkhunthian, J. Sirithunyalug, and S. Okonogi, "Effect of rice variety and reaction parameters on synthesis and antibacterial activity of silver nanoparticles," *Drug Discov. Ther.*, vol. 12, no. 5, pp. 267–274, Oct. 2018, doi: 10.5582/ddt.2018.01058.
[184] S. Thanganadar Appapalam and R. Panchamoorthy, "Aerva lanata mediated phytofabrication of silver nanoparticles and evaluation of their antibacterial activity against wound associated bacteria," *J. Taiwan Inst. Chem. Eng.*, vol. 78, pp. 539–551, Sep. 2017, doi: 10.1016/j.jtice.2017.06.035.
[185] N. T. K. Thanh, N. Maclean, and S. Mahiddine, "Mechanisms of Nucleation and Growth of Nanoparticles in Solution," *Chem. Rev.*, vol. 114, no. 15, pp. 7610–7630, Aug. 2014, doi: 10.1021/cr400544s.
[186] C. Vanlalveni, K. Rajkumari, A. Biswas, P. P. Adhikari, R. Lalfakzuala, and L. Rokhum, "Green Synthesis of Silver Nanoparticles Using Nostoc linckia and its Antimicrobial Activity: a Novel Biological Approach," *BioNanoScience*, vol. 8, no. 2, pp. 624–631, Jun. 2018, doi: 10.1007/s12668-018-0520-9.
[187] R. Varghese, M. A. Almalki, S. Ilavenil, J. Rebecca, and K. C. Choi, "Silver nanopaticles synthesized using the seed extract of Trigonella foenum-graecum L. and their antimicrobial mechanism and anticancer properties," *Saudi J. Biol. Sci.*, vol. 26, no. 1, pp. 148–154, Jan. 2019, doi: 10.1016/j.sjbs.2017.07.001.
[188] R. Vazquez-Muñoz *et al.*, "Toxicity of silver nanoparticles in biological systems: Does the complexity of biological systems matter?," *Toxicol. Lett.*, vol. 276, pp. 11–20, Jul. 2017, doi: 10.1016/j.toxlet.2017.05.007.
[189] D. K. Verma, S. H. Hasan, and R. M. Banik, "Photo-catalyzed and phyto-mediated rapid green synthesis of silver nanoparticles using herbal extract of Salvinia molesta and its

antimicrobial efficacy," *J. Photochem. Photobiol. B*, vol. 155, pp. 51–59, 2016, doi: 10.1016/j.jphotobiol.2015.12.008.
[190] Y. Wu, Y. Yang, Z. Zhang, Z. Wang, Y. Zhao, and L. Sun, "A facile method to prepare size-tunable silver nanoparticles and its antibacterial mechanism," *Adv. Powder Technol.*, vol. 29, no. 2, pp. 407–415, Feb. 2018, doi: 10.1016/j.apt.2017.11.028.
[191] M. Wypij, P. Golinska, H. Dahm, and M. Rai, "Actinobacterial-mediated synthesis of silver nanoparticles and their activity against pathogenic bacteria," *IET Nanobiotechnol.*, vol. 11, no. 3, pp. 336–342, 2017, doi: 10.1049/iet-nbt.2016.0112.
[192] M. Wypij, J. Czarnecka, M. Świecimska, H. Dahm, M. Rai, and P. Golinska, "Synthesis, characterization and evaluation of antimicrobial and cytotoxic activities of biogenic silver nanoparticles synthesized from Streptomyces xinghaiensis OF1 strain," *World J. Microbiol. Biotechnol.*, vol. 34, no. 2, 2018, doi: 10.1007/s11274-017-2406-3.
[193] Q. H. Xia, Y. J. Ma, and J. W. Wang, "Biosynthesis of Silver Nanoparticles Using Taxus yunnanensis Callus and Their Antibacterial Activity and Cytotoxicity in Human Cancer Cells," *Nanomater. Basel*, vol. 6, no. 9, p. 160, 2016, doi: http://dx.doi.org/10.3390/nano6090160.
[194] H. Xu *et al.*, "Making Good Use of Food Wastes: Green Synthesis of Highly Stabilized Silver Nanoparticles from Grape Seed Extract and Their Antimicrobial Activity," *Food Biophys.*, vol. 10, no. 1, pp. 12–18, Mar. 2015, doi: 10.1007/s11483-014-9343-6.
[195] F. Zandpour, A. R. Allafchian, M. R. Vahabi, and S. A. H. Jalali, "Green synthesis of silver nanoparticles with the Arial part of Dorema ammoniacum D. extract by antimicrobial analysis," *IET Nanobiotechnol.*, vol. 12, no. 4, pp. 491–495, 2018, doi: 10.1049/iet-nbt.2017.0216.
[196] A. Ananth, S. Dharaneedharan, M.-S. Heo, and Y. S. Mok, "Copper oxide nanomaterials: Synthesis, characterization and structure-specific antibacterial performance," *Chem. Eng. J.*, vol. 262, pp. 179–188, 2015, doi: 10.1016/j.cej.2014.09.083.
[197] S. Babaei, A. Abbasi, and N. Sohrabi, "Investigating the Susceptibility and Death Kinetic of Pseudomonas Aeruginosa Bacterium Standard and Clinical Strains to the Copper Oxide Nanoparticle," *J. Res. Med. Dent. Sci.*, vol. 6, no. 2, p. 6, 2018.
[198] R. Chakraborty, R. K. Sarkar, A. K. Chatterjee, U. Manju, A. P. Chattopadhyay, and T. Basu, "A simple, fast and cost-effective method of synthesis of cupric oxide nanoparticle with promising antibacterial potency: Unraveling the biological and chemical modes of action," *Biochim. Biophys. Acta BBA - Gen. Subj.*, vol. 1850, no. 4, pp. 845–856, Apr. 2015, doi: 10.1016/j.bbagen.2015.01.015.
[199] A. H. Keihan, H. Veisi, and H. Veasi, "Green synthesis and characterization of spherical copper nanoparticles as organometallic antibacterial agent," *Appl. Organomet. Chem.*, vol. 31, no. 7, p. e3642, 2017, doi: 10.1002/aoc.3642.
[200] T. Kruk, K. Szczepanowicz, J. Stefańska, R. P. Socha, and P. Warszyński, "Synthesis and antimicrobial activity of monodisperse copper nanoparticles," *Colloids Surf. B Biointerfaces*, vol. 128, pp. 17–22, Apr. 2015, doi: 10.1016/j.colsurfb.2015.02.009.
[201] R. Pandit, S. Gaikwad, and M. Rai, "Biogenic fabrication of CuNPs, Cu bioconjugates and in vitro assessment of antimicrobial and antioxidant activity," *IET Nanobiotechnol.*, vol. 11, no. 5, pp. 568–575, 2017, doi: 10.1049/iet-nbt.2016.0165.
[202] S. Shiravand, H. Mahmoudvand, and K. Ebrahimi, "Biosynthesis of copper nanoparticles using aqueous extract of Capparis spinosa fruit and investigation of its antibacterial

activity," *Marmara Pharm. J.*, vol. 21, no. 4, pp. 866–871, Oct. 2017, doi: 10.12991/mpj.2017.31.
[203] A. Chahardoli, N. Karimi, F. Sadeghi, and A. Fattahi, "Green approach for synthesis of gold nanoparticles from *Nigella arvensis* leaf extract and evaluation of their antibacterial, antioxidant, cytotoxicity and catalytic activities," *Artif. Cells Nanomedicine Biotechnol.*, vol. 46, no. 3, pp. 579–588, Apr. 2018, doi: 10.1080/21691401.2017.1332634.
[204] M. Hamelian, S. Hemmati, K. Varmira, and H. Veisi, "Green synthesis, antibacterial, antioxidant and cytotoxic effect of gold nanoparticles using Pistacia Atlantica extract," *J. Taiwan Inst. Chem. Eng.*, vol. 93, pp. 21–30, Dec. 2018, doi: 10.1016/j.jtice.2018.07.018.
[205] M. Hamelian, K. Varmira, and H. Veisi, "Green synthesis and characterizations of gold nanoparticles using Thyme and survey cytotoxic effect, antibacterial and antioxidant potential," *J. Photochem. Photobiol. B*, vol. 184, pp. 71–79, Jul. 2018, doi: 10.1016/j.jphotobiol.2018.05.016.
[206] M. Jafari *et al.*, "Cytotoxic and antibacterial activities of biologically synthesized gold nanoparticles assisted by Micrococcus yunnanensis strain J2," *Biocatal. Agric. Biotechnol.*, vol. 15, pp. 245–253, 2018, doi: 10.1016/j.bcab.2018.06.014.
[207] A. U. Khan *et al.*, "Photocatalytic and antibacterial response of biosynthesized gold nanoparticles," *J. Photochem. Photobiol. B*, vol. 162, pp. 273–277, Sep. 2016, doi: 10.1016/j.jphotobiol.2016.06.055.
[208] S. Layeghi-Ghalehsoukhteh, J. Jalaei, M. Fazeli, P. Memarian, and S. S. Shekarforoush, "Evaluation of 'green' synthesis and biological activity of gold nanoparticles usingTragopogon dubiusleaf extract as an antibacterial agent," *IET Nanobiotechnol.*, vol. 12, no. 8, pp. 1118–1124, 2018, doi: 10.1049/iet-nbt.2018.5073.
[209] N. Srivastava and M. Mukhopadhyay, "Biosynthesis and Characterization of Gold Nanoparticles Using Zooglea ramigera and Assessment of Its Antibacterial Property," *J. Clust. Sci.*, vol. 26, no. 3, pp. 675–692, May 2015, doi: 10.1007/s10876-014-0726-0.
[210] S. G. Daghdari, M. Ahmadi, H. D. Saei, and A. A. Tehrani, "The effect of ZnO nanoparticles on bacterial load of experimental infectious wounds contaminated with Staphylococcus aureus in mice," p. 5, 2017.
[211] S. Fanny Chiat Orou *et al.*, "Antibacterial activity by ZnO nanorods and ZnO nanodisks: A model used to illustrate 'Nanotoxicity Threshold,'" *J. Ind. Eng. Chem.*, vol. 62, pp. 333–340, Jun. 2018, doi: 10.1016/j.jiec.2018.01.013.
[212] O. Kahraman, R. Binzet, E. Turunc, A. Dogen, and H. Arslan, "Synthesis, characterization, antimicrobial and electrochemical activities of zinc oxide nanoparticles obtained from sarcopoterium spinosum (L.) spach leaf extract," *Mater. Res. Express*, vol. 5, no. 11, p. 115017, Sep. 2018, doi: 10.1088/2053-1591/aad953.
[213] M. Khatami, H. Q. Alijani, H. Heli, and I. Sharifi, "Rectangular shaped zinc oxide nanoparticles: Green synthesis by Stevia and its biomedical efficiency," *Ceram. Int.*, vol. 44, no. 13, pp. 15596–15602, 2018, doi: 10.1016/j.ceramint.2018.05.224.
[214] C. Mahendra *et al.*, "Antibacterial and antimitotic potential of bio-fabricated zinc oxide nanoparticles of Cochlospermum religiosum (L.)," *Microb. Pathog.*, vol. 110, pp. 620–629, 2017, doi: 10.1016/j.micpath.2017.07.051.
[215] M. Maruthupandy, G. Rajivgandhi, T. Muneeswaran, J.-M. Song, and N. Manoharan, "Biologically synthesized zinc oxide nanoparticles as nanoantibiotics against ESBLs producing gram negative bacteria," *Microb. Pathog.*, vol. 121, pp. 224–231, Aug. 2018, doi: 10.1016/j.micpath.2018.05.041.

[216] A. Oquendo-Cruz and O. Perales-Pérez, “Synthesis, Characterization and Bactericide Properties of Pure and Li Doped ZnO Nanoparticles for Alternative Water Disinfection Methods,” *J. Electron. Mater.*, vol. 47, no. 10, pp. 6260–6265, 2018, doi: 10.1007/s11664-018-6541-x.
[217] G. Patrinoiu, J. M. Calderón-Moreno, C. M. Chifiriuc, C. Saviuc, R. Birjega, and O. Carp, “Tunable ZnO spheres with high anti-biofilm and antibacterial activity via a simple green hydrothermal route,” *J. Colloid Interface Sci.*, vol. 462, pp. 64–74, Jan. 2016, doi: 10.1016/j.jcis.2015.09.059.
[218] C. Pholnak, M. Lertworapreecha, C. Sirisathitkul, and S. Suwanboon, “Antibacterial and physical properties of ZnO with pH-sensitive morphology,” *J. Exp. Nanosci.*, vol. 11, no. 17, pp. 1320–1330, Nov. 2016, doi: 10.1080/17458080.2016.1214984.
[219] H. Rokbani, F. Daigle, and A. Ajji, “Combined Effect of Ultrasound Stimulations and Autoclaving on the Enhancement of Antibacterial Activity of ZnO and SiO2/ZnO Nanoparticles,” *Nanomaterials*, vol. 8, no. 3, Feb. 2018, doi: 10.3390/nano8030129.
[220] J. P. Shabaaz Begum, M. K. Sateesh, H. Nagabhushana, and R. B. Basavaraj, “Averrhoa carambola L. assisted phytonanofabrication of zinc oxide nanoparticles and its anti-microbial activity against drug resistant microbes,” *Mater. Today Proc.*, vol. 5, no. 10, Part 1, pp. 21489–21497, Jan. 2018, doi: 10.1016/j.matpr.2018.06.559.
[221] K. Steffy, G. Shanthi, A. S. Maroky, and S. Selvakumar, “Potential bactericidal activity of S. nux-vomica–ZnO nanocomposite against multidrug-resistant bacterial pathogens and wound-healing properties,” *J. Trace Elem. Med. Biol.*, vol. 50, no. Complete, pp. 229–239, 2018, doi: 10.1016/j.jtemb.2018.07.009.
[222] E. Zare, S. Pourseyedi, M. Khatami, and E. Darezereshki, “Simple biosynthesis of zinc oxide nanoparticles using nature’s source, and it’s in vitro bio-activity,” *J. Mol. Struct.*, vol. 1146, pp. 96–103, Oct. 2017, doi: 10.1016/j.molstruc.2017.05.118.
[223] L. B. Reller, M. Weinstein, J. H. Jorgensen, and M. J. Ferraro, “Antimicrobial Susceptibility Testing: A Review of General Principles and Contemporary Practices,” *Clin. Infect. Dis.*, vol. 49, no. 11, pp. 1749–1755, 2009, doi: 10.1086/647952.
[224] CLSI, “Methods for Dilution Antimicrobial Susceptibility Tests for Bacteria That Grow Aerobically, 11th ed.,” Clinical and Laboratory Standards Institute, CLSI Standard M07, Jan. 2018.
[225] A. M. El Badawy, R. G. Silva, B. Morris, K. G. Scheckel, M. T. Suidan, and T. M. Tolaymat, “Surface Charge-Dependent Toxicity of Silver Nanoparticles,” *Environ. Sci. Technol.*, vol. 45, no. 1, pp. 283–287, Jan. 2011, doi: 10.1021/es1034188.
[226] G. Tetz, D. Vikina, and V. Tetz, “Antimicrobial activity of mul-1867, a novel antimicrobial compound, against multidrug-resistant Pseudomonas aeruginosa,” *Ann. Clin. Microbiol. Antimicrob.*, vol. 15, no. 1, p. 19, Mar. 2016, doi: 10.1186/s12941-016-0134-4.
[227] Y. S. Park *et al.*, “Acquisition of extensive drug-resistant Pseudomonas aeruginosa among hospitalized patients: risk factors and resistance mechanisms to carbapenems,” *J. Hosp. Infect.*, vol. 79, no. 1, pp. 54–58, Sep. 2011, doi: https://doi.org/10.1016/j.jhin.2011.05.014.
[228] J. F. Acar, F. W. Goldstein, M. D. Kitzis, and L. Gutmann, “Activity of imipenem on aerobic bacteria,” *J. Antimicrob. Chemother.*, vol. 12, no. suppl D, pp. 37–45, Jan. 1983, doi: 10.1093/jac/12.suppl_D.37.
[229] P. Ball, “Emergent resistance to ciprofloxacin amongst Pseudomonas aeruginosa and Staphylococcus aureus :clinical significance and therapeutic approaches,” *J. Antimicrob.*

Chemother., vol. 26, no. suppl_F, pp. 165–179, Jan. 1990, doi: 10.1093/jac/26.suppl_F.165.
[230] C. I. Bustamante, G. L. Drusano, B. A. Tatem, and H. C. Standiford, "Postantibiotic effect of imipenem on Pseudomonas aeruginosa," *Antimicrob. Agents Chemother.*, vol. 26, no. 5, pp. 678–682, Nov. 1984, doi: 10.1128/aac.26.5.678.
[231] M. A. Cohen, M. D. Huband, J. W. Gage, S. L. Yoder, G. E. Roland, and S. J. Gracheck, "In-vitro activity of clinafloxacin, trovafloxacin, and ciprofloxacin," *J. Antimicrob. Chemother.*, vol. 40, no. 2, pp. 205–211, Aug. 1997, doi: 10.1093/jac/40.2.205.
[232] J. M. Hyatt, D. E. Nix, and J. J. Schentag, "Pharmacokinetic and pharmacodynamic activities of ciprofloxacin against strains of Streptococcus pneumoniae, Staphylococcus aureus, and Pseudomonas aeruginosa for which MICs are similar," *Antimicrob. Agents Chemother.*, vol. 38, no. 12, pp. 2730–2737, Dec. 1994, doi: 10.1128/aac.38.12.2730.
[233] M. H. Limoncu, S. Ermertcan, Ç. B. Çetin, G. Cosar, and G. Dinç, "Emergence of phenotypic resistance to ciprofloxacin and levofloxacin in methicillin-resistant and methicillin-sensitive Staphylococcus aureus strains," *Int. J. Antimicrob. Agents*, vol. 21, no. 5, pp. 420–424, May 2003, doi: 10.1016/s0924-8579(03)00006-2.
[234] A. P. MacGowan, M. Wootton, and H. A. Holt, "The antibacterial efficacy of levofloxacin and ciprofloxacin against Pseudomonas aeruginosaassessed by combining antibiotic exposure and bacterial susceptibility," *J. Antimicrob. Chemother.*, vol. 43, no. 3, pp. 345–349, Mar. 1999, doi: 10.1093/jac/43.3.345.
[235] D. J. Mason, E. G. Power, H. Talsania, I. Phillips, and V. A. Gant, "Antibacterial action of ciprofloxacin," *Antimicrob. Agents Chemother.*, vol. 39, no. 12, p. 2752, Dec. 1995, doi: 10.1128/aac.39.12.2752.
[236] J. P. Quinn, E. J. Dudek, C. A. DiVincenzo, D. A. Lucks, and S. A. Lerner, "Emergence of Resistance to Imipenem During Therapy for Pseudomonas aeruginosa Infections," *J. Infect. Dis.*, vol. 154, no. 2, pp. 289–294, Aug. 1986, doi: 10.1093/infdis/154.2.289.
[237] N. J. Robillard and A. L. Scarpa, "Genetic and physiological characterization of ciprofloxacin resistance in Pseudomonas aeruginosa PAO," *Antimicrob. Agents Chemother.*, vol. 32, no. 4, pp. 535–539, Apr. 1988, doi: 10.1128/aac.32.4.535.
[238] M. O. Santos-Ferreira and J. O. Vital, "In-vitro antibacterial activity of imipenem compared with four other [3- lactam antibiotics (ceftazidime, cefotaxime, piperacillin and azlocillin) against 828 separate clinical isolates from a Portuguese hospital," p. 4.
[239] W. M. Scheld and J. M. Keeley, "Imipenem therapy of experimental Staphylococcus aureus and Streptococcus faecalis endocarditis," *J. Antimicrob. Chemother.*, vol. 12, no. suppl D, pp. 65–78, Jan. 1983, doi: 10.1093/jac/12.suppl_D.65.
[240] Y. Sumita, M. Fukasawa, and T. Okuda, "Comparison of two carbapenems, SM-7338 and imipenem. Affinities for penicillin-binding proteins and morphological changes," *J. Antibiot. (Tokyo)*, vol. 43, no. 3, pp. 314–320, 1990, doi: 10.7164/antibiotics.43.314.
[241] H. J. Zeiler, "Evaluation of the in vitro bactericidal action of ciprofloxacin on cells of Escherichia coli in the logarithmic and stationary phases of growth," *Antimicrob. Agents Chemother.*, vol. 28, no. 4, pp. 524–527, Oct. 1985, doi: 10.1128/aac.28.4.524.
[242] K. S. Butler, D. J. Peeler, B. J. Casey, B. J. Dair, and R. K. Elespuru, "Silver nanoparticles: correlating nanoparticle size and cellular uptake with genotoxicity," *Mutagenesis*, vol. 30, no. 4, pp. 577–591, Jul. 2015, doi: 10.1093/mutage/gev020.

[243] O. Choi and Z. Hu, “Size Dependent and Reactive Oxygen Species Related Nanosilver Toxicity to Nitrifying Bacteria,” *Environ. Sci. Technol.*, vol. 42, no. 12, pp. 4583–4588, Jun. 2008, doi: 10.1021/es703238h.
[244] H. Yang *et al.*, “Detailed insight into the formation of protein corona: Conformational change, stability and aggregation,” *Int. J. Biol. Macromol.*, vol. 135, pp. 1114–1122, Aug. 2019, doi: 10.1016/j.ijbiomac.2019.06.014.
[245] D. K. Ban and S. Paul, “Protein corona over silver nanoparticles triggers conformational change of proteins and drop in bactericidal potential of nanoparticles: Polyethylene glycol capping as preventive strategy,” *Colloids Surf. B Biointerfaces*, vol. 146, pp. 577–584, Oct. 2016, doi: 10.1016/j.colsurfb.2016.06.050.
[246] M. R. Salvadori, R. A. Ando, C. A. O. Nascimento, and B. Corrêa, “Extra and Intracellular Synthesis of Nickel Oxide Nanoparticles Mediated by Dead Fungal Biomass,” *PLOS ONE*, vol. 10, no. 6, p. e0129799, Jun. 2015, doi: 10.1371/journal.pone.0129799.
[247] S. V. Otari, R. M. Patil, S. J. Ghosh, N. D. Thorat, and S. H. Pawar, “Intracellular synthesis of silver nanoparticle by actinobacteria and its antimicrobial activity,” *Spectrochim. Acta. A. Mol. Biomol. Spectrosc.*, vol. 136, pp. 1175–1180, Feb. 2015, doi: 10.1016/j.saa.2014.10.003.
[248] A. Ahmad *et al.*, “Intracellular synthesis of gold nanoparticles by a novel alkalotolerant actinomycete,Rhodococcusspecies,” *Nanotechnology*, vol. 14, no. 7, pp. 824–828, Jun. 2003, doi: 10.1088/0957-4484/14/7/323.
[249] G. Singaravelu, J. S. Arockiamary, V. G. Kumar, and K. Govindaraju, “A novel extracellular synthesis of monodisperse gold nanoparticles using marine alga, Sargassum wightii Greville,” *Colloids Surf. B Biointerfaces*, vol. 57, no. 1, pp. 97–101, May 2007, doi: 10.1016/j.colsurfb.2007.01.010.
[250] M. Kowshik *et al.*, “Extracellular synthesis of silver nanoparticles by a silver-tolerant yeast strain MKY3,” *Nanotechnology*, vol. 14, no. 1, pp. 95–100, Dec. 2002, doi: 10.1088/0957-4484/14/1/321.
[251] P. Mukherjee *et al.*, “Extracellular Synthesis of Gold Nanoparticles by the Fungus Fusarium oxysporum,” *ChemBioChem*, vol. 3, no. 5, pp. 461–463, May 2002, doi: 10.1002/1439-7633(20020503)3:5<461::AID-CBIC461>3.0.CO;2-X.
[252] S. P. Chandran, M. Chaudhary, R. Pasricha, A. Ahmad, and M. Sastry, “Synthesis of Gold Nanotriangles and Silver Nanoparticles Using Aloevera Plant Extract,” *Biotechnol. Prog.*, vol. 22, no. 2, pp. 577–583, 2006, doi: 10.1021/bp0501423.
[253] N. A. Begum, S. Mondal, S. Basu, R. A. Laskar, and D. Mandal, “Biogenic synthesis of Au and Ag nanoparticles using aqueous solutions of Black Tea leaf extracts,” *Colloids Surf. B Biointerfaces*, vol. 71, no. 1, pp. 113–118, Jun. 2009, doi: 10.1016/j.colsurfb.2009.01.012.
[254] J. Y. Song and B. S. Kim, “Rapid biological synthesis of silver nanoparticles using plant leaf extracts,” *Bioprocess Biosyst. Eng.*, vol. 32, no. 1, p. 79, Apr. 2008, doi: 10.1007/s00449-008-0224-6.
[255] E. Lam, K. B. Male, J. H. Chong, A. C. W. Leung, and J. H. T. Luong, “Applications of functionalized and nanoparticle-modified nanocrystalline cellulose,” *Trends Biotechnol.*, vol. 30, no. 5, pp. 283–290, May 2012, doi: 10.1016/j.tibtech.2012.02.001.

[256] S. Beck, J. Bouchard, and R. Berry, “Dispersibility in Water of Dried Nanocrystalline Cellulose,” *Biomacromolecules*, vol. 13, no. 5, pp. 1486–1494, May 2012, doi: 10.1021/bm300191k.
[257] M. Mariano, N. E. Kissi, and A. Dufresne, “Cellulose nanocrystals and related nanocomposites: Review of some properties and challenges,” *J. Polym. Sci. Part B Polym. Phys.*, vol. 52, no. 12, pp. 791–806, 2014, doi: 10.1002/polb.23490.
[258] M. Yadav, Y.-K. Liu, and F.-C. Chiu, “Fabrication of Cellulose Nanocrystal/Silver/Alginate Bionanocomposite Films with Enhanced Mechanical and Barrier Properties for Food Packaging Application,” *Nanomaterials*, vol. 9, no. 11, Art. no. 11, Nov. 2019, doi: 10.3390/nano9111523.
[259] F. Luzi, E. Fortunati, A. Jiménez, D. Puglia, A. Chiralt, and L. Torre, “PLA Nanocomposites Reinforced with Cellulose Nanocrystals from Posidonia oceanica and ZnO Nanoparticles for Packaging Application,” *J. Renew. Mater.*, vol. 5, no. 2, pp. 103–115, Apr. 2017, doi: 10.7569/JRM.2016.634135.
[260] K. K. Sadasivuni, D. Ponnamma, H.-U. Ko, H. C. Kim, L. Zhai, and J. Kim, “Flexible NO2 sensors from renewable cellulose nanocrystals/iron oxide composites,” *Sens. Actuators B Chem.*, vol. 233, pp. 633–638, Oct. 2016, doi: 10.1016/j.snb.2016.04.134.
[261] K. B. R. Teodoro, F. L. Migliorini, W. A. Christinelli, and D. S. Correa, “Detection of hydrogen peroxide (H2O2) using a colorimetric sensor based on cellulose nanowhiskers and silver nanoparticles,” *Carbohydr. Polym.*, vol. 212, pp. 235–241, May 2019, doi: 10.1016/j.carbpol.2019.02.053.
[262] K. Bethke *et al.*, “Functionalized Cellulose for Water Purification, Antimicrobial Applications, and Sensors,” *Adv. Funct. Mater.*, vol. 28, no. 23, p. 1800409, 2018, doi: 10.1002/adfm.201800409.
[263] S. Y. H. Abdalkarim, H.-Y. Yu, C. Wang, L.-X. Huang, and J. Yao, “Green synthesis of sheet-like cellulose nanocrystal–zinc oxide nanohybrids with multifunctional performance through one-step hydrothermal method,” *Cellulose*, vol. 25, no. 11, pp. 6433–6446, Nov. 2018, doi: 10.1007/s10570-018-2011-0.
[264] Th. I. Shaheen and A. Fouda, “Green approach for one-pot synthesis of silver nanorod using cellulose nanocrystal and their cytotoxicity and antibacterial assessment,” *Int. J. Biol. Macromol.*, vol. 106, pp. 784–792, Jan. 2018, doi: 10.1016/j.ijbiomac.2017.08.070.
[265] Y. Wen, S. Pan, X. Luo, X. Zhang, W. Zhang, and M. Feng, “A biodegradable low molecular weight polyethylenimine derivative as low toxicity and efficient gene vector,” *Bioconjug. Chem.*, vol. 20, no. 2, pp. 322–332, Feb. 2009, doi: 10.1021/bc800428y.
[266] Z. Shi *et al.*, “Enhanced colloidal stability and antibacterial performance of silver nanoparticles/cellulose nanocrystal hybrids,” *J. Mater. Chem. B*, vol. 3, no. 4, pp. 603–611, Dec. 2014, doi: 10.1039/C4TB01647E.
[267] F. Liu, V. Kozlovskaya, O. Zavgorodnya, C. Martinez-Lopez, S. Catledge, and E. Kharlampieva, “Encapsulation of anticancer drug by hydrogen-bonded multilayers of tannic acid,” *Soft Matter*, vol. 10, no. 46, pp. 9237–9247, 2014, doi: 10.1039/C4SM01813C.
[268] T. Ahmad, “Reviewing the Tannic Acid Mediated Synthesis of Metal Nanoparticles,” *Journal of Nanotechnology*, 2014. https://www.hindawi.com/journals/jnt/2014/954206/ (accessed Mar. 02, 2020).

[269] S. K. Sivaraman, I. Elango, S. Kumar, and V. Santhanam, “A green protocol for room temperature synthesis of silver nanoparticles in seconds,” *Curr. Sci.*, vol. 97, no. 7, p. 5, 2009.
[270] Z. Yi *et al.*, “Green, effective chemical route for the synthesis of silver nanoplates in tannic acid aqueous solution,” *Colloids Surf. Physicochem. Eng. Asp.*, vol. 392, no. 1, pp. 131–136, Dec. 2011, doi: 10.1016/j.colsurfa.2011.09.045.
[271] Z. Fu and R. Chen, “Study of Complexes of Tannic Acid with Fe(III) and Fe(II),” *Journal of Analytical Methods in Chemistry*, 2019. https://www.hindawi.com/journals/jamc/2019/3894571/ (accessed Nov. 04, 2019).
[272] P. Kraal, B. Jansen, K. G. J. Nierop, and J. M. Verstraten, “Copper complexation by tannic acid in aqueous solution,” *Chemosphere*, vol. 65, no. 11, pp. 2193–2198, Dec. 2006, doi: 10.1016/j.chemosphere.2006.05.058.
[273] J. Tang, Z. Shi, R. M. Berry, and K. C. Tam, “Mussel-Inspired Green Metallization of Silver Nanoparticles on Cellulose Nanocrystals and Their Enhanced Catalytic Reduction of 4-Nitrophenol in the Presence of β-Cyclodextrin,” *Ind. Eng. Chem. Res.*, vol. 54, no. 13, pp. 3299–3308, Apr. 2015, doi: 10.1021/acs.iecr.5b00177.
[274] Z. Hu, R. M. Berry, R. Pelton, and E. D. Cranston, “One-Pot Water-Based Hydrophobic Surface Modification of Cellulose Nanocrystals Using Plant Polyphenols,” *ACS Sustain. Chem. Eng.*, vol. 5, no. 6, pp. 5018–5026, Jun. 2017, doi: 10.1021/acssuschemeng.7b00415.
[275] A. Barbasz, M. Oćwieja, and J. Barbasz, “Cytotoxic Activity of Highly Purified Silver Nanoparticles Sol Against Cells of Human Immune System,” *Appl. Biochem. Biotechnol.*, vol. 176, no. 3, pp. 817–834, Jun. 2015, doi: 10.1007/s12010-015-1613-3.
[276] R. Sankar, R. Maheswari, S. Karthik, K. S. Shivashangari, and V. Ravikumar, “Anticancer activity of Ficus religiosa engineered copper oxide nanoparticles,” *Mater. Sci. Eng. C*, vol. 44, pp. 234–239, Nov. 2014, doi: 10.1016/j.msec.2014.08.030.
[277] Y. Abboud *et al.*, “Biosynthesis, characterization and antimicrobial activity of copper oxide nanoparticles (CONPs) produced using brown alga extract (Bifurcaria bifurcata),” *Appl. Nanosci.*, vol. 4, no. 5, pp. 571–576, Jun. 2014, doi: 10.1007/s13204-013-0233-x.
[278] B. Chudasama, A. K. Vala, N. Andhariya, R. V. Mehta, and R. V. Upadhyay, “Highly bacterial resistant silver nanoparticles: synthesis and antibacterial activities,” *J. Nanoparticle Res.*, vol. 12, no. 5, pp. 1677–1685, Jun. 2010, doi: 10.1007/s11051-009-9845-1.
[279] T. Dadosh, “Synthesis of uniform silver nanoparticles with a controllable size,” *Mater. Lett.*, vol. 63, no. 26, pp. 2236–2238, Oct. 2009, doi: 10.1016/j.matlet.2009.07.042.
[280] K. Ranoszek-Soliwoda *et al.*, “The role of tannic acid and sodium citrate in the synthesis of silver nanoparticles,” *J. Nanoparticle Res.*, vol. 19, no. 8, p. 273, Aug. 2017, doi: 10.1007/s11051-017-3973-9.
[281] J. W. Slot and H. J. Geuze, “A new method of preparing gold probes for multiple-labeling cytochemistry,” *Eur. J. Cell Biol.*, vol. 38, no. 1, pp. 87–93, Jul. 1985.
[282] L. J. Johnston *et al.*, “Determination of sulfur and sulfate half-ester content in cellulose nanocrystals: an interlaboratory comparison,” *Metrologia*, vol. 55, no. 6, pp. 872–882, Nov. 2018, doi: 10.1088/1681-7575/aaeb60.
[283] J. M. Rifkind, Y. A. Shin, J. M. Heim, and G. L. Eichhorn, “Cooperative disordering of single-stranded polynucleotides through copper crosslinking,” *Biopolymers*, vol. 15, no. 10, pp. 1879–1902, 1976, doi: 10.1002/bip.1976.360151002.

[284] T. Huang and X.-H. Nancy Xu, “Synthesis and Characterization of Tunable Rainbow Colored Colloidal Silver Nanoparticles Using Single-Nanoparticle Plasmonic Microscopy and Spectroscopy,” *J. Mater. Chem.*, vol. 20, no. 44, pp. 9867–9876, Jan. 2010, doi: 10.1039/C0JM01990A.
[285] H. I. Badi’ah, F. Seedeh, G. Supriyanto, and A. H. Zaidan, “Synthesis of Silver Nanoparticles and the Development in Analysis Method,” *IOP Conf. Ser. Earth Environ. Sci.*, vol. 217, p. 012005, Jan. 2019, doi: 10.1088/1755-1315/217/1/012005.
[286] A. G. M. da Silva, T. S. Rodrigues, S. J. Haigh, and P. H. C. Camargo, “Galvanic replacement reaction: recent developments for engineering metal nanostructures towards catalytic applications,” *Chem. Commun.*, vol. 53, no. 53, pp. 7135–7148, Jun. 2017, doi: 10.1039/C7CC02352A.
[287] C. Bhattacharya, N. Arora, and B. R. Jagirdar, “Digestive-Ripening-Facilitated Nanoengineering of Diverse Bimetallic Nanostructures,” *Langmuir*, vol. 35, no. 20, pp. 6493–6505, May 2019, doi: 10.1021/acs.langmuir.8b02208.
[288] X. M. Lin, C. M. Sorensen, and K. J. Klabunde, “Digestive Ripening, Nanophase Segregation and Superlattice Formation in Gold Nanocrystal Colloids,” *J. Nanoparticle Res.*, vol. 2, no. 2, pp. 157–164, Jun. 2000, doi: 10.1023/A:1010078521951.
[289] Advanced Materials Research Lab., Department of Physics, College of Science, University of Sulaimani, Qlyasan Street, Sulaimani, Kurdistan Regional Government-Iraq and S. B. Aziz, “Investigation of Metallic Silver Nanoparticles through UV-Vis and Optical Micrograph Techniques,” *Int. J. Electrochem. Sci.*, pp. 363–373, Jan. 2017, doi: 10.20964/2017.01.22.
[290] A. Zielińska, E. Skwarek, A. Zaleska, M. Gazda, and J. Hupka, “Preparation of silver nanoparticles with controlled particle size,” *Procedia Chem.*, vol. 1, no. 2, pp. 1560–1566, Nov. 2009, doi: 10.1016/j.proche.2009.11.004.
[291] K. Okazaki, T. Kiyama, K. Hirahara, N. Tanaka, S. Kuwabata, and T. Torimoto, “Single-step synthesis of gold–silver alloy nanoparticles in ionic liquids by a sputter deposition technique,” *Chem. Commun.*, vol. 0, no. 6, pp. 691–693, 2008, doi: 10.1039/B714761A.
[292] K. Mallik, M. Mandal, N. Pradhan, and T. Pal, “Seed Mediated Formation of Bimetallic Nanoparticles by UV Irradiation: A Photochemical Approach for the Preparation of ‘Core−Shell’ Type Structures,” *Nano Lett.*, vol. 1, no. 6, pp. 319–322, Jun. 2001, doi: 10.1021/nl0100264.
[293] H. M. Chen, R. S. Liu, L.-Y. Jang, J.-F. Lee, and S. F. Hu, “Characterization of core–shell type and alloy Ag/Au bimetallic clusters by using extended X-ray absorption fine structure spectroscopy,” *Chem. Phys. Lett.*, vol. 421, no. 1, pp. 118–123, Apr. 2006, doi: 10.1016/j.cplett.2006.01.043.
[294] N. M. Zain, A. G. F. Stapley, and G. Shama, “Green synthesis of silver and copper nanoparticles using ascorbic acid and chitosan for antimicrobial applications,” *Carbohydr. Polym.*, vol. 112, pp. 195–202, Nov. 2014, doi: 10.1016/j.carbpol.2014.05.081.
[295] S. D. House, Y. Chen, R. Jin, and J. C. Yang, “High-throughput, semi-automated quantitative STEM mass measurement of supported metal nanoparticles using a conventional TEM/STEM,” *Ultramicroscopy*, vol. 182, pp. 145–155, Nov. 2017, doi: 10.1016/j.ultramic.2017.07.004.
[296] S. Valsalam *et al.*, “Rapid biosynthesis and characterization of silver nanoparticles from the leaf extract of Tropaeolum majus L. and its enhanced in-vitro antibacterial, antifungal,

antioxidant and anticancer properties," *J. Photochem. Photobiol. B*, vol. 191, pp. 65–74, Feb. 2019, doi: 10.1016/j.jphotobiol.2018.12.010.
[297] M. A. Asghar *et al.*, "Iron, copper and silver nanoparticles: Green synthesis using green and black tea leaves extracts and evaluation of antibacterial, antifungal and aflatoxin B1 adsorption activity," *LWT*, vol. 90, pp. 98–107, Apr. 2018, doi: 10.1016/j.lwt.2017.12.009.
[298] S. W. Brown, S. G. Oliver, D. E. F. Harrison, and R. C. Righelato, "Ethanol inhibition of yeast growth and fermentation: Differences in the magnitude and complexity of the effect," *Eur. J. Appl. Microbiol. Biotechnol.*, vol. 11, no. 3, pp. 151–155, 1981, doi: 10.1007/BF00511253.
[299] M. J. Winans and J. E. G. Gallagher, "Metallomic and lipidomic analysis of S. cerevisiae response to cellulosic copper nanoparticles uncovers drivers of toxicity," *Metallomics*, vol. 12, no. 5, pp. 799–812, 2020, doi: 10.1039/D0MT00018C.